DEVELOPMENT OF PLASTIC HINGE MODELS FOR CORRODED REINFORCEMENT IN RC BEAMS

A Thesis

Submitted in partial fulfilment of the requirement for the award of degree

of

Doctor of Philosophy

In

Civil Engineering

Submitted By

Divyashree

Reg. No.: 951002011

Supervisor(s)

Dr. Naveen Kwatra,
Professor
Department of Civil Engineering
Thapar Institute of Engineering & Technology
Patiala

Dr. Pankaj Agarwal,
Professor & Head
Department of Earthquake Engineering
IIT Roorkee
Roorkee

DEPARTMENT OF CIVIL ENGINEERING

THAPAR INSTITUTE
OF ENGINEERING & TECHNOLOGY
(Deemed to be University)

PATIALA-147004

July, 2021

CERTIFICATE

I, Divyashree, hereby declare that the thesis entitled, "Development of plastic hinge models for corroded reinforcement in RC beams," submitted to Thapar Institute of Engineering & Technology, Patiala, in partial fulfilment of the requirement for the award of Degree of **Doctor Of Philosophy** in **Civil Engineering** is a record of original and independent research work done by me during 2011-2021. This thesis has been conducted under the supervision and guidance of Dr. Naveen Kwatra, Professor, Department of Civil Engineering, Thapar Institute of Engineering & Technology, and Dr. Pankaj Agarwal, Professor, Department of Earthquake Engineering, IIT Roorkee. It has not formed the basis for the award of any Degree to any candidate of any university.

Divyashree
Reg. No.: 951002011

Date: 7/6/2021

This is to certify that above statement made by the candidate is correct to the best of my knowledge.

Dr. Naveen Kwatra

Supervisor
Professor
Civil Engineering Department
Thapar Institute of Engineering & Technology

Dr. Pankaj Agarwal

Supervisor
Professor
Earthquake Engineering Department
IIT Roorkee

ii

ABSTRACT

Earthquake can cause great amount of damage to humanity among all-natural hazards. In order to avoid collapse of building during major earthquakes, most of the multistoried buildings are designed and detailed to combine strength and ductility. To attain the required ductility, they need to be proportionally adjusted to ensure that in the event of a large earthquake, the beam swing failure mode takes precedence over the cylindrical swing failure mode. The designated area in the structure (called a potential plastic hinge) is designed to withstand inelastic deformation, while the rest of the structure undergoes elastic deformation. Dynamic performance of building is determined through these plastic hinges once yielding has occurred.

Also, deformation capability of plastic hinge in RCC structure are dependent on quality of steel. Reinforcing steel bars have been corroded to different levels due to environmental effects in already existing structures. Further, corroded reinforcements will not allow the structure to behave as ductile moment resisting building during earthquake. Therefore, incorporating plastic hinge model of corroded RC beams to make sure weak beam- strong column behaviour is the base of this research to prevent collapse of RC structures during earthquakes.

In this work, plastic hinge model of RC beam under flexure loading incorporating the effect of 10%, 20% and 30% corrosion in reinforcement bar has been attempted. Nonlinear behaviour of Reinforced Concrete structures is observed using developed plastic hinge model.

The study of the effect of corroded old reinforcement is done on the plastic hinge parameters of RCC structures. For this, the effect of different grade of concrete and different reinforcement bar along with the condition of reinforcement (bars have been corroded outside the beam) on a RC beam is studied under flexure loading. The beams are simply supported under four-point loading to ensue flexure behaviour. The moment carrying capacity is increased when the concrete grade is increased. For the same concrete grade when yield strength of the reinforcement is increased, there is a decrease observed in curvature value. Also, plastic hinge length is maximum in the RC beams with no corroded bars used and decreases as the corrosion level increases in all four cases. Further, the bars when inside the RC beam is experimentally investigated to different durations by impressed current corrosion technique as a pilot study using two cases for comparison. However, the work has been extended by taking corrosion of reinforcement outside before casting the beam. Also, reinforced concrete (RC) beams have been analysed through nonlinear finite element modeling considering the effect of reinforcement corrosion loss observed. Plastic hinge model with corroded reinforcement is developed after comparing experimental and

analytical results. Then, a simple empirical equation is reported for maximum moment including the percentage of corrosion, using soft computing technique of Genetic Programming (GP).

The efficacy of developed hinge models of corroded RC beams on a two-storey frame by performing pushover analysis analytically is investigated. Base shear decreased with increase in level of corrosion as observed from pushover curve.

It is observed that corrosion-induced damage in RC structures can effectively be incorporated in developing plastic hinge models for seismic analysis of Reinforced Concrete buildings. This will greatly help the seismic assessment of the remaining bearing capacity of the steel bars, which will greatly help in formulating the design strategy of the existing Reinforced Concrete frame structure.

ACKNOWLEDGEMENT

First and Foremost, I am beholden to the Almighty and I bow before him for his blessings and bestowing in me the grit and confidence to carry out the research work.

I convey heartfelt and sincere gratitude to my research supervisors **Dr. Naveen Kwatra**, Professor, Civil Engineering Department and **Dr. Pankaj Agarwal**, Professor & Head, Earthquake Engineering Department, IIT Roorkee. Their valuable support, advice, and encouragement inspired me to complete the research work on time.

I extend my thanks to **Dr. Prem Pal Bansal**, Head of the department, Civil Engineering, Thapar Institute of Engineering and Technology, for his support and advice in my journey of Ph.D.

I am honour bound and profoundly thankful to the doctoral committee members- **Dr. Shruti Sharma**, Associate Professor, Civil Engineering Department, **Dr. Maneek Kumar**, Professor, Civil Engineering Department, and **Dr. Rajesh Kumar,** Professor, School of Physics, Thapar Institute of Engineering and Technology, for their support and invaluable comments.

Further, I wish to thank all technicians & workers in structural and concrete lab, particularly Mr. Ram Sumiran, Mr. Virender Sharma, Mr. Roop Kumar and many others.

I am grateful to my husband, Mr. Jitender who stood like a rock in my difficult times and worked relentlessly to provide me full support. I would also like to thank my family: my father, Sh. S.P. Yadav, my mother, Smt. Prita Kaur, Tanushree Thorat (sister) for their endless support. Their love, patience, persistent encouragement, and good virtuous understanding enabled me to complete the research work successfully. My father believed in me, enrolled me in Ph.D. degree, and provided full enthusiasm in this beautiful research journey. I also thank God for blessing me with the best parents of the world.

Divyashree

Regn No. 951002011

TABLE OF CONTENTS

Certificate

Abstract

Acknowledgement

Table of Contents

List of Figures

List of Tables

Acronyms and Abbreviations

Chapter 1: Introduction

1.1 Background

1.2 Motivation for research

1.3 Objectives of research

1.4 Thesis Outline

1.5 Closing remarks

Chapter 2: Plastic hinge models of RC beam and Pushover analysis for RCC frame- A Review

2.1 Introduction

2.2 Plastic hinge

2.2.1 Plastic hinge concept

2.2.1.1 Analysis of plastic hinge

2.2.1.2 Types of plastic hinge

2.2.2 Review of plastic hinges for seismic analysis of plastic hinge length

2.3 Pushover Analysis

2.3.1 Description of Pushover Analysis

2.3.2 Key elements of the pushover analysis and its significance

2.3.3 Pushover Analysis- Analytically

2.3.4 Review of Pushover analysis for RC frame with non-corroded and corroded bars

2.4 Closing Remarks

Chapter 3: Evaluation of plastic hinge parameters with corroded reinforcement

3.1 General

3.2 Experimental Investigation and methodology

3.2.1 Reinforced Concrete (RC) beam design

3.2.2 Accelerated corrosion in RC beam (When reinforcement bar is inside RC beam)

3.2.3 Inducing Accelerated Corrosion in Reinforcement Bar (Outside before casting RC beam)

3.2.4 Comparison of load -deflection behaviour of RC beams when corrosion is induced in Reinforcement Outside and Inside the beam

3.2.5 Accelerated corrosion in Reinforcement Bar Individually for Evaluation of Plastic hinge parameters

3.2.6 Tensile properties of reinforcement bar

3.3 Behaviour of RC beam under Flexure loading

3.3.1 Effect of 10% corrosion on R1/R2 RC beam

3.3.2 Effect of 20% corrosion on R1/R2 RC beam

3.3.3 Effect of 30% corrosion on R1/R2 RC beam

3.4 Experimental Moment-Curvature Behaviour

3.5 Analysis of plastic hinge length

3.6 Closing Remarks

Chapter 4: Development of plastic hinge model with corroded reinforcement

4.1 General

4.2 Finite Element Modeling

4.2.1 Modeling of Concrete

4.3.1.1 Fixed crack model

4.2.2 Modeling of reinforcement

4.2.3 Modeling of Bond-Slip relationship

4.3 Results and Discusssions

4.3.1 Load-Discplacement Behaviour

4.3.2 Moment-Rotation Relationship

4.4 Development of Mathematical relation using Genetic Programming

4.4.1 Advantage of Genetic Programming

4.4.2 Methodology

4.4.3 Model Formulation and Results

4.5 Closing Remarks

Chapter 5: Efficacy of developed plastic hinge model of RC beam by pushover analysis

5.1 General

5.2 Description and modelling of RC frame structure
5.3 Pushover Methodology
5.3.1 Moment-curvature and Pushover curve
5.3.2 Plastic hinges mechanism
5.4 Closing remarks
Chapter 6: Conclusions
6.1 General
6.2 Concluding Remarks
6.2.1 Evaluation of plastic hinge parameters with corroded reinforcement
6.2.2 Development of plastic hinge model with corroded reinforcement
6.2.3 Efficacy of developed plastic hinge model of RC beam by pushover analysis
6.3 Recommendations for future research
List of publications
References

LIST OF FIGURES

1.1	Moment- chord rotation relation and performance levels of RC plastic hinges (FEMA-356, 2000)	3
2.1	Schematic Curvature Distribution along Beam at Ultimate Stage: (a) Beam, (b) Bending Moment Diagram, (c) Curvature Diagram [Kheyroddin&Naderpour]	7
2.2	Formation of uni-directional and reversing plastic hinges [Douglas, Davidson & Fenwick]	9
2.3 (a)	Flowchart explaining Pushover analysis	13
2.3 (b)	Schematics depicting the development of an equivalent SDOF system for a pushover curve (FEMA 440, 2005).	13
2.4	Values for determining the vertical distribution of the lateral loads	14
2.5	Bilinear relation of base shear Vs roof displacement plot	14
2.6 (a)	Performance Evaluation of structure in terms of Capacity and Demand	17
2.6 (b)	Nonlinear analysis procedure	18
2.7	Typical seismic demand Vs. Capacity (a) Safe Design (b) Unsafe Design	20
2.8	Force-Deformation for pushover hinge	21
3.1	(a) Geometry and Details of test specimen (b) Two- point loading setup of 42 RC beam	31
3.2	Corrosion of R1, R2 bars inside RC beams by accelerated Anodic Impressed Current corrosion technique	32
3.3	Schematic setup of accelerated corrosion of RC beam	32
3.4	Corrosion of R1 and R2 Bars Individually by Impressed Current method	34
3.5	Comparison of Load-deflection curve of RC beams when corrosion is induced individually outside and inside RC beam with R1 and R2 bars (10% corroded bars)	35
3.6	Condition of extracted bars at different levels of corrosion	37
3.7	Spatial distribution of bottom bar diameter along the specimen length at different levels of corrosion	38
3.8	Failure patterns of RC beams. a- M1R1 (4cases), b- M1R2 (4cases), c- M2R1 (4 cases), d- M2R2 (4cases)	40 41
3.9	Load-deflection curve of RC beams with R1 bars (Without corrosion)	43
3.10	Load-deflection curve of RC beams with R2 bars (Without corrosion)	43
3.11	Load-deflection curve of RC beams with R1 bars (10% corroded bars)	43
3.12	Load-deflection curve of beams with R2 bars (10% corroded bars)	43

3.13	Load-deflection curve of RC beams with R1 bars (20% corroded bars)	44
3.14	Load-deflection curve of RC beams with R2 bars (20% corroded bars)	44
3.15	Load-deflection curve of RC beams with R1 bars (30% corroded bars)	44
3.16	Load-deflection curve of RC beams with R2 bars (30% corroded bars)	44
3.17	Moment- curvature Curve of M1 R1 (all cases)	45
3.18	Moment- curvature curve of M1 R2 (all cases)	45
3.19	Moment- curvature Curve of M2 R1 (all cases)	46
3.20	Moment- curvature curve of M2 R2 (all cases)	46
3.21	Variation in plastic hinge length for M1R1 (4 cases)	47
3.22	Variation in plastic hinge length for M1R2 (4 cases)	47
3.23	Variation in plastic hinge length for M2R1(4 cases)	47
3.24	Variation in plastic hinge length for M2R2(4 cases)	47
3.25	Effect of Ductility on RC beams (all cases)	48
4.1	FEM model along with mesh generation	52
4.2	(a) Geometry of brick elements and stages of crack openings	53
4.2	(b) Bilinear stress-strain law for reinforcement	53
4.2	(c) Bond-slip relationship	53
4.2	(d) Fixed crack model. Stress and strain state.	53
4.3	Comparison of Experimental and FEM results (No corrosion)	55
4.4	Comparison of Experimental and FEM results (10% corroded)	55
4.5	Comparison of Experimental and FEM results (20% corroded)	56
4.6	Comparison of Experimental and FEM results (30% corroded)	56
4.7	(a). Failure patterns of RC beams after FE analysis (flexure in all cases)	57
4.7	(b). Failure patterns of RC beams after FE analysis (shear failure observed)	57
4.8	Analytical moment- rotation curve of M1R1	58
4.9	Analytical moment- rotation curve of M1R2	59
4.10	Analytical moment- rotation curve of M2R1	59
4.11	Analytical moment- rotation curve of M2R2	60
4.12	Moment-rotation curve of Experimental and FEM results (No corrosion)	61
4.13	Moment-rotation curve of Experimental and FEM results (10% corrosion)	61
4.14	Moment-rotation curve of Experimental and FEM results (20% corrosion)	62
4.15	Moment-rotation curve of Experimental and FEM results (30% corrosion)	62
4.16	Moment- chord rotation relation of RC plastic hinges in category NC of transverse reinforcement	64

4.17	Moment-chord rotation relation for RC beam plastic hinges using 0%, 20%, 35% corroded bar	64
4.18	Relationship between moment carrying capacity and percentage of steel weight loss using Experimental, Analytical & GP based relationships	67
5.1	RC frame Model (SAP 2000)	70
5.2	Force-Deformation for pushover hinge	72
5.3	Moment-Curvature of Developed hinge model (Case M1R1) and Default-hinge model	72
5.4	Pushover curves of RC frame for all four cases a)M1R1 b) M1R2 c)M2R1 d) M2R2	74
5.5	Plastic hinge patterns of M1R1 RC frame a) No corrosion b) 10% corrosion c) 20% corrosion d) 30% corrosion	75
5.6	Plastic hinge patterns of M1R2 RC frame a) No corrosion b) 10% corrosion c) 20% corrosion d) 30% corrosion	76
5.7	Plastic hinge patterns of M2R1 RC frame a) No corrosion b) 10% corrosion c) 20% corrosion d) 30% corrosion	77
5.8	Plastic hinge patterns of M2R2 RC frame a) No corrosion b) 10% corrosion c) 20% corrosion d) 30% corrosion	78

LIST OF TABLES

2.1	Values for modification factor Co	14
2.2	Values for modification factor C2	16
2.3	Equations for loading type and target displacement according to FEMA 356 [16]	16
3.1	Details of beams used in the study	30
3.2	Material and Compressive Properties of concrete	31
3.3	Corrosion levels achieved in different bars corroded inside RC beam	33
3.4	Calculation of % corrosion of longitudinal, Stirrups (R1, R2) Steel bar before casting Beam	34
3.5	Calculation of % corrosion of longitudinal (R1, R2) Steel bar before casting Beam	36
3.6	Calculation of % corrosion of Stirrups (R1, R2) before casting Beam	36
3.7	Tensile Properties of Steel bars	38
3.8	Experimental data of RC beams	39
3.9	Plastic hinge length of RC beams	42
4.1	Details of beams used in FEM study	51
4.2	Material properties used	54
4.3	Modeling parameters and acceptance criteria of RC beams for nonlinear analysis	63
4.4	Results of GP model	66
5.1	Member Section Properties	69
5.2	Yield Strengths of Steel bar	70
5.3	Pushover Analysis cases	71

ACRONYMS AND ABBREVIATIONS

ACI	American Concrete Institute
ASCE	American Society of Civil Engineers
ATENA	Advanced Tool for Engineering Nonlinear Analysis
BF	Bare Frame
CE	Coefficient of Efficiency
CFRP	Carbon Fibre Reinforced Polymer
CP	Collapse Prevention
CSM	Capacity Spectrum Method
ETABS	Extended Three-Dimensional Analysis of Building System
FE	Finite Element
FEM	Finite Element Modeling
FEMA-356	Federal Emergency Management Agency
GA	Genetic Algorithms
GP	Genetic Programming
INF	Infilled Frame
IO	Immediate Occupancy
LS	Life Safety
Lp	Plastic hinge length
LVDT	Linear Variable Differential Transducer
M1	Concrete Mix 1
M2	Concrete Mix 2
MASFI	Modified Axial-Shear-Flexure Interaction
MASFI-C	Modified Axial-Shear-Flexure Interaction considering Reinforcement corrosion
MLR	Multi Linear Regression
NC	Non-Conforming
NSP	Nonlinear Static Procedure
R1	Reinforcement Bar 1
R2	Reinforcement Bar 2
RC	Reinforced Concrete
RCC	Reinforced Cement Concrete

RMSE	Root Mean Squared Error
SAP2000	Structural Analysis Program 2000
SBF	Steel Braced Frame
SDOF	Single Degree of Freedom System
UTS	Ultimate Tensile Strength
YS	Yield Strength

CHAPTER 1
INTRODUCTION

1.1 BACKGROUND

The issues concerning to the seismic vulnerability of existing structures have been disseminated due to young earthquakes occurring in numerous places of the world. Inelastic Performance of reinforced concrete (RC) member partly leads to reallocation of moments and forces, resulting in increased component's affordability to carry load. As loading increases, hinge begins to form continuously at places where plastic moment capacity of component is reached. Additionally, the hinges keep on rotating with increase in load until the last hinge is formed, transforming structure into mechanism, which leads to failure. Due to development of mechanism, study of formation of hinges is a very important area of research.

Several researchers have proposed various models predicting plastic hinge length or rotation capacity. Plastic hinge length is considered as an equivalent length, at which the given plastic curvature is assumed to be constant, to integrate the section curvature along the length of the RC member to account for the flexural deflection and plastic rotation capacity of the member. Documents like FEMA-356 or ATC 40 have given hinge models of individual components of RC frame. Hinge models or plastic hinge formation have been evaluated experimentally or analytically through moment-curvature behaviour of individual components. The formation of plastic hinges is studied by various researchers based on its dependence on number of parameters such as yield strength of steel bar, cross-section details of component, concrete compressive strength, loading type and corrosion level of reinforcement bars (Lopes and Bernardo, 2003; Zhao, Wu, Leung & Lam, 2011; Zhou, Zhao, Zhang & Yang, 2015; Ou& Nguyen, 2014). It has been observed, that unexpected large-scale elongation and shear deformation have occurred in zones of plastic hinges.

Seismic qualification of existing RC structures has become highly crucial under plastic hinge formation condition. Seismic qualification ultimately guides to the retrofitting of deficient buildings. Seismic rehabilitation of structures is built on a performance-based design method which deviates from the traditional methods for seismic design of structures. Displacement Coefficient Method or Capacity Spectrum Approach for pushover analysis and evaluation of performance of structure are mostly used for seismic evaluation. A crucial task in performance-based design is to evaluate earthquake demands for buildings to depict its performance level with credence. There are four traditional methods to evaluate the structure under earthquake forces, which are linear static, linear dynamic, ‘non-linear static’ or ‘pushover analysis’ and non-linear dynamic. Seismic analysis of existing structure is performed using Pushover analysis based on displacement coefficient method or capacity spectrum method. Pushover

analysis or Nonlinear static analysis, has been evolved over the past so many years from 1990's onwards. It has become the most adopted analysis procedure for seismic performance evaluation purposes as the method is comparatively simple compared to the nonlinear dynamic analysis and consider plastic (post elastic) behaviour. Pushover analysis is a static procedure that uses a simplified nonlinear technique to estimate seismic structural deformations. Pushover analysis can be performed experimentally as well as analytically. In performing nonlinear pushover analytically, modelling of each component of a structure is an essential step. The model should examine 'non-linear' behaviour of structural components which is required as to describe the plastic hinge properties at various locations in the building. For performing pushover of a structure, it is necessary to understand overall yield point and ultimate point of the structure, which gives details regarding ductility. The significant increase in ductility in ultimate limit state is the main criteria for design of RC beams in bending (Baker. 1956). This can be observed by the development of large deformations before the collapse, and make large deformations and energy dissipation possible during the earthquake (Carpinteri et al. 2009). The ductility of structural component can be assessed in terms of various plastic hinge parameters (plastic hinge length, plastic hinge rotation capacity, hinging pattern etc.). The energy dissipation is expected to occur through plastic hinges formed and hinges should form in beams to ensure strong column-weak beam behaviour for a seismically efficient structure.

Hinge models of reinforced concrete structures can be defined with the help of plastic hinges, which are assumed to be either distributed or concentrated (lumped). Most of the models developed by Panagiotakos and Fardis (2001), Biskinis and Fardis (2010) have assumed concentrated plastic hinges in columns and beams. After defining plastic hinge models, hinge rotation capacity at yielding, ultimate state and plastic hinge length are calculated from their geometry, yield strength of reinforcement and concrete grade. In this context, Panagiotakos and Fardis (2001) proposed expressions for the 'yield chord rotation', 'yield moment' and 'ultimate chord rotation'. The above-mentioned expressions are developed from database of around 1000 experiments correspondent to columns, beams and shear walls.The moment-rotation relationship of the Reinforced Concrete plastic hinge is given in the curve, **Fig. 1.1** below as defined in FEMA-356. In this curve, terminologies like curvature, strain, elongation and rotation are used to represent deformations. Parameters a and b represents deformation that appears after yielding, that is, plastic deformation. The parameter c is the reduced resistance after the sudden reduction from C to D. Numerical explanation of RC beams is defined by parameters a, b and c, which are shown in Table 6-7 of FEMA-356. 3 structural performance levels are described by FEMA-356, known as 'immediate occupancy' IO, 'life safety' LS and 'collapse prevention' CP. The performance level of building is represented by force-deformation curve of plastic hinge are shown in **Fig. 1.1.**

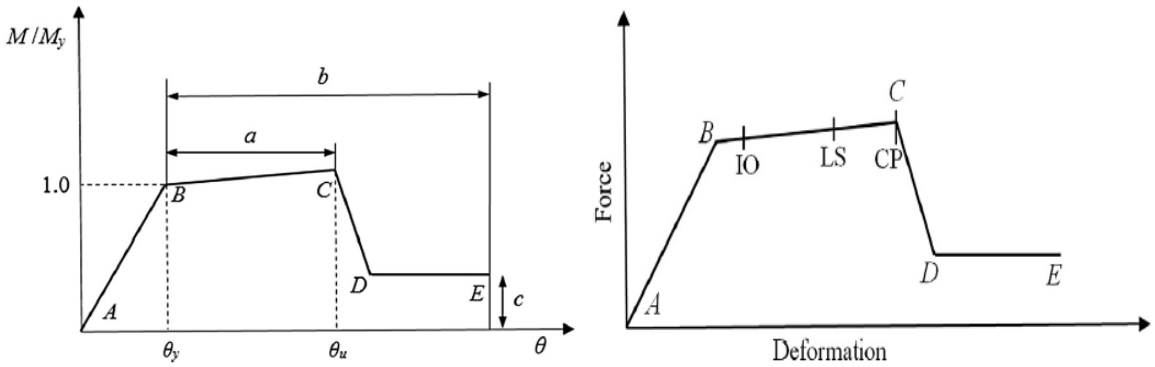

Fig. 1.1 Moment- chord rotation relation and performance levels of RC plastic hinges (FEMA-356, 2000)

According to the moment-chord rotation relation and structural performance levels for RC plastic hinges, modelling parameters and acceptance standards for linear and non-linear behaviour are given for RC columns, beams, walls, beam-column joints in FEMA-356.

Various researchers have assessed the earthquake performance of RC frames exposed to rebar corrosion and noticed progressive deterioration of frames over time can cause serious reductions on the load-bearing capacity (Saetta et al. 2008, Yuksel and Coskan. 2013, Yalciner and Marar. 2012).The plastic hinge models or plastic hinge parameters studied in previous years have not focussed much on the behaviour of components of RC frame incorporating corrosion of steel.

The present work attempts to develop the plastic hinge models of Reinforced Concrete (RC) beams for retrofitting and seismic evaluation of old buildings by performing experiments to analyse outcome of different grades of concrete, yield strength of reinforcement bar along with the condition of reinforcement. Therefore, the present work has been focussed on evaluation and development of plastic hinge models by taking into account the corrosion of reinforcement bar up to 35% in RC beam. The corrosion has been induced in the steel bar by corroding it outside the beam as well as inside the beam. However, the plastic hinge models have been developed and presented based on corrosion when induced in reinforcement bar inside the RC beam. Later, the work has been extended to check the behaviour of a two-storey frame on the basis of plastic hinge models developed for seismic evaluation of the structure. When reinforced concrete hinges are corroded at up to 35%, the moment-chord rotation shows that the ductility decreases with the increase of the corrosion degree of the steel bar, making it vulnerable to damage in earthquakes, which can be used to predict nonlinear behavior of existing structure by performing pushover analysis. Following section provides an insight to plastic hinge models and pushover analysis of RC structures for its seismic evaluation.

1.2 MOTIVATION FOR RESEARCH

Plenty of research work has been described on seismic evaluation of RC structures by performing pushover analysis using plastic hinge models already developed. Several experimental and analytical research is done to assess the plastic hinge regions of corrosion affected RC members. But, development of plastic hinge models of Reinforced Concrete (RC) beams needs to be investigated for retrofitting and seismic evaluation of old buildings. This forms the motivation of research to study the effect of different grades of concrete and yield strength of reinforcement bar along with the condition of reinforcement by developing plastic hinge models. It is also proposed to investigate the efficacy of plastic hinge models developed which is extremely important for seismic analysis of existing RC structures.

1.3 OBJECTIVES OF THE RESEARCH

The objective of this research work is to examine plastic hinge models of RC beams developed to study the effect of various parameters (concrete grade, yield strength of reinforcement, condition of reinforcement etc.) for retrofitting and seismic evaluation of old buildings. Moment-rotation relations and the failure modes observed from experimental data of RC beams are then compared and investigated analytically through nonlinear finite element analysis. The major objectives of the proposed work are as below –

1. To study the behaviour of RCC beams experimentally by varying type of reinforcement, corrosion of reinforcement and grade of concrete.
2. To study the behaviour of RCC beams analytically by varying type of reinforcement, corrosion of reinforcement and grade of concrete.
3. Development of mathematical model for moment carrying capacity and plastic hinge length of RC beams using Artificial Intelligence
4. Generalised Hinge models would be developed based on above experimental & analytical studies of RCC beams.
5. To test the suitability of developed Hinge models on a two-storey frame by performing pushover analysis analytically

1.4 THESIS OUTLINE

The thesis is organised in following manner:

Chapter 1 introduces the problem of plastic hinge models already developed. Gaps in the research area are identified and objectives of the study is outlined.

Chapter 2 includes literature review in two parts. The first part includes various researches done on plastic hinges of RC beams with corroded reinforcement. In the second study, suitability of plastic hinge models developed are tested on a two-storey frame by performing pushover analysis analytically.

Chapter 3 focusses on the behaviour of RCC beams experimentally including effects of concrete grade and type of reinforcement along with condition of reinforcement (10, 20. and 30% corroded reinforcement) by applying two-point loading.

Chapter 4 focusses on the behaviour of RCC beams analytically including effects of concrete grade and type of reinforcement along with condition of reinforcement (10, 20. and 30% corroded reinforcement) and generalised models are developed with the comparison between experimental and analytical results.

Chapter 5 presents the suitability of plastic hinge models developed on a two-storey frame by performing pushover analysis analytically.

Chapter 6 presents the conclusions and provides a few recommendations for further study.

1.5 CLOSING REMARKS

In this chapter, a discussion on the importance of plastic hinge models of RC structures are given. The advantages of pushover analysis with the help of hinge parameters for seismic analysis are highlighted. Finally, the significance of plastic hinge length to be applied on frame structures for the pushover analysis is highlighted. Aims and objectives of the research work are outlined. The succeeding chapter brings out a review of recent works done utilizing plastic hinge of RC beams and pushover analysis for seismic qualification in RC structures.

CHAPTER 2
PLASTIC HINGE MODELS OF RC BEAM AND PUSHOVER ANALYSIS FOR RCC FRAME- A REVIEW

2.1 INTRODUCTION

Seismic resistance capacity of existing buildings is frequently raised questions due to earthquakes occurring in many parts of the world. These raised questions can be answered by predicting the seismic performance of buildings incorporating various numerical models which can predict the outcome generated by earthquake actions on buildings. Seismic analysis of a structure can be conducted by different methods and using nonlinear analyses is necessary to represent behaviour of buildings under earthquake effects. Nonlinear static analysis is the most commonly used procedures by researchers as it is easy to implement through the specifications as given in FEMA-356 or ATC-40. A characteristic non-linear force-deformation graph can be ordained for building corresponding to moment-curvature relationship up to plastic hinge formation of individual components in nonlinear pushover analysis. The design of any structure is based on inelastic section. If there is no significant rebar yield, the building persists to function in a linear elastic way even under factored loads. If yielding of reinforcement occurs, then under-reinforced sections exhibits ductile behavior because of the capacity of components to experience large curvatures close to constant moment following steel yielding.

Dissipation of seismic energy is mostly attained through flexural yielding, because the compression and shear ductility of reinforced concrete is relatively small. Ductile moment resisting frame is defined as a frame of continuous construction, containing flexural members, columns and their connections, designed and detailed to contain reversible lateral displacements after the development of plastic hinges (without decrease in strength). The ductile behavior allows the structure to go into an inelastic phase, wherein the sections which have attained their ultimate moment capacities undergo rotations (under constant moment). An imaginary hinge is first introduced at the component under consideration, it can be column, beam or beam-column joint and a rotation initiated therein in a direction correspondent to the moment desired. So, in elastoplastic behavior of structure, the excess energy produced under seismic forces, will get dissipated by the plastic hinge. Thus, while ductility improves in decreasing induced forces and in dissipating some input energy, which also demands large deformations to be accommodated by the structure. So, in a structure composed of ductile moment resisting frame, the required inelastic response progresses by the formation of plastic hinges in RC members.

The chapter throws light on plastic hinge parameters and pushover analysis along with the review of the latest works done with focus on developing plastic hinge models.

2.2 PLASTIC HINGE

This section provides an insight into the detailed analysis of plastic hinge formation for seismic evaluation.

2.2.1 Plastic Hinge concept

2.2.1.1 Analysis of Plastic Hinge

Under action of bending moment, beam is completely plastic, which will cause the members to behave as if they were hinged on the neutral axis with an attempt to increase the moment. It is defined as a plastic hinge. Under a constant moment equal to plastic moment of the section, an infinitely large rotation can occur at the plastic hinge. The plastic hinge can be explained as the yield area due to the bending of the component of structure, in which it can rotate indefinitely under the constant plastic moment of the section. For a specific structure, under a given load condition, the number of hinges required to fail will not change, although a part of the building may independently fail due to the development of less number of hinges. The structural component works as a hinge mechanism, and in doing so, adjacent hinges rotate in opposite directions. In theory, it is presumed that a plastic hinge occurs at point of occurrence of plastic rotation. The performance of plastic hinges is reproving to the deformation and load-bearing capacity of components.

The conditions of the ultimate load state when a particular cantilever beam is exposed to uniform load are shown in **Fig. 2.1** [Kheyroddin&Naderpour. 2007].

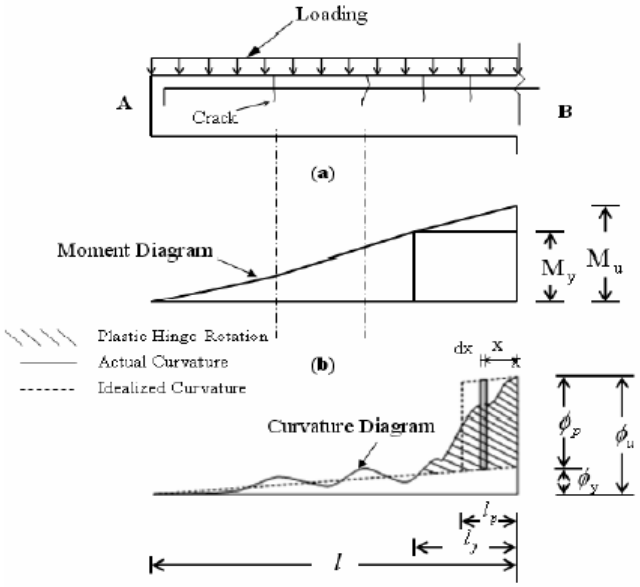

Fig. 2.1. Schematic Curvature Distribution along Beam at Ultimate Stage: (a) Beam, (b) Bending Moment Diagram, (c) Curvature Diagram [Kheyroddin&Naderpour, 2007]

For load values less than the yield moment, *My*, the curvature gradually increases from the free end of the cantilever (Point A) to the face of the column (point B). The curvature of the tension steel increases greatly when it first yields. In the ultimate load stage, the curvature value of the support suddenly increases, resulting in large inelastic deformation. Since the concrete between the cracks may be subjected to a certain tension (tension-stiffening), the curvature will fluctuate along the length of the beam. Each curvature peak corresponds to the crack position. The actual curvature distribution at a stage of ultimate load can be idealized into elastic and plastic regions [**Fig. 2.1**], thus the total rotation, θt, over the beam length can be divided into elastic, θe, and plastic, θp, rotations. The curvature at yielding can be used to obtain the elastic rotation, θe until the steel yields. With reference to **Fig. 2.1**, the plastic hinge rotation, θp, on each side of the critical section, can be determined from equation 1:

$$\theta_p = \int_0^{l_y} [\phi(x) - \phi_y] dx \qquad (1)$$

In which *ly*, is the beam length where the bending moment is greater than the yield moment, *My*, or the distance between the critical zone and the first yield position of tension steel and $\varphi(x)$ is the curvature at a distance *x* from the critical section at the ultimate load stage.

2.2.1.2 Types of Plastic Hinge

Two forms of plastic hinge may develop in beams subjected to seismic actions, with the type of plastic hinge depending upon the relative magnitudes of the seismic and gravity loads which act are:

(a) Uni-directional Plastic Hinge

(b) Reversing Plastic Hinge

Where the gravity loading dominates as illustrated in the **Fig. 2.2** shown below, as the structure sways backward and forward negative moment plastic hinges form in beam at the column faces and positive moment plastic hinges in the span of the beam. With each inelastic displacement the vertical deflection of the beam increases and the inelastic rotations sustained by the plastic hinges increase in magnitude. As each of these zones sustains inelastic rotations in one direction only, they are referred to as uni-directional plastic hinges. The load deflection characteristics of structures which form uni-directional plastic hinges show little stiffness degradation when subjected to inelastic cyclic deflections. The situation where the seismic actions dominate is shown in **Fig. 2.2**. In this case, as the structure sways backward and forward, negative and positive moment plastic hinges form in beam at column faces, with direction of rotation in each of these reversing with the direction of motion. These are referred to as reversing plastic hinges [Douglas, Davidson & Fenwick, 1996].

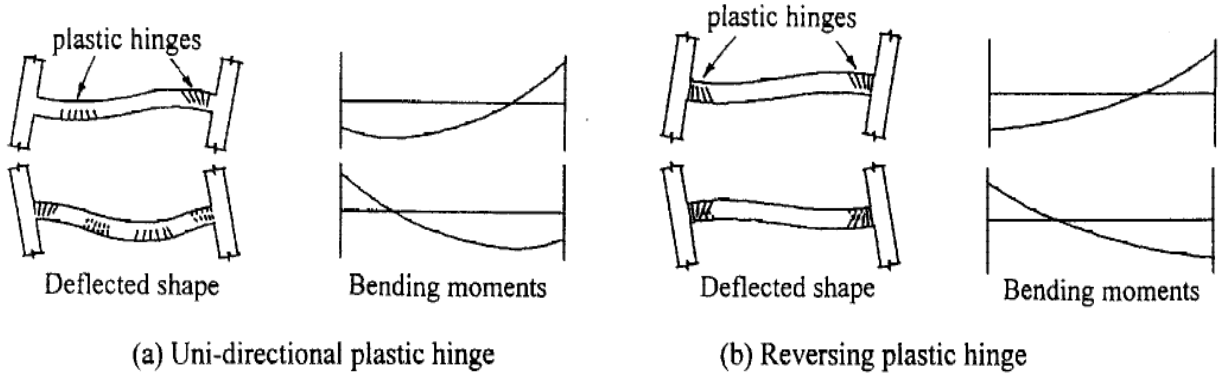

Fig. 2.2 Formation of uni-directional and reversing plastic hinges [Douglas, Davidson & Fenwick, 1996]

2.2.2 Review of Plastic Hinges for seismic analysis of plastic hinge length

A review of the latest works analyzing plastic hinges of corroded and non-corroded RC beams are briefed below:

Douglas et al. (1996) developed a finite element sub-structure model, which represents uni-directional and reversing plastic hinges in RC beams and implemented in a dynamic structural analysis program. The model allows for the increase in plastic hinge length as strain hardening occurs, and it is capable of predicting flexural, shear and elongation deformations. Though the stirrups have been a part to withstand significantly more shear than maximum value, the experimental results represent considerable shear deformation that develops in reversing plastic hinges. Also, considerable elongation has been seen occurring both in unidirectional and reversing plastic hinges.

Lopes and Carmo (2006) studied effect of concrete strength and ductility of steel over plastic rotation capacity. A theoretical model of plastic hinges in RC beams has been presented for assessment of moment-rotation curves. The conclusions showed that with increase in shear reinforcement ratio, plastic rotation capacity has been observed increasing which was more in normal strength concrete than high concrete strength. Also, with increase in shear force, decrease in plastic rotation capacity has been verified.

Lopes and Bernardo(2003) studied plastic rotation capacity of high strength RC beams experimentally. The effect of longitudinal tensile reinforcement ratio and strength of concrete on plastic rotation magnitude is analysed. Compressive strength of concrete has varying influence on rotation capacity of high strength beams. The results showed increase in compressive strength of concrete for similar reinforcement ratios shows increase in rotation capacity.

Eligehausen and Langer(1986) calculated rotation capacity of plastic hinges through a mathematical model in RC beams & slabs. The model is presented by taking into consideration shifting of tensile force by shear cracks and concrete between cracks. It was reported that with increasing shear stresses the

rotation capacity decreases. When shear cracks are formed, the rotation capacity is significantly increased because of shifting of the tensile force and the corresponding increase of the plastic hinge length.

Kheyroddin and Naderpour(2007) performed the research work to examine the effect of bending moment distribution and tension steel index on ultimate displacement characteristics of RC beams. Under three different loading conditions, the analytical results with varying amounts of tension reinforcement ratio for 15 simply supported RC beams are presented. Plastic hinge rotation capacity has been observed to be increasing when the loading is revised from concentrated load at centre to three-point loading. Also, plastic hinge rotation capacity is observed to be maximum for uniformly distributed load. It was concluded that influence of type of loading on capacity of plastic rotation of heavily reinforced beams is not as important as compared to lightly ones.

Zhao et al.(2011) built and verified a model including rotational capacity, stress and strain distributions of reinforcement and load-deflection response with experimental data already existing. Plastic hinge length is also investigated after doing parametric studies in terms of member dimensions, reinforcement ratio and material properties of rebar and concrete. It was concluded that numerical results of length of plastic hinge decreases with rise in the value of *fc* and *fy* while plastic hinge length increase as ratio of distance between critical section and contraflexure point to overall depth of beam and effective depth of beam increase.

Zhao et al.(2012) investigated plastic hinge region of reinforced concrete beams from FE numerical results in detail. Examination of concrete crushing zone, curvature localization zone and Rebar yielding zone are done in detail. Numerical results show that plastic hinge length increases with increase in effective depth, d. Among all the parameters, tensile reinforcement ratio ρs, compressive reinforcement ratio ρsc, hardening modulus of steel *Esh*, effective depth of beam *d* and ratio of distance between critical section and point of contraflexure to overall depth of the beam *z/h* are noticed to influence the physical plastic hinge to a great extent. Flexural capacity and length of plastic hinge is also observed getting affected by diameter of reinforcement in tension *db* due to its effect on strength of bond.

Dadi and Agarwal(2015) evaluated the resultant ductility and the specimen's relative post-yield behavior. Cyclic testing and pushover testing of RC beam specimen was done with confinement and without as well. Cyclic loading was evaluated in unconfined as well as confined conditions and specimens of eight beams were assessed under pushover loading. ASCE/SEI 41-06 mentions the non-linear modeling parameter "a" tested beam specimen was even more assessed in accordance with pushover and cyclic test outcomes. One of the major results of the study is that the Non- modelling parameter "a" value attained was smaller as compare to the values attained from the pushover testing which are quite larger. As per the ASCE/SEI 41-06, either under pushover or cyclic test performance of the post yield beam specimens shows that the additional controlling parameters for the flexure

components is based on the type of steel as the characteristics of steel bar is reflected in the beam due to the behavior of plastic hinges.

Ou and Nguyen(2014) did research to find out the influence of steel corrosion on length of plastic hinge *Lp* of RC beams. A nonlinear FE analysis was done and validated with experimental data of corroded RC beams. To examine the effect of corrosion level, compressive strength of concrete, longitudinal tension steel ratio, and shear span on plastic hinge length of RC beams, a parametric review was done. The outcome of the research work showed that plastic hinge length is not firmly dependent on longitudinal tension reinforcement ratio or compressive strength of concrete. However, *Lp* is positively depending on shear span for corroded and uncorroded beams. Furthermore, with increase in corrosion, length of plastic hinge decreases which is also dependent on depletion of flexural-strength hardening ratio effected by corrosion.

Ou and Nguyen (2016) investigated the seismic behaviour of corroded RC beams experimentally. Through electrochemical accelerated corrosion method, corrosion has been induced to steel at many locations in RC beams. The testing of beams was done to examine their seismic performance under cyclic loading after accelerated corrosion. Corrosion was induced to both top, bottom longitudinal steel and also to transverse steel. The outcome showed that failure mode of RC beam changed to flexural tension caused by fracture of tension steel from flexural shear caused by crushing of concrete core as the level of corrosion is increased in tension steel. Corrosion of compression steel, longitudinal tension, and transverse steel had insignificant influence on peak load and yield load. However, corrosion induced in compression steel negatively forced the yield drift during the flexural shear failure mode.

Ou and Chen (2014) assessed the reinforced concrete beam's seismic performance with corrosion where it is induced by cycle loading in transverse steel reinforcement. The transverse reinforcement fulfilled the earthquake design provisions in ACI 318 code whereas the beams were being designed with the spaced steel hoops closely. Without Corrosion only one beam has been used. Six level of corrosion was put through the other sic beams by an electrochemical method in potential plastic hinge region. With the increase in corrosion level, it has been noticed that pitting corrosion increased while performing experiments. At a corrosion mass loss of 35%, hoops were fractured. The beams were able to support a corrosion mass loss of 6% in hoops as indicated by cyclic test results, still maintaining the ductile flexural behavior in the beam. The deformation capacity of the beam was adversely affected by corrosion in hoops, but it did not affect load carrying capacity of RC beams. Due to splitting cracks by corrosion, there is decrease observed in shear strength of cover concrete.

Ou and Nguyen (2016) described Two new axial-shear-bending interaction methods, the improved axial-shear-bending interaction (MASFI) method and its extensions to consider the effect of steel corrosion (MASFI-C) to predict the future Force-displacement behavior of non-corroded and corroded RC beams, respectively. MASFI considers the influence of shear forces on the confinement of concrete

and buckling of longitudinal steel bars, as well as the softening effect of the tensile strain of transverse steel bars on the compression zone of flexural concrete. MASFI-C considers the influence of steel corrosion by applying corrosion constitutive model of concrete, steel and its bond. It was found that MASFI recorded the behavior of uncorroded beams well, and the effect of shear on the confined and bending of longitudinal steel was important to estimate post-peak performance. MASFI-C with the mean value of residual cross-sectional area and average strength of the corroded residual steel bars well captures the initial stiffness and strength performance of corroded reinforced concrete beams before the corroded steel bars break.

2.3 PUSHOVER ANALYSIS

Pushover analysis is desired analysis method for design and most importantly for the aim to do seismic performance assessment as the method is comparatively simple compared to the nonlinear dynamic analysis and consider plastic (post elastic) behavior. Pushover analysis has become the main restoration criterion and the preferred method for evaluating seismic performance of structures because it is simple in concept and calculation. Pushover analysis can track the yielding sequence and failure at the component and structural levels, along with the progression of the overall capacity curve of building.
The following sub-sections provide an explanation to pushover analysis, description, its key elements, uses and analytically performing pushover analysis.

2.3.1 Description of Pushover Analysis

Pushover analysis is an approximate analysis method in which building is exposed to monotonously increasing lateral forces, and the height direction distribution remains unchanged till target displacement is attained. Pushover analysis is explained in the flowchart given below.

Force-controlled or displacement controlled are two procedures to perform Pushover analysis. When gravity loading is known, it is defined as force-controlled pushover method. Pushover analysis is mostly implemented as displacement-controlled. The extent of load which is applied is not familiar in advance is defined as displacement-controlled pushover procedure. Till a defined value of the control displacement is reached, a necessary increase or reduction in capacity of load combination is noticed. Displacement at roof is defined as control displacement when it is acting at the centre of mass of structure.

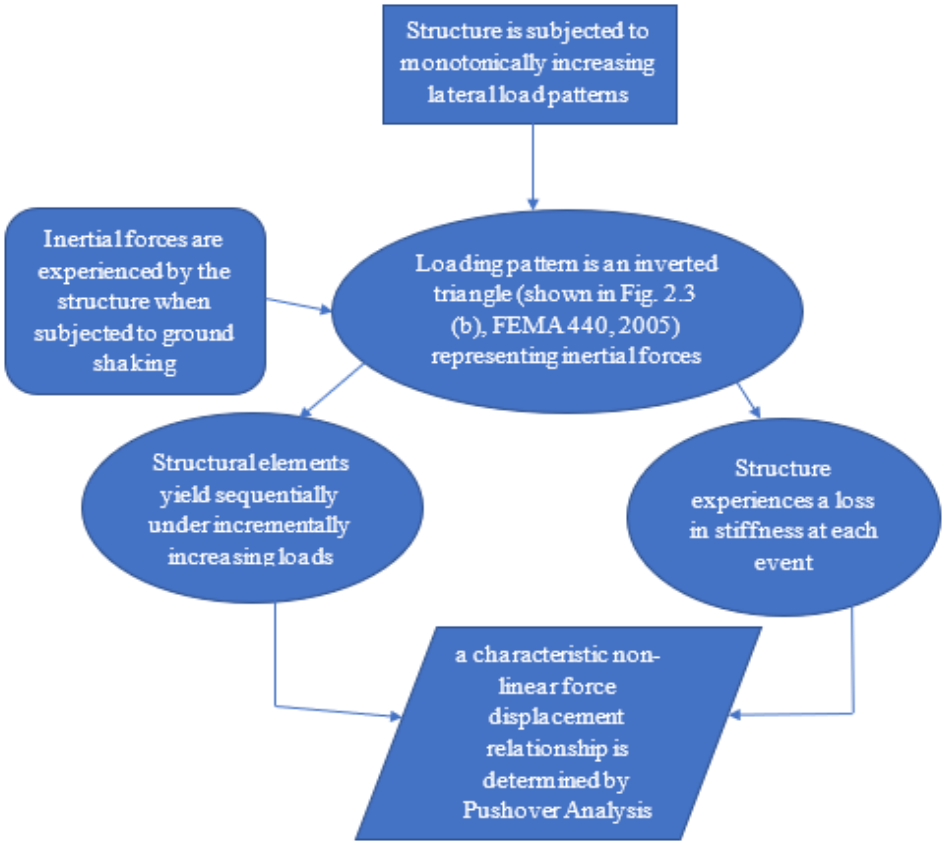

Fig. 2.3 (a) – Flowchart explaining Pushover Analysis

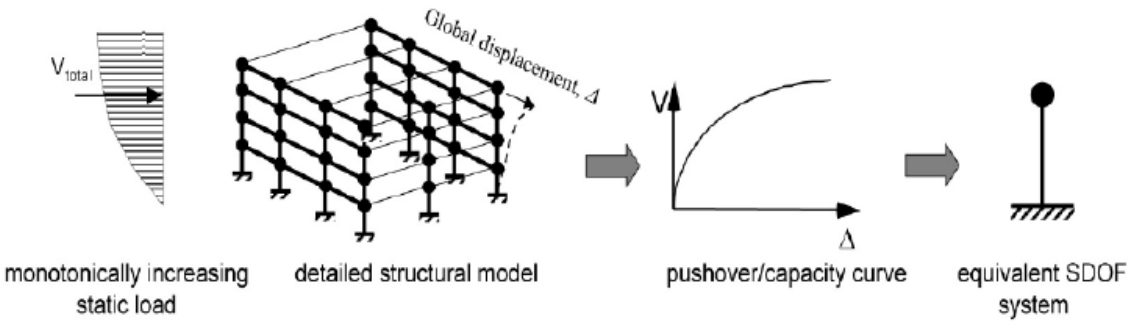

Fig. 2.3 (b) – Schematic diagram showing development of an equivalent SDOF system for a pushover curve (FEMA 440, 2005)

As per definition in Federal Emergency Management Document 356 [6], Pushover analysis is defined as a numerical model explaining the nonlinear load-deformation parameters of all the elements of frame. Elements of structure is exposed to monotonously increasing lateral loads which is depicting inertia forces in an earthquake till target displacement is surpassed. The maximum deformation, which is supposed to be embodied throughout design earthquake, represents target displacement.

In performing the pushover analysis according to FEMA 356 [6], the following table (**Table 2.3**) elaborates the equations used for loading type and target displacement.

Table 2.1- Values for modification factor Co

	Shear Buildings[2]		Other Buildings
Number of Stories	Triangular Load Pattern (1.1, 1.2, 1.3)	Uniform Load Pattern (2.1)	Any Load Pattern
1	1.0	1.0	1.0
2	1.2	1.15	1.2
3	1.2	1.2	1.3
5	1.3	1.2	1.4
10+	1.3	1.2	1.5

1. Linear interpolation shall be used to calculate intermediate values.
2. Buildings in which, for all stories, interstory drift decreases with increasing height.

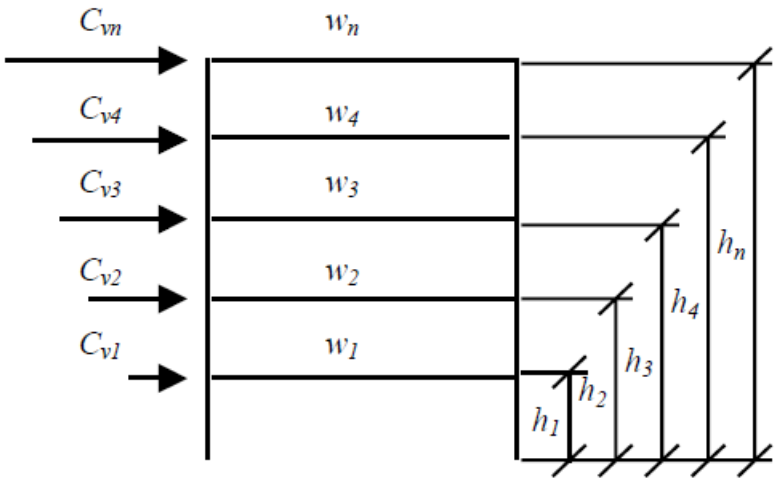

Fig. 2.4 Values for determining the vertical distribution of the lateral loads

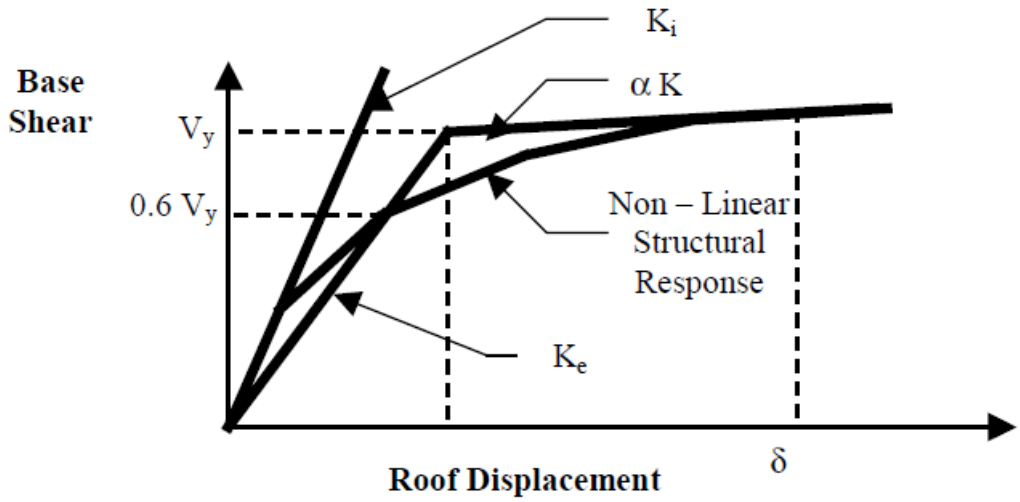

Fig. 2.5. - Bilinear relation of base shear Vs roof displacement plot

Table 2.2-Values for modification factor C2

Loads and Target Displacement	Equations	Components of equation
Gravity Loads	$Q_G = 1.1(Q_D + QL + QS)$	Q_G = Total Gravity force QD = Dead-load (action). QL = Effective live load (action), equal to 25% of the unreduced design live load, but not less than the actual live load. QS = Effective snow load (action) contribution to W
Vertical distribution of the lateral loads	$C_{vx} = \frac{w_x h_x^{\,k}}{\sum_{i=1}^{n} w_i h_i^{\,k}}$	C_{vx} = Vertical distribution factor k = 2.0 for T>2.5 seconds = 1.0 for T< 0.5 seconds Linear interpolation shall be used to calculate values of k for intermediate values of T w_i = Portion of the total building weight W located on or assigned to floor level i w_x = Portion of the total building weight W located on or assigned to floor level x h_i = Height (in ft) from the base to floor level i h_x = Height (in ft) from the base to floor level x
Target Displacement	$\delta_t = C_0 C_1 C_2 C_3 S_a \frac{T_e^{\,2}}{4\pi^2} g$ $C_1 = 1.0$ for $T_e \geq T_o$ $C_1 = [1.0 + (R-1)\, T_0/T_e]/R$ for $T_e < T_0$ $R = \frac{S_a}{V_y / W} \frac{1}{C_0}$	g= acceleration due to gravity, C_0 = modification factor equal to spectral displacement and likely building roof displacement. C_0 values are given in FEMA 356 which is related to the total number of stories of the structure and are shown in **Table 2.1** given below. $C1$ = modification factor which is related with expected maximum inelastic displacements and displacements calculated for linear elastic response. Te is defined as effective fundamental period of the structure. To is the characteristic period of the response spectrum R is the ratio of elastic strength demand to calculated yield strength coefficient Sa is the Response Spectrum Acceleration, in g's, V_y is the yield strength calculated using the results of the Pushover Analysis, where the non – linear force displacement

	$C_3 = 1.0 + \frac{\lvert\alpha\rvert(R-1)^{3/2}}{T_e}$ $T_e = T\sqrt{\frac{K_i}{K_e}}$	curve of the building is characterized by a bilinear relation as shown in **Fig. 2.5**. *W* is the total dead load and anticipated live load *C2* is a modification factor that represents the effect of hysteresis shape on the maximum displacement response of the structure. Values for *C2* are tabulated in FEMA 273 and are a function of Building Performance Level, framing type, and the fundamental period of the structure. They are included in **Table 2.2**. [6] *C3* is a modification factor to represent increased displacements due to dynamic P–Δ effects. For buildings with positive post – yield stiffness, *C3* shall be set equal to 1.0. Te = The effective fundamental period of the structure in the direction under consideration, *T* is the elastic fundamental period of the structure (in seconds) in the direction under consideration calculated by elastic dynamic analysis. *Ki* is the elastic lateral stiffness of the building in the direction under consideration and is found from the initial stiffness of the non – linear base shear vs. roof displacement curve as shown in **Fig. 2.5**. *Ke* is the effective lateral stiffness of the building in the direction under consideration and is defined as the slope of the line which connects the point of intersection of the post – yield stiffness line with the horizontal line at the yield base shear value to zero, while intersecting the original base shear vs. roof displacement curve at 60% of the yield base shear value. *Ki* and *Ke* are shown in **Fig. 2.5**.

Table 2.3 Equations for loading type and target displacement according to FEMA 356

	$T \le 0.1$ second[3]		$T \ge T_S$ second[3]	
Structural Performance Level	**Framing Type 1[1]**	**Framing Type 2[2]**	**Framing Type 1[1]**	**Framing Type 2[2]**
Immediate Occupancy	1.0	1.0	1.0	1.0
Life Safety	1.3	1.0	1.1	1.0
Collapse Prevention	1.5	1.0	1.2	1.0

1. Structures in which more than 30% of the story shear at any level is resisted by any combination of the following components, elements, or frames: ordinary moment-resisting frames, concentrically-braced frames, frames with partially-restrained connections, tension-only braces, unreinforced masonry walls, shear-critical, piers, and spandrels of reinforced concrete or masonry.
2. All frames not assigned to Framing Type 1.
3. Linear interpolation shall be used for intermediate values of *T*.

The force and deformation corresponding to the deformation of the control node of any member equally or exceeding the target displacement will meet the acceptance criteria. Therefore, it is pointed out in FEMA 356 that the expected deformation capacity should not be less than the highest displacement determined at target displacement. Unless explicitly stated in the modeling and analysis, the flexural plastic hinge must not be far from the end of the part.

Pushover analysis is a rationalised non-linear analysis procedure to determine the demands coming on a building through earthquake ground vibrations. Ideally, performance evaluation of a structure should be formed on the basis of non-linear "time history" analysis depending on representative ground vibrations. However, the pushover analysis can identify critical regions of high force and deformation demands and provide reasonable estimates of overall structural behavior and expected damage. At target displacement, internal forces and displacements are determined through pushover analysis which are taken as approximate values of inelastic deformation and strength demands which is to be compared with obtainable capacities of structure for "performance check". The capacity, performance and demand are explained in the form of flowchart in **Fig. 2.6 (a)** given below.

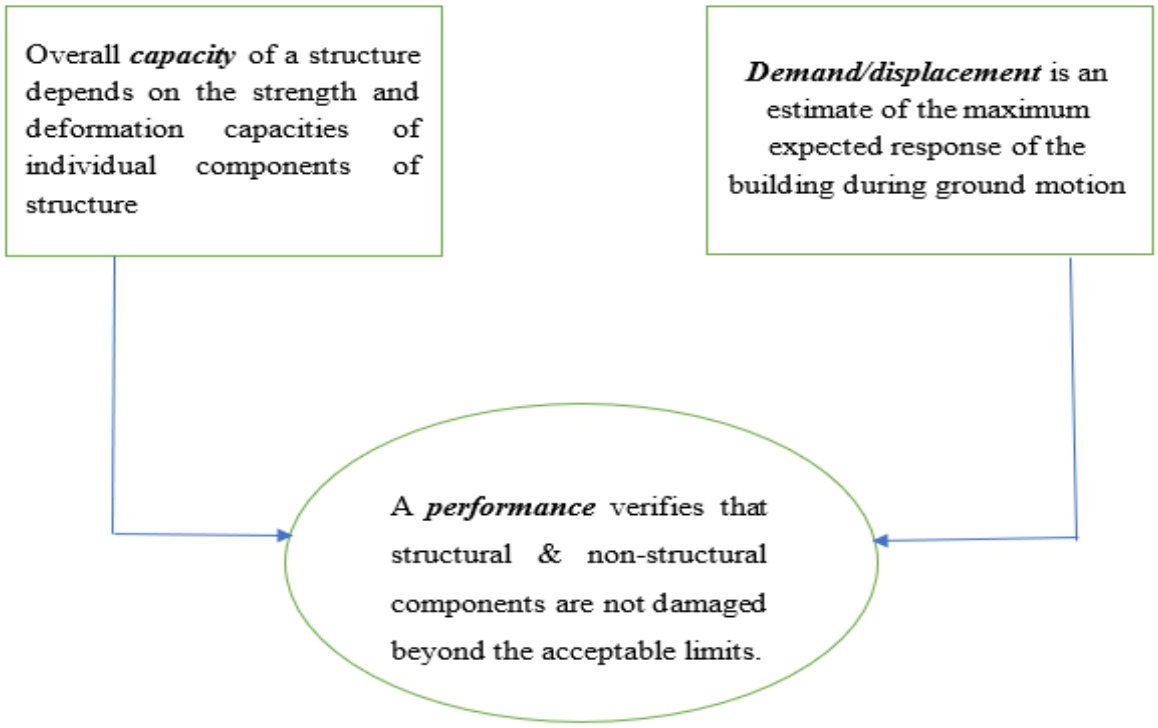

Fig. 2.6 (a) Performance Evaluation of structure in terms of Capacity and Demand

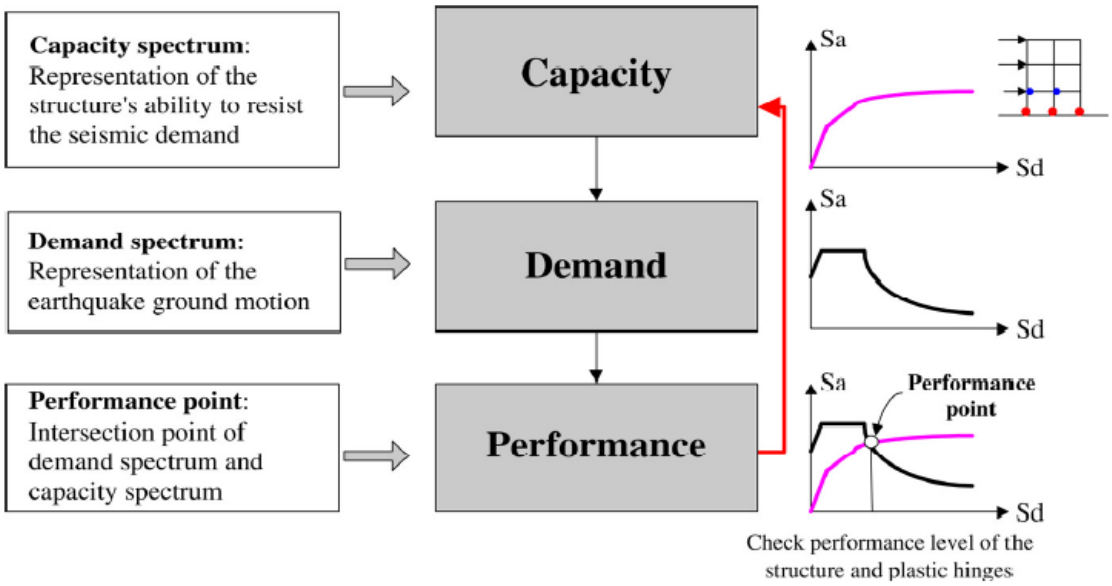

Fig. 2.6 (b) Nonlinear analysis procedure

As presented in the above two figures, **Fig. 2.6 (a) and (b)**, three main elements are determined from nonlinear static procedure: “capacity”, “demand” and “performance”. The first response mode of building is the basis of obtaining capacity spectrum from pushover analysis, presuming that fundamental mode of vibration is dominant reaction of building. Capacity graph acquired after pushover analysis estimates the behaviour of structure past elastic limit for seismic loadings. The demand spectrum curve is usually estimated by using the spectrum reduction method to reduce the standard elastic 5% damping design spectrum. Capacity and demand curves obtained by pushover analysis when intersects at a point is defined as performance point. The response of result of building should be examined for a defined acceptability criterion, checked at performance point (as shown in **Fig. 2.6 (b))**.

2.3.2 Key Elements of the Pushover Analysis and its significance

The distinctive information which is provided by pushover, cannot be extricated through either elastic static or dynamic analysis [Habibullah, A. and Pyle (1998), Krawinkler, H. and Seneviratna (1998)]:

• The practical force demands for capable elements which are brittle.
• Deformation demand approximation on inelastic elements which are deformed for dissipating energy.
• Decrease in strength of components which will influence the overall stability of structure.
• Finding the critical places with significant inelastic predicted deformations.
• Finding the strength irregularities in elevation or plan.
• Interstorey drift approximation which is responsible for break in stiffness or strength.

• Considering non-structural and structural components of frame by confirming the suitability of load path

• Component's yielding order and formation of hinge along with progression of capacity curve of building.

Usually, in the push-over procedure, the structure will be loaded with a predetermined or adaptive "lateral load pattern" and statically pushed into the "target displacement". Lateral load can be stated as a "force" or "displacement" and draw a "capacity curve". The load is monotonic, affected by cyclic behavior and load reversal, and has a damping approximation. As the load increases, weak links and failure modes of the structure are found [Habibullah, A. and Pyle(1998)]. The fundamental components of pushover analysis are: [M. Seifi et al.,(2008)].

Lateral load pattern: For performance evaluation, the choice of load mode may be more critical than the accurate determination of the target displacement. Since it should deform building in similar manner to when an earthquake occurs, it plays an important role. Conventionally, inverted triangles or uniform shapes are used to conform to the coded static lateral force distribution, but the use of adaptive load shapes is increasing. When the response is not controlled by a single mode, the importance of the loading shape increases

Target displacement: The target displacement estimates the expected overall displacement caused by the design earthquake corresponding to the selected performance level. The roof displacement at center of mass of building is an appropriate definition of target displacement. It can be calculated by considering any process in which the nonlinear response affects the displacement amplitude.

Applied forces vs. applied displacements: Essentially and due to historical developments in the understanding of structural dynamics, current seismic design is based on force rather than displacement. Although today's design procedures have become more rigorous in their applications, this basic force-based approach has not changed much since its introduction in the early 1900s. On the other hand, structural displacement is the main cause of damage in structures subjected to earthquakes. Simple techniques for estimating structural displacement can clearly develop design methods based on expected displacements. Therefore, displacement-based methods are considered effective structural design and control methods.

Capacity Curve: The overall force-displacement characteristic of the structure is defined by its capacity curve, which is obtained by plotting the relationship between base shear force *(Vb)* and top displacement of structure during entire pushover analysis. Capacity Spectroscopy (CSM) is a method that allows graphical comparisons between structural bearing capacity and seismic demand. The lateral resistance of structure is presented by force-deformation behaviour acquired by pushover analysis. Also, called push-down curve. According to FEMA-356, non-linear behaviour is expected to occur in frame structure components of centralized plastic hinges. The primary result of pushover analysis is the relationship

between response demand and capacity. The structure has good impendence, if convergence point between demand and capacity curve is near to the elastic range (as shown in **Fig. 2.7**). If the meeting of demand and capacity curve is at a point when the strength and deformability are hardly preserved, then it can be concluded that building will perform poorly when subjected to earthquake excitation.

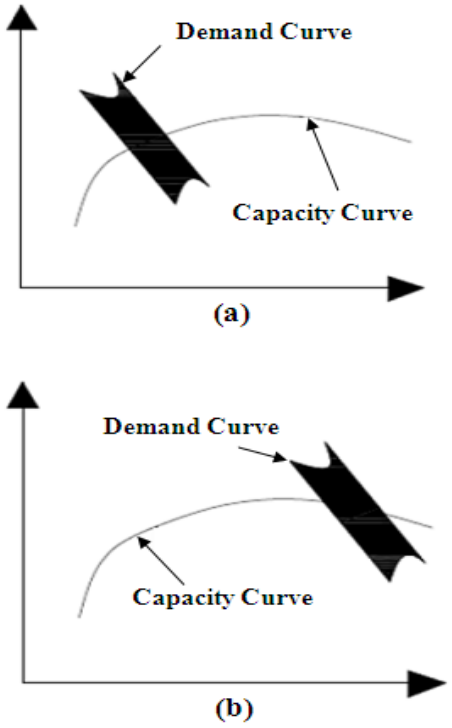

Fig. 2.7. Typical seismic demand Vs. Capacity (a) Safe Design (b) Unsafe Design

Pushover analysis shows the design problems which may be invisible in elastic analysis. These are the excessive deformation requirements, story mechanism, overload on potentially brittle components and uneven strength. The actual strength of the building can be well approximated by pushover analysis. Non-linear static analysis can better understand structure, and can more accurately evaluate the earthquake of the building, because the destruction and destruction process can be tracked. The Pushover curve generated by Pushover analysis is composed of capacity range, demand range and performance points. Maximum base shear capacity and performance level of building components are well shown by pushover.

2.3.3 Pushover Analysis- Analytically

The capacity curve of pushover analysis is the basis of detailed seismic assessment methods. Many commercial programs, such as ETABS and SAP2000, can perform nonlinear static analysis, also defined as Pushover analysis. Documents like FEMA-456 have formed a modeling program, acceptance criteria

and analysis program for the same. FEMA-456 and other documents define standards of force-deformation relationship for hinges assigned in pushover analysis as shown in **Fig. 2.8** below.

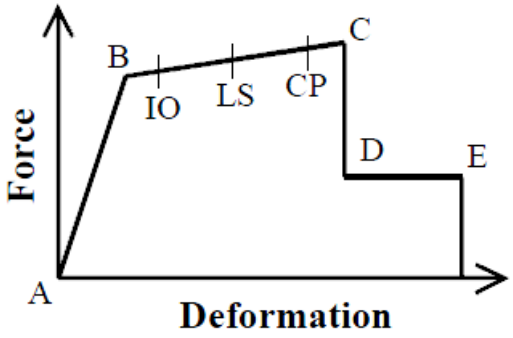

Fig. 2.8. Force-Deformation for pushover hinge

The value assigned to each point varies depending on member type and many other parameters as per definition given in FEMA document. The steps of pushover analysis are given below:

1 The fundamental two- or three-dimensional model is created in the software.

2 The properties and acceptance criteria for pushover hinges are stated (for e.g. in SAP it includes "default-hinge properties" based on the tables of FEMA-273 and "user-defined" too which has to be given by the user).

3 The nonlinear response of the structure is limited to the nonlinear hinges allocated on the structural elements of the structure. Shear hinges, axial hinges and moment hinges are the types of non-linear hinges. Then assign the hinges to the beams and columns of the structure.

4 Lateral load or pushover load including gravity load and monotonously increasing transverse load shall be given. The lateral load is applied to building corresponding to inertial force distribution.

5 Check the force-displacement curve or pushing curve, and then check the number. It is also necessary to check the number of hinges developed in each state, as if to strengthen a component, which can also be done immediately by changing the component properties and again running the analysis.

The hinge properties are defined by research papers or experimental data. The types of output available at every pushover step are frame's 'member properties', 'hinge forces', 'displacement' etc. which can be reviewed.

2.3.4 Review of Pushover analysis for RC frame with non-corroded and corroded bars

Hsiaoet al. (2006) performed seismic assessment method through nonlinear program (ETABS) for Reinforced Concrete school structure with pushover analysis. The verification of this seismic assessment is done with the help of experiment data after in-situ tests are performed by NCREE in Taiwan. For analytical results, moment hinges are allocated to each end of beam or column, shear hinge as well in the

centre of beam or column to represent failure in shear. And, for performing experimental pushover test, the research team used an old school building of Kouhu elementary school, Yunlin, which is about to be demolished as the case study of pushover test. The structure was tested by applying static lateral load and pushed to total collapse. Comparison proves that analytical model represents well prediction before pushover curve is decurved. The maximum base shear value from experiment and analysis is approximately near. The mismatching of unloading area of the pushover curve has been put as agenda for future research by authors.

Tu et al. (2006) carried out 4 in-site "push-over" testing of school structures by using pushover analysis to study effects of different retrofitting measures and to verify seismic assessment methods. 6 hydraulic actuators were placed at the top of all floors of each specimen to provide lateral loading along the longitudinal direction. A seismic assessment method is introduced and the comparison between analytical method and test result is done.

Several common failure patterns were found in the pictures of the 4 specimens when they were severe damaged. Since school buildings usually have identical plan in every floor and usually the 1st floor carries the largest lateral load, it's expectable that most damage and deformation happened in 1F of all the specimens. However, although two of the specimens has vertical members retrofitted by wing walls, the strong-beam-weak-column effect still showed in every specimen. The beams and slabs remained almost non-damaged even when the columns and wing walls failed and the specimens nearly collapse. The "X" marks represent the analytical collapse point, which is defined by appearance of shear failure of any vertical member or the strength decreasing to be less than 80% of the maximum strength. Some modifications were made during the analysis. Since the RC wing walls have higher height to width ratio, they were modeled as columns but not walls. Then the columns beside brick wing walls were considered only fail by shear so the analysis could be corresponding to real structural behavior.

Lee & Kang (2000) verified the association amongst analytical & experimental responses of a high-rise RC structure with non-seismic details. The design of structure is done as per current Korean seismic code on a 1:12 scale as a plane frame mode. The reversed lateral load & monotonic pushover test upto the maximum capacity of the used displacement transducer at roof were performed quasi-statically under the displacement control. Lateral force distribution is taken as inverse triangle (whiffle tree) to simulate earthquake effect. From the tests, lateral force, storey displacements & local rotations were measured by using transducers installed on the reference frame. The whiffle tree was constructed to pull the specimen & lateral force distribution was main-framed. The load cell on the whiffle tree was set up in the mid height of the first storey column to calculate shear force at each column. The analytical modeling of the same frame was done by DRAIN-2DX, analysis was done by using plastic hinge beam-column element. The ultimate strength of the whole structure and the vertical distribution of story drifts can be predicted

with high reliability even if there may be some errors in the input information on the section properties. The sequence of distribution and occurrence of plastic hinges are similar to experimental results.

Erdem et al. (2004) examined and compared the 2 types of strengthening techniques experimentally and analytically both of reinforced concrete structures by performing pushover analysis. Two 1/3 scaled, Two- storey, Three-bay test specimens are prepared representing two cases as infill RC wall (S1), and CFRP strengthened hollow clay tile wall (S2). To experimentally evaluate the stiffness and lateral strength of the frames, envelope curves were formed. The plots of response envelop curves of both S1 and S2 with that of bare frame are compared. The stiffness and strength of bare frame is less than both S1 and S2 frames. Also, initial stiffness and strength of specimen S2 is observed close to specimen S1. But, the decrease in strength in Specimen S2 beyond the maximum value was faster and more relevant when compared to S1 Specimen. It is related to the failure of the CFRP anchor dowels in foundation. CFRP sheets were no longer as effective, after failure of CFRP anchor dowels. So, from infill to exterior columns, a large part of lateral loads has been transferred. As a result, there is a drastic decrease observed in lateral load capacity of specimen S2.

Paul and Agarwal (2012) acquired pushover curves experimentally of a 1/4 size Reinforced Concrete frame models without and with infill wall. In order to calibrate nonlinear analysis model of building, steel bracing has been used. The three non-ductile frame models were tested by push-over method under quasi-static conditions, namely bare frame (BF), infill frame (INF) and steel support (SBF) frame. The nonlinear analysis model is further expanded to be used for seismic assessment and repair of a 4-story 2D frame using infill walls and steel bracing. In this case; first, different versions of IS: 456 and IS: 1893 are used to analyse and design the 4-storey 2D RC frame structure. These frames have been re-evaluated, using masonry infill and steel bracing as renovation options, using pushover analysis. It was found that the existing 4-story RC frame structure in the fourth zone of the earthquake, designed and constructed using the old Indian standards, was insufficient to meet the current code specifications. According to IS 1893 in 1970, 1975 and 1984, the maximum basic shear force calculated was lower than 2.40, 2.0 and 1.25 times the basic shear force calculated according to the existing IS: 1893 (Part-I), respectively. The frame model experiment and analytic push-over analysis show that the effective stiffness, yield and ultimate load have increased due to incorporating infill walls, and the above three parameters have also increased due to the addition of steel bracing.

Inel and Ozmen (2006) did research on the differences between default and user defined non-linear properties of component in the outcomes of pushover analysis. There are some programs available based on ATC-40 and FEMA-356 guidelines, to carry out pushover analysis for both user defined or default non-linear hinge properties. Low and medium rise structures are represented through four and seven story building for this research. SAP2000 has been used to perform the analysis. To perform pushover analysis, a 2-D model of each frame is generated in SAP2000. Column and beam elements are modelled

by defining plastic hinges at both their ends with lumped plasticity. Pushover analysis has been performed for five cases, CASE A represents default hinge properties in SAP2000, and four cases of user defined hinge properties by incorporating variabilities in length of plastic hinge and transverse reinforcement spacing. These four cases are: (i) Case B2: *L p* with Eq. proposed by Park and Paulay and transverse reinforcement spacing, *s* = 100 mm; (ii) Case B3: *L p* with Eq. proposed by Priestley et al. and *s* = 100 mm; (iii) Case C3: *s* = 150 mm and *L p* with Eq. proposed by Priestley et al.; and (iv) Case D3: *s* = 200 mm and *L p* with Eq. proposed by Priestley et al. Base shear capacity of all five cases are similar for both different L p and transverse reinforcement spacing, it was observed to be less than 5%. Therefore, it proves that base share capacity does not gets affected by either user defined or default hinge properties. Length of plastic hinge has significant influence on deformation capacity of structures. A variation with respect to 30% in displacement capacities is observed due to plastic hinge length. Hinging pattern comparison of both models, CASE A and CASE B3, evaluated development of plastic hinge at yielding state effectively. But, important differences in hinging patterns are noticed at ultimate position.

Marques and Delgado (2010) aims to go through the concentrated plasticity modeling possibility, considering different approaches for the element bars' stiffness-degrading. Majorly, two alternatives nonlinear modeling's are considered: The fibre-based model- examining the plasticity distribution along the components, where material nonlinearities are presented with regard to inelastic deformations and the plastic hinges model, considering the plasticity concentrated in the element's extremities. Two RC frames are analysed to pushover analyses using a fibre-based software (SS) and a plastic-hinges based software (PNL), by an imposing non-adaptive force (Nadapt) or an adaptive displacement (Adapt). Considering a permanent elastic stiffness joint between plastic hinges is importantly dissolved when studying a full structure, in contrast with a single element analysis. Strategy (i) a detailed element scenario or the conventional plastic hinges' modeling with an elastic stiffness joint reveal similar results on both structures, particular when used an adaptive pushover procedure. This aspect permits to conclude that inelasticity is well obtained within plastic hinges' length. An additional issue is referred to the joint element stiffness scheme proposals. Herein, slightly differences are identified in mod4 frame, however in what concerns to mod6 structure it can be seen that strategy (ii) is less accurate, revealing a poor performance because of overestimating the amount of stiffness degradation.

Olteanu et al. (2011) investigated productive answers using pushover analysis to make the plastic hinges formed in beams instead of columns to prevent collapse of building. As weak beam-strong column is used amongst the basic design concepts. In order to determine formation of plastic hinge, stress influence in steel and crack development in concrete, a 3-D ground storey structure was examined in this study. Different experiments were performed varying the steel and slab geometry. Computer program ATENA was used with finite element for stress analysis. An RC frame structure in 3D was

taken with 3m height of level and openings of 6m in both directions. At the roof of building, a steel plate was established for application of horizontal loading. Analyses and comparison of four cases of frame structure were done, (i) Frame without slab, (ii) with slab of 15 cm thickness (iii) with slab of 15 cm thickness and material replacement in corner (iv) with slab of 15 cm thickness and joints in corner. The first case of frame without slab is the majorly effective at horizontal load of 1000kN after the analysis is done. Also, plastic hinges in case (i) is formed in beams first as per the basic design concepts. The effect of slab is to redirect formation of plastic hinges in columns.

Poluraju& Rao (2011) did the performance evaluation by means of non-linear pushover analysis using SAP200 under expected earthquakes in the future of the framed buildings. Analysed a G+3 building. This research shows that a well-designed frame performs good under seismic loads. As per the ISI1893:2002, pushover analysis is done for design of the RC frames. Once beams and columns go through the elastic actions, the pushover curve of the G+3 building starts to deviate from linearity. The curve comes back to its linear state when the building is forced to go back to its inelastic range. Estimated results can be occupied for the curve by a bilinear relationship. The journey of the plastic hinge begins with the lower stories of the beam ends and base columns moving on to the upper stories where the interior intermediate columns are continued in upper stories. The amount of damage is limited in the building as the yielding only occurs in B, IO and LS.

Kadid and Boumrkik (2008) performed pushover analysis using SAP2000 to examine framed buildings performance in the expected future earthquakes. Here, the analysis is done for three framed buildings with the use of 5,8 and 12 stories respectively. PMM and M3 hinges for columns and beams respectively are recommended by SAP2000 and gives default hinge properties which is explained in FEMA-356. The features are same as the mentioned three capacity curves. When the beams and columns go through the inelastic actions, they begin to deviate from the linearity. When forced to go to the previous state which is inelastic range, curves were seen linear again with less slope. Capacity curve pattern is same for the three buildings. The yielding is continued in upper stories of interior intermediate columns followed by the plastic hinge formation in the lower stories along with the beam ends and columns that moves to the upper stories. The damage occurred in the three buildings as mentioned is limited because the yielding occurred in B, IO and LS events respectively.

Shuraim and Charif (2007) concluded that the nonlinear static analysis program (Pushover) given by ATC-40 is used to evaluate existing design of the new RC structure to test its applicability. The potential structural defects of the structure under moderate earthquake loads are estimated through the seismic design code and the pushover method. The design is assessed by redesigning under a selected seismic combination to show which components require additional steel bar in the first method. The results show that most of the columns require a lot of additional reinforcement, indicating their pregnable nature to seismic forces. However, the nonlinear pushover procedure indicates that the frame can withstand

assumed seismic forces and has a certain yield on all beams and one column. The location of vulnerabilities in the two methods is significantly different. This article discusses the reasons behind the apparent difference, which is mainly because the default assumptions of the software implementation method are related to the code assumptions about the reduction factor and the maximum allowable limit. In the new building design, the code always maintains certain safety factors, these factors come from load factors, material reduction factors, and ignore some characteristics after yielding. The reduction factor is assumed as1, and to consider hardening, in modeling assumption of ATC-40.

Goel and Chopra (2001) derived an improved "Direct Displacement-Based Design Procedure" for Performance-Based seismic design of structures. Direct displacement-based design requires a simpler step by step procedure to predict the seismic deformation of an inelastic SDOF system, related to the first i.e. elastic mode of vibration of the structure. This step is usually achieved by performing analysis on an "equivalent" linear system with the help of elastic design spectra. In this study, the developed procedure was based on the concepts of inelastic design spectra. This process provides: (1) relatively accurate values of displacement and ductility demands, and (2) design of structure satisfying the required design criteria for allowable plastic rotation. In contrast, the existing procedure involving elastic design spectra is shown to underestimate considerably the displacement and ductility demands.

Lopez-Lopez et al. (2016) studied the effect of different plastic hinge models on nonlinear behavior of reinforced concrete structures. In order to achieve the same purpose, considering the following plastic hinge models, several nonlinear analyses were performed using software SAP2000: (i) FEMA-356 model included in SAP2000, and (ii) the other two developed by some researchers through experience by taking the expression of the model calibration with different experimental data. The conclusion shows that plastic hinges modeled by empirical expressions can be used by structural engineers to more accurately model the behavior of structural elements in ordinary RC structures located in earthquake areas, and to compare with the results provided by the model included in the seismic building design code.

Krishna and Sengupta (2017) introduced a comprehensive summary of research on the seismic vulnerability of corroded reinforced concrete buildings, so that the substantive findings of the research will be useful for researchers and practical engineers in the future in this field. The conclusion is that chloride ion, oxygen penetration, insufficient coverage, carbonation, etc. are the potential causes of corrosion in the reinforcement of RC buildings. Although, the degree of damage due to steel corrosion depends only on the corrosion rate, the amount of corrosion, the location of corrosion, the corrosion of longitudinal or sheared steel bars, the loss of cross-sectional area of steel bars, etc. Therefore, corroded RC structure will exhibit insufficient seismic resistance when subjected to strong ground motion, which will eventually lead to full or partial collapse.

Presti et al. (2018) proposed an analysis and research on the residual structural bearing capacity of the corroded steel RC frame due to reduction of the strength and the reduction of cross-section of steel bar, which considers layout and details of steel bar. This work shows how the degree of corrosion affects the pushover response of the RC frame, and an in-depth analysis of the numerical results. Numerical analysis was performed to evaluate bending moment-curvature of RC sections under corrosion. The analysis proves that corrosion reduces ductility and ultimate strength. Ultimately, the nonlinear response of planar RC frame as part of actual structure was assessed. The distribution of plastic hinges is almost same as uncorroded condition. In contrast, the influence of corrosion on overall performance of RC frames leads to a decrease in ductility and strength, which confirms need for further research on this issue in order to propose a more accurate prediction model.

Pandit et al. (2011) studied behaviour of RC structure due to rebar corrosion analytically. A Pushover analyses present in Structure Analysis Program (SAP)-2000 is used for the analysis. The Pushover tool is nonlinear static analysis tool and is very sensitive to strength of steel. The analysis is done on the bare frame when exterior beams and columns are corroded. From the results it is seen that there will be decrease in load capacity and also ductility of structure of all tests taken into consideration. Also, ductile to brittle type shift in failure pattern is seen for some of the cases. From the results it is concluded that the corrosion is an essential phenomenon need to be incorporated analytically in design of buildings.

Saetta et al. (2008) investigated the preliminary results concerning influence of corrosion of reinforcement showing seismic behaviour of Reinforced Concrete structures. Analysis of some of the case studies for moderate attack of corrosion and the results of same are shown with regard to capacity curves along with comparing to the European Code provisions. The comparison between the obtained results and the European Code provisions suggests the opportunity to modify the code expression of the rotation capacity accounting for the effects of corrosion attacks. Further research is necessary for a more accurate calibration of the moment-rotation relationships of corroded hinges in order to account for cover cracking and rebars slippage, which may occur in case of particularly aggressive attack.

Yuksel and Coskan (2013) researched on the earthquake performance of RC frames exposed to rebar corrosion. A typical two-bay, four-story reinforced concrete (RC) frame is designed. Two different rebar corrosion scenarios and a design spectrum are selected. The deteriorated condition in these scenarios are included which are changes in mechanical properties of steel bars, loss in diameter of rebar, bond strength and changes in damage limits of concrete sections. The RC frame is evaluated using a nonlinear static analysis method in sound condition as well as deteriorated conditions. The rebar corrosion effect on the global level is investigated by comparing the responses of each scenario with respect to response of sound condition of frame. The result shows that the progressive deterioration of frames over time can cause serious reductions on load-bearing capacity. Hence overall seismic behaviour of frame is adversely affected.

Yalciner and Marar (2012) evaluated the effects on the time dependent seismic output levels of the corroded RC buildings of default and user-defined hinge properties based on FEMA 356 (FEMA-356, 2000). In order to estimate the building's capacity curve using the normal default and user-defined plastic hinges (t: 25 years and t: 50 years), the supposed corrosion rate has been used. The effects of defective and user specified hinge properties on levels of history have been considered in two, four and seven stories of RC buildings. The tests conducted and the IDA clearly showed that the use of the plastic hinge properties based on ready documents and user-defined harness characteristics had substantial differences. If user understands the program capabilities, where the SAP2000 (CSI, 2008) automatically stops analyzing the curvature of a plastic hinge, ready document plastic hinge characteristics may be applied to the fast and preliminary RC building assessment. However, time-dependent results showed clearly that defined plastic hinge characteristics give better and correct results rather than default hinge characteristics.

Colajanni et al. (2019) analyzed the non-linear behavior of the reinforced concrete framework, by investigating the effect of corrosion damage on the seismic reactions of existing RC buildings. For accurate performance evaluation of multidegree freedom systems, additional studies are also needed. The degradation of strength and decrease of the steel rebar cross-section have been examined and in numerical analyses considered. A number of numerical analysis has been conducted to evaluate RC cross-sectional, corrosive phenomenal bending relations. They show that corrosion dramatically decreases RC cross-section ductility and ultimate strength. Finally, it assessed the nonlinear, static behavior of an existing RC framework that is part of an actual corrosion building. The plastic hinges are distributed in much the same way as the non-corroded case.

In this work, it is proved that the deformation and ductility factors evaluated when designing the building components are much smaller than the deformation and ductility requirements calculated by the nonlinear analysis of the system using the inelastic design spectrum. Also, seismic response of RC structures for different percentages of corrosion needs to be investigated by taking the moment-curvature analysis of RC components of structure.

2.4 CLOSING REMARKS

In this chapter, the procedure as well as fundamentals of plastic hinges and pushover analysis are described in detail. The basics of plastic hinges and Pushover testing techniques are also discussed. Additionally, an extensive literature review was carried out on plastic hinges and Pushover testing techniques for seismic evaluation of RC Structures separately. The review established the efficacy of plastic hinges and pushover testing for seismic evaluation of reinforced concrete structures. But before it can be applied to civil engineering buildings, research is still needed.

CHAPTER 3
EVALUATION OF PLASTIC HINGE PARAMETERS WITH CORRODED REINFORCEMENT

3.1 GENERAL

Due to earthquakes occurring in the world, seismic qualification of old buildings is of major concern. It is crucial to make sure that a seismically efficient structure should behave in a ductile manner and should be capable to take large deformations at maximum load to prevent collapse. Deformation capability in RCC structure is dependent on quality of steel. Since in existing structure, reinforcing steel bars have been corroded to different levels due to environmental effects which questions the deformation capability of existing structures. Further, corroded reinforcements will not allow the structure to behave as ductile moment resisting building during earthquake. A seismically efficient building possesses "strong-column"-"weak-beam" behaviour. "Strong column-weak beam" behaviour ensures maximum plastic hinges to form in beams. Plastic hinges formed are represented by the parameters which include length of plastic hinge (l_p) and plastic hinge rotation capacity. Plastic hinge parameters of old structures depend upon corrosion levels of reinforcing steel bar, its yield strength and concrete strength.

The chapter reports the study of effect of corroded steel bar on plastic hinge parameters of RCC structures. The corrosion of steel bar is done outside individually as well as inside before and after casting the RC beam respectively as a pilot study. The effect of different grade of concrete and different reinforcement bar along with the condition of reinforcement (corroded upto 30% level), when corroded outside before casting the RC beam for the development of plastic hinge have been reported.

3.2 EXPERIMENTAL INVESTIGATION AND METHODOLOGY

3.2.1 Reinforced Concrete (RC) Beam Design

Sixteen different types of RC beams are tested with the variation of concrete grade and reinforcement bar. RC beams are designated by two different concrete mix design, M1, M2 (details of same are given in **Table 3.2**). Also, RC beams are represented by two types of reinforcement used with different yield strength, R1, R2 (details of the same are given in **Table 3.5**). The two types of reinforcements were corroded at different percentages (10%, 20%, 30%) to represent existing old structures. The method of inducing corrosion to the bars is explained in next section. **Table 3.1** gives the details of sixteen types of RC beams used in the study. For each type, three samples have been casted and tested. Average test results of three samples have been used as final test result. Therefore, in total forty-eight beams have been tested which measured 1.5 metres in length with an effective span length of 1.3m. RC beam with a cross-section of 230 × 300mm is used. All RC beams have been provided with four bars of longitudinal

reinforcement for tension as well as compression (2 bars of 12mm at top and bottom respectively) with the concrete cover of 25mm. Shear reinforcement of 8mm diameter (diameter is represented by *Y* in **Fig. 3.1a**) bars spaced at 200mm centre to centre are provided. The geometry and details of the test specimen along with two-point loading arrangement is shown in **Fig. 3.1(a)** and **Fig. 3.1(b)** respectively. RC beams are simply supported with four-point loading to ensure flexure behaviour (as shown in **Fig. 3.1** (a) and (b)). The RC beam has been designed to fail in flexure.

Table 3.1 Details of beams used in the study

Beam No.	RC beam	Concrete Grade	Reinforcement Bar
A	M1 R1	M1	R1
B	M1 R1 C10	M1	R1C10 (Corroded at 10%)
C	M1 R1 C20	M1	R1C20 (Corroded at 20%)
D	M1 R1 C30	M1	R1C30 (Corroded at 30%)
E	M1 R2	M1	R2
F	M1 R2 C10	M1	R2C10 (Corroded at 10%)
G	M1 R2 C20	M1	R2C20 (Corroded at 20%)
H	M1 R2 C30	M1	R2C30 (Corroded at 30%)
I	M2 R1	M2	R1
J	M2 R1 C10	M2	R1C10 (Corroded at 10%)
K	M2 R1 C20	M2	R1C20 (Corroded at 20%)
L	M2 R1 C30	M2	R1C30 (Corroded at 30%)
M	M2 R2	M2	R2
N	M2 R2 C10	M2	R2C10 (Corroded at 10%)
O	M2 R2 C20	M2	R2C20 (Corroded at 20%)
P	M2 R2 C30	M2	R2C30 (Corroded at 30%)

The load has been applied by a hydraulic jack of capacity 500kN with 250mm displacement capacity. The load has been increased till the failure of the RC beam. LVDT's (Displacement transducers) have been used to measure the vertical displacements as shown in **Fig. 3.1 (b)**. Settlement of supports have not been allowed. Total three LVDT's have been placed equidistant to each other with one placed at centre of span and at quarters of the span. These LVDT's have been connected to data acquisition system for recording deflection and producing load-deflection curves.

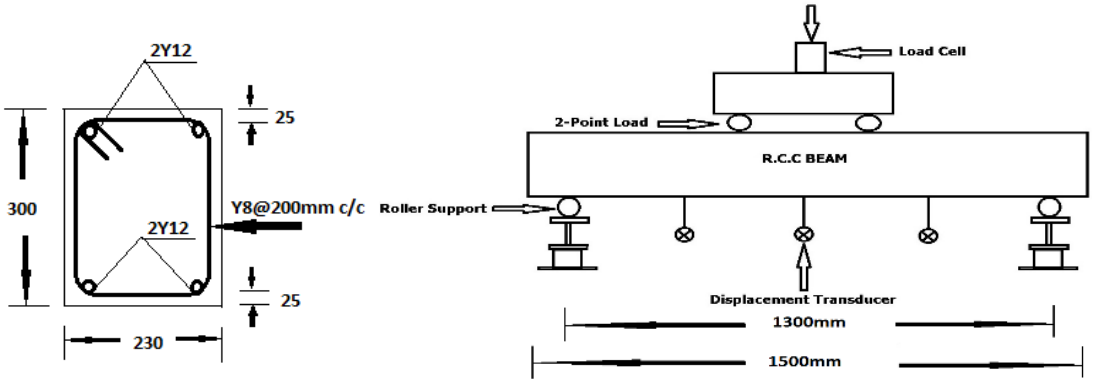

Fig. 3.1(a) Geometry and details of test specimen

Fig. 3.1(b) Two- point loading setup of RC beam

Fig. 3.1 (a) Geometry and Details of test specimen **(b)** Two- point loading setup of RC beam

Two different types of mix of concrete M1 and M2 have been used. The concrete mix design ratio and compressive strength of the concrete at 7, 21 and 28-days are shown in **Table 3.2.**

Table 3.2 Material and Compressive Properties of concrete

Beam No.	Concrete mix	C: FA : CA	7-days compressive strength (MPa)	21-days compressive strength (MPa)	28-days compressive strength (MPa)
1	M1	1: 1.6388 : 3.1244	22.09	23.46	24.96
2	M2	1: 1.11: 2.39	24.495	28.6	30.4

The concrete mix ratio of cement: fine aggregate: coarse aggregate (C: F.A: C.A) of M1 and M2 grade have been taken as 1: 1.6388: 3.1244 with water-cement ratio= 0.5 and 1: 1.11: 2.39 with water-cement ratio= 0.46.

Two types of reinforcement bars R1, R2 are used along with the condition of reinforcement bars (Corroded at 10%, 20%, 30%). Corrosion of reinforcement bar at 10%, 20% and 30% level are attained by impressed current method. The details of the same has been presented in section 3.2.2.

3.2.2 Accelerated Corrosion in RC Beam (When Reinforcement bar is inside RC Beam)

A pilot study has been done to assess the difference between the load-deflection behaviour of RC beams when bars are corroded before and after casting. Initially, six RC beams have been corroded using two types of rebars R1, R2 (3 RC beams for each case). These six beams are corroded to different durations by impressed current corrosion technique for approximately 25, 40 and 60 days.

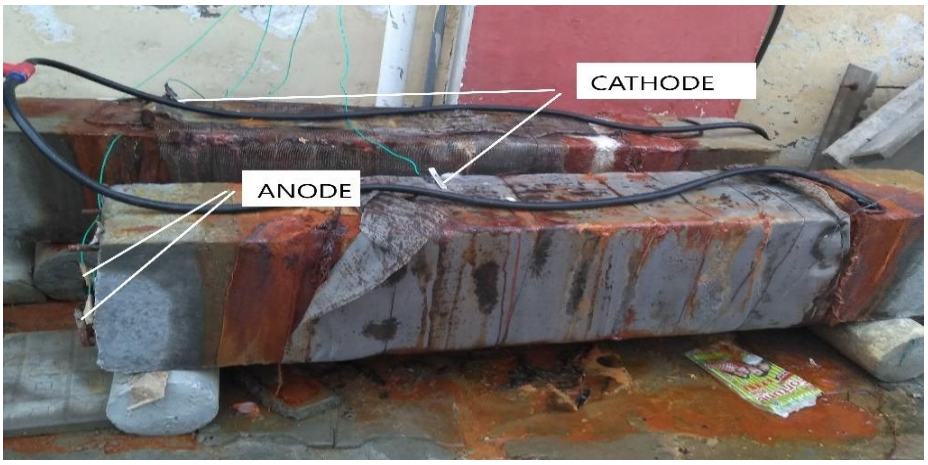

Fig. 3.2. Corrosion of R1, R2 bars inside RC beams by accelerated Anodic Impressed Current corrosion technique

Reinforcement bar is made anode and stainless-steel wire mesh is wrapped on the cotton gauge in the middle 1000mm length of the beam is made cathode. A drip of 3.5% NaCl has been done in middle 1m of wrapped beam with schematic arrangement for accelerated corrosion shown in **Fig. 3.3** below. Corrosion has been induced at 20V using a constant voltage power supply (APLAB make, 64V capacity). Current has been observed varying with increase in corrosion level. The range of corrosion current is between 0 to 2 Amperes. Different corrosion levels have been achieved in approximately more than 25 days which is in accordance to the mass loss observed by Sharma et. al. 2017.

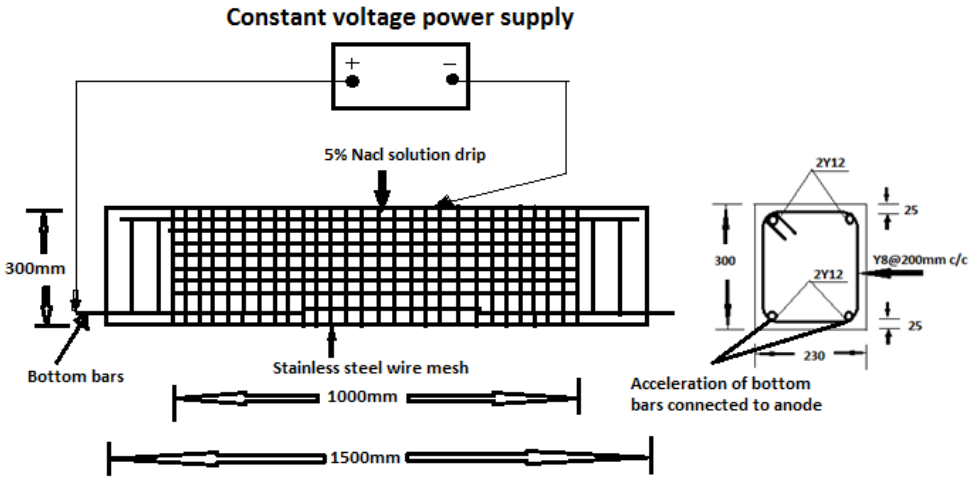

Fig. 3.3. Schematic setup of accelerated corrosion of RC beam

The levels of corrosion achieved are determined by measuring the % mass loss in top, bottom and spiral reinforcement after extracting them from the corroded beams. **Table 3.3** shows the corrosion levels achieved in different bars. Stirrups of 8mm diameter are corroded only upto 8%, whereas bottom bars are corroded upto 20% when corroded for 50 days.

Table 3.3. Corrosion levels achieved in different bars corroded inside RC beam

Steel bar	Steel bar, R1			Steel bar, R2		
	Initial Mass (kg)	Final Mass (kg)	Corrosion level (%)	Initial Mass (kg)	Final mass (kg)	Corrosion Level (%)
Bottom bars	1.34	1.20	10.45%	1.268	1.132	10.73%
	1.334	1.061	20.46%	1.268	1.008	20.50%
Top Bars	1.331	1.285	3.46%	1.264	1.205	4.74%
	1.337	1.144	14.44%	1.265	1.080	14.62%
Stirrups	0.572	0.530	7.4%	0.536	0.494	7.835%
	0.573	0.529	7.6%	0.539	0.530	7.37%

3.2.3 Inducing Accelerated Corrosion in Reinforcement Bar (Outside before casting RC beam)

Corrosion process takes many years to take place in natural environments. Salt spray, chloride diffusion, alternate drying and wetting in salt water, and application of anode current are various methods in the literature that can be used to induce accelerated corrosion. However, impressed anodic current technique is the fastest method used for inducing corrosion. Corrosion is induced in the reinforcement bars separately (R1, R2) at 10%, 20% and 30% level in which 3.5% NaCl is added to 1 litres of water (Simulation of marine conditions). Reinforcement bar is made anode and stainless-steel wire mesh is made cathode with the electrolyte as (3.5% NaCl + water) (Maddawy et al. 2005). Corrosion was induced at 20V using a constant voltage power supply (Aplab make, 64V capacity). The reinforcement bars are constantly soaked in the electrochemical solution throughout its length for accelerated corrosion. The required reduction of the mass of the individual reinforcement bar took more than 30 days. The accelerated corrosion setup of individual reinforcement is shown in **Fig. 3.4**. Intitially, six beams have been casted after inducing corrosion in reinforcement individually.

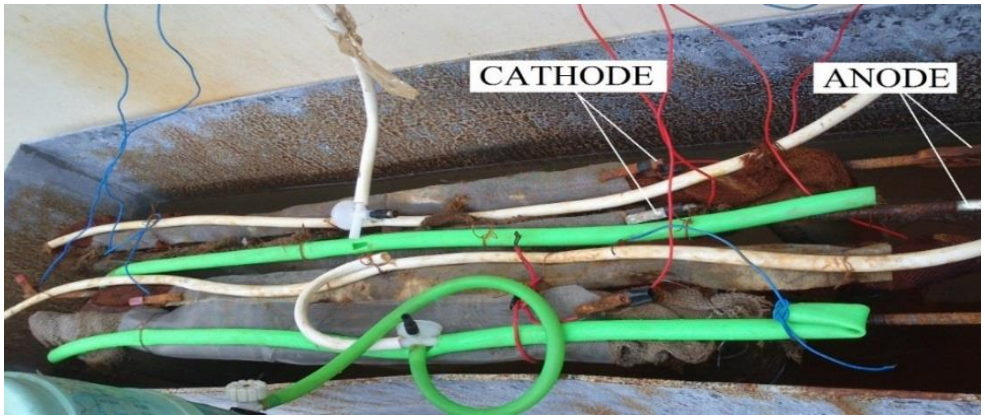

Fig. 3.4. Corrosion of R1 and R2 Bars Individually by Impressed Current method

Mass of reinforcing bar is noted before and after the corrosion. Before and after applying corrosion, clean the bar with 5% nitric acid solution to remove scale and rust products and then weighed (Hou et al.). **Table 3.4** shows the percentage of corrosion of steel bars corroded outside before casting the beam.

TABLE 3.4 Calculation of % corrosion of longitudinal, Stirrups (R1, R2) Steel bar before casting Beam

Steel Bar	**Initial Mass (kg)**	**Final Mass (kg)**	**10% corrosion C10**	**Initial mass (kg)**	**Final Mass (kg)**	**20% corrosion C20**	**Initial mass (kg)**	**Final Mass (kg)**	**30% corrosion C30**
R1	1.329	1.190	10.52%	1.330	1.0549	20.74%	1.332	0.929	30.28%
R1 (Stirrup)	0.5719	0.514	10.04%	0.571	0.456	20.16%	0.573	0.401	30.01%
R2	1.26	1.133	10.08%	1.261	1.007	20.14%	1.261	0.88	30.21%
R2 (Stirrup)	0.539	0.483	10.05%	0.537	0.429	20.07%	0.537	0.376	30.05%

3.2.4 Comparison of load -deflection behaviour of RC beams when corrosion is induced in Reinforcement Outside and Inside the beam

The load deflection curve from the **Fig. 3.5** below shows that there is not much difference in load carrying capacity of RC beam when reinforcement is corroded outside the beam to corrosion induced inside.

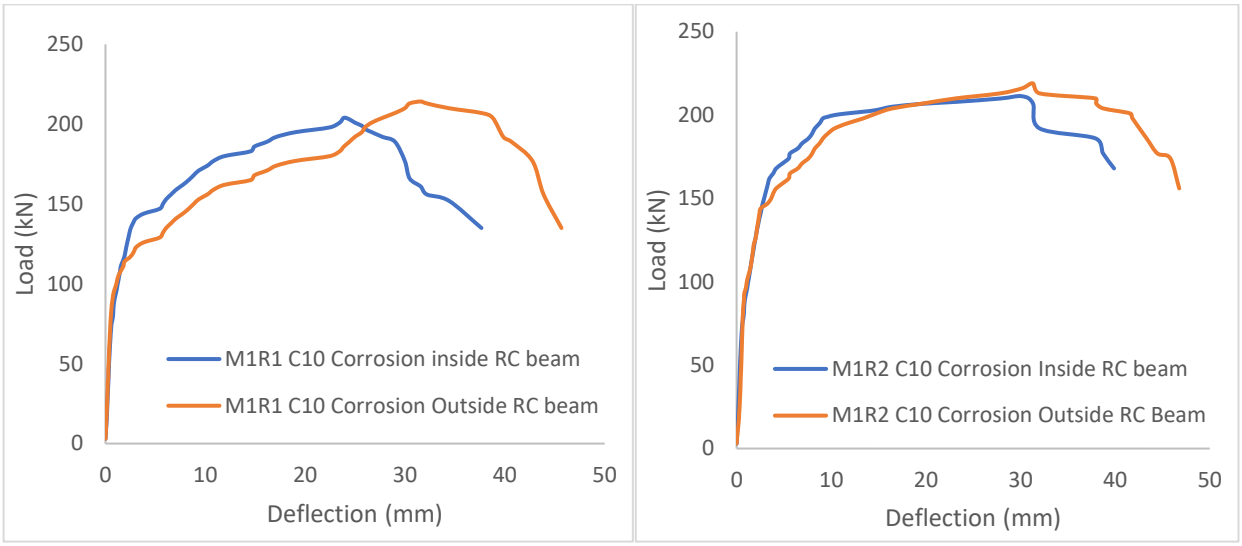

Fig. 3.5. Comparison of Load-deflection curve of RC beams when corrosion is induced individually outside and inside RC beam with R1 and R2 bars (10% corroded bars)

However, 10% to 15% less deformation capacity has been observed in RC beam when corrosion is induced inside the RC beam due to bond behaviour between steel and concrete. The bond behaviour between the reinforcement and surrounded concrete is not same as in case of actual or field conditions. It can be observed that load-deflection behaviour of RC beam when corrosion is induced in reinforcement inside the RC beam is close to the behaviour when corrosion is induced to the reinforcement individually before casting.

Therefore, the work has been extended towards the evaluation of plastic hinge parameters in section below by adopting the corrosion to be induced individually to reinforcement before casting. The % corrosion loss and tensile properties of reinforcement bars when corroded outside before casting RC beam and experimental results of all sixteen RC beams obtained from load-deflection graphs are presented in the section below.

3.2.5 Accelerated corrosion in Reinforcement Bar Individually for Evaluation of Plastic hinge parameters

Percentage of corrosion of longitudinal bars (compression and tension) and stirrups of both the types of reinforcement bars R1 and R2 at 10%, 20% and 30% level are given below in **Table 3.5** and **Table 3.6**. Steel bars are corroded before casting to ensure the degree of corrosion and it does not induce immediate cracking in concrete due to the lateral confinement that exists around steel bar (Ouglova et al. 2004). The bond behaviour between the reinforcement and surrounded concrete is not same as in case of actual or field conditions. This is one of the limitations of the lab study on the corroded reinforcement. It is very difficult to corrode the reinforcement after casting the specimens with in a fixed time frame by artificial mechanism as shown in section 2.3.2. The adherence or bond is affected at higher levels of

stirrup corrosion and the transference of the diagonal tension forces is disturbed resulting in accumulating the shear stress at the interference of stirrup and the concrete (Juarez et al. 2011). Increasing the corrosion level within a certain range will limit the bond deterioration. After several months of exposure to the chloride environment, the broken beam failed due to the rupture of a tensile rod (Valente. 2012). Corrosion caused the steel to be more brittle during tension. Corroded tensile bar is observed failing after several months of corrosion rather than concrete-steel bond failure. Therefore, spalling stresses generated in the concrete are neglected.

TABLE 3.5 Calculation of % corrosion of longitudinal (R1, R2) Steel bar before casting Beam

Steel Bar	Initial Mass (kg)	Final Mass (kg)	10% corrosion C10	Initial mass (kg)	Final Mass (kg)	20% corrosion C20	Initial mass (kg)	Final Mass (kg)	30% corrosion C30
R1	1.331	1.191	10.52%	1.331	1.055	20.74%	1.331	0.928	30.28%
R1	1.337	1.203	10.02%	1.334	1.061	20.46%	1.334	0.921	30.96%
R1	1.339	1.205	10.01%	1.333	1.064	20.18%	1.332	0.929	30.26%
R1	1.34	1.2	10.45%	1.332	1.053	20.95%	1.335	0.925	30.71%
R2	1.26	1.133	10.08%	1.261	1.007	20.14%	1.261	0.88	30.21%
R2	1.267	1.129	10.89%	1.264	1.009	20.17%	1.264	0.884	30.06%
R2	1.263	1.131	10.45%	1.269	1.01	20.41%	1.265	0.881	30.36%
R2	1.268	1.137	10.33%	1.268	1.012	20.19%	1.262	0.882	30.11%

TABLE 3.6 Calculation of % corrosion of Stirrups (R1, R2) before casting Beam

Steel Bar	Initial Mass (kg)	Final Mass (kg)	10% corrosion C10	Initial mass (kg)	Final Mass (kg)	20% corrosion C20	Initial mass (kg)	Final Mass (kg)	30% corrosion C30
R1	0.5724	0.515	10.04%	0.572	0.457	20.16%	0.574	0.402	30.01%
R1	0.573	0.515	10.09%	0.577	0.461	20.10%	0.573	0.401	30.05%
R1	0.5768	0.519	10.02%	0.576	0.461	20.01%	0.576	0.403	30.11%
R1	0.578	0.520	10.03%	0.574	0.459	20.03%	0.578	0.404	30.10%
R2	0.5382	0.484	10.05%	0.538	0.430	20.07%	0.538	0.377	30.05%
R2	0.536	0.482	10.07%	0.536	0.428	20.10%	0.536	0.375	30.04%
R2	0.5398	0.485	10.15%	0.539	0.431	20.16%	0.538	0.376	30.11%
R2	0.5342	0.480	10.11%	0.537	0.430	20.04%	0.534	0.373	30.15%

After the reinforcement bars have undergone corrosion, for the desired percentages, loss of metal is observed in a small zone at 10% corrosion level in both types of reinforcement. At 20% corrosion level, loss of metal has spread over a larger area and pitting corrosion at some places is visible at 30% corrosion level with substantial loss of metal. Additionally, loss of cross-section of reinforcement is

discernible at this point. For the corrosion at and beyond 20% level, it is exacerbating the corrosion further.

Fig. 3.6 shows the condition of corroded bars at different levels. Spatial distribution and pitting are represented through the reduction in diameter at various corrosion levels (0%,10%, 20%, 30%) in **Fig. 3.7**. The diameter is measured using digital Vernier caliper and confirmed manually also. Distribution of cross-section loss (in terms of diameter of bar) along the reinforcement bar is spatially non-uniform and cross-section loss of bar significantly increases with the increase in percentage of corrosion. Maximum cross-section loss is observed in steel bar, between 750m-1000mm (near the centre of the rebar) of 1.45m length as shown in **Fig. 3.7**. At initial level of corrosion, loss of metal had been restricted to a small area. With increase in percentage level or days, corrosion has been seen spreading over larger area with traces of pitting and substantial loss of metal in reinforcement bar. At this stage, localised reduction in cross-section of bar is perceptible. Therefore, higher level of corrosion is observed in corroded bars at central portion.

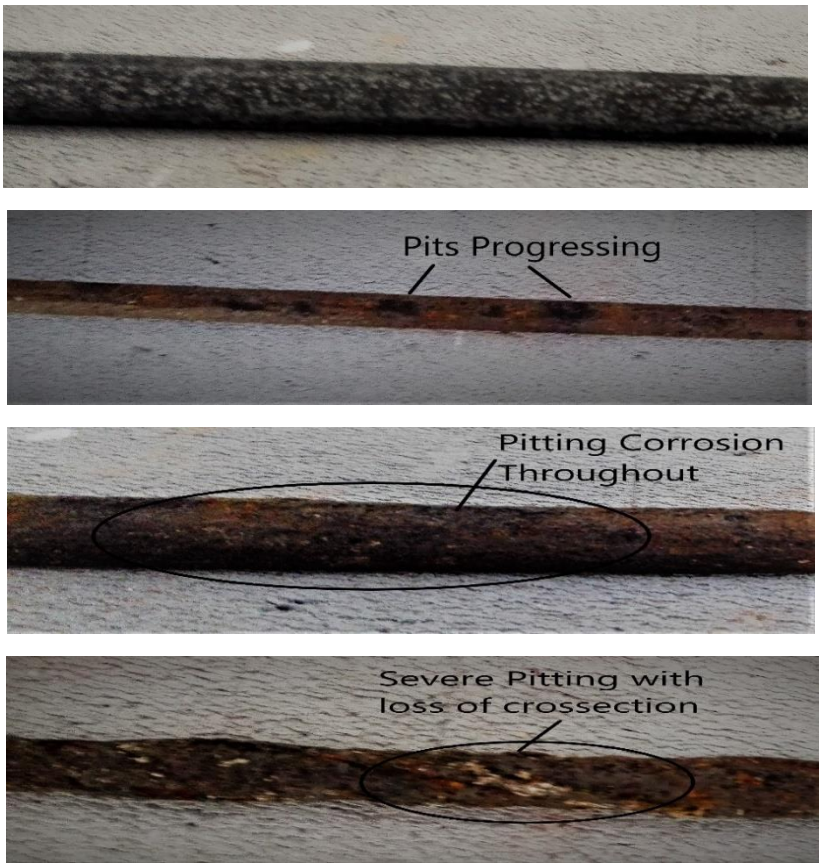

a) 0% corroded bar,R1

b) 10% corroded bar, R1

c) 20% corroded bar, R1

d) 30% corroded bar, R2

Fig. 3.6. Condition of extracted bars at different levels of corrosion

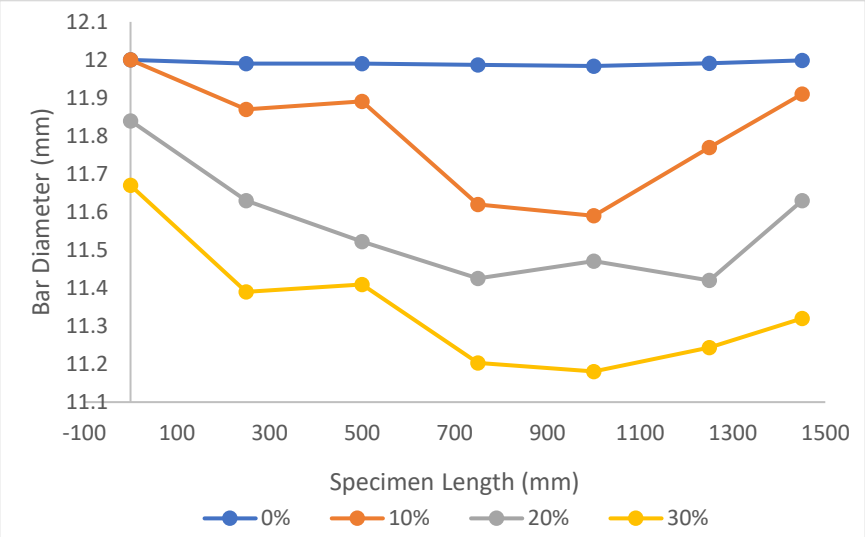

Fig. 3.7. Spatial distribution of bottom bar diameter along the specimen length at different levels of corrosion

3.2.6 Tensile Properties of Reinforcement Bar

After performing tensile tests, the tensile properties comprising of yield strength (*YS*), ratio of ultimate tensile strength and *YS* (*UTS/YS*) and % elongation at ultimate tensile strength are calculated from load-deflection graphs as summarised below in **Table 3.7**. Yield strength of the corroded bars have been observed using the reduced cross-sectional area. Yield strength of bars are observed decreasing when the corrosion percentage is increasing. The specified minimum *UTS/YS* ratio should be minimum 1.25 which helps to impart ductility to structures as given by various researchers (Rai et al. 2012). *UTS/YS* ratio of R1 and R2 (No corrosion) is more than 1.25 which represents high ductility preventing early failure. It is noticed that bars corroded to 10% still have ductility as the *UTS/YS* ratio was close to 1.25 whereas bars corroded to 20% and 30% level is having low ductility as *UTS/YS* ratio is much less than 1.25.

TABLE 3.7 Tensile Properties of Steel bars

Reinforcement Bar	**Yield Strength (MPa)**	**UTS/YS Ratio**	**Max. Load (kN)**	**% Elongation**
R1	369	1.33	67.255	0.297
R1 C10 (10% corroded)	335	1.22	59.605	0.264
R1 C20 (20% corroded)	323	1.2	57.40	0.253
R1 C30 (30% corroded)	300	1.12	44.01	0.195
R2	445	1.31	71.91	0.311
R2 C10 (10% corroded)	425	1.25	60.465	0.267
R2 C20 (20% corroded)	360	1.15	46.78	0.207
R2 C30 (30% corroded)	340	1.14	43.91	0.194

During inelastic deformation low *UTS/YS* ratio in corroded bars have low energy absorption and dissipation capability which is undesirable for seismic qualification of old buildings.

3.3 BEHAVIOUR OF RC BEAM UNDER FLEXURE LOADING

The mode of failure of almost all RC beams after performing the tests by applying four-point bending test have behaved in a flexure manner as designed except in few beams corroded to 30%.

Load Vs Deflection graph is obtained from the data acquisition system till the failure of the beam which is discussed in the next section in detail. The experimental results are obtained from load-deflection graphs, including first flexure crack load, flexure yield load, ultimate load and ultimate crack width, which are presented in **Table 3.8**.

TABLE 3.8 Experimental data of RC beams

Beam No.	**RC Beam**	**First Flexure Crack Load (kN)**	**Flexure Yield Load (kN)**	**Ultimate Load (kN)**	**Ultimate Crack Width (cm)**
A	M1 R1	44	81	214.2	1
B	M1 R1 C10	38	63	204.6	2.1
C	M1 R1 C20	40	51	189	8.3
D	M1 R1 C30	36	45	165	12.2
E	M1 R2	47	75	219	0.7
F	M1 R2 C10	40	72	201	1.9
G	M1 R2 C20	38	57	185.04	7.4
H	M1 R2 C30	37	48	172.2	11
I	M2 R1	52	83	227.55	0.5
J	M2 R1 C10	50	78	204.78	1.4
K	M2 R1 C20	46	75	192.6	6.9
L	M2 R1 C30	47	42	180	8.5
M	M2 R2	60	87	236.28	0.3
N	M2 R2 C10	62	84	219	1.1
O	M2 R2 C20	56	78	207	5.1
P	M2 R2 C30	50	66	195	7.8

Yield load and ultimate load is observed to be reducing with increase in corrosion percentage of reinforcement. Reduced bonding due to corrosion may have less impact on peak loads because partial corrosion occurred in the reinforcement bar at potential plastic hinge regions and bond strength

degradation has also been observed due to repeated cyclic loads (Maddawy et al. 2005, Wang and Liu. 2010, Valente. 2012). It is also reflecting that the yield and ultimate load is increasing with increase in concrete grade and yield strength of reinforcement as well. However, the percentage increase is higher when strength of concrete grade is increased.

Fig. 3.8 shows the failure patterns at ultimate load of all the four cases: **Fig. 3.8a**- M1R1 (0%,10%,20%,30%), **Fig. 3.8b**-M1R2 (0%,10%,20%,30%),**Fig.3.8c**- M2R1 (0%,10%,20%,30%), **Fig.3.8d**- M2R2 (0%,10%,20%,30%). Almost all the beams showed flexure failure (**Figs. 3.8a and 3.8c**) but shear failure is also observed in some corroded beams. Shear failure has been observed in the beams when yield strength of the bar is increased from R1 to R2 mostly at 30% corrosion level with both concrete grades. The reason for shear failure is the decrease in ultimate strain and length of yield plateau with increase in yield strength of reinforcement (Paulay and Priestley. 1992).

1. M1 R1

2. M1 R1C10(10% corroded)

3. M1 R1C20(20% corroded)

4. M1 R1C30 (30% corroded)

Fig 3.8a- M1R1 (4 cases)

5. M1 R2

6. M1 R2C10 (10% corroded)

7. M1 R2C20 (20% corroded)

8. M1 R2C30 (30% corroded)

Fig 3.8b- M1 R2 (4 Cases)

9. M2 R1

10. M2 R1C10 (10% corroded)

11. M2 R1C20 (20% corroded)

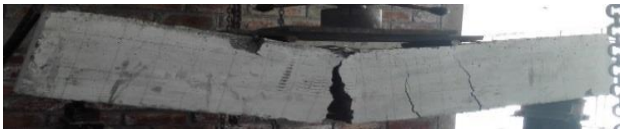

12. M2 R1C30 (30% corroded)

Fig 3.8c- M2R1 (4 cases)

13. M2 R2

14. M2 R2C10 (10% corroded)

15. M2 R2 C20(20% corroded)

16. M2 R2C30 (30% corroded)

Fig 3.8d- M2R2 (4 cases)

Fig. 3.8 Failure patterns of RC beams. **Fig. 3.8a**- M1R1 (4cases), **Fig. 3.8b**- M1R2 (4cases), **Fig. 3.8c**- M2R1 (4 cases), **Fig. 3.8d**- M2R2 (4cases)

From observation of failure pattern of RC beams at ultimate load, flexure ductile failure in RC beams without any corroded bars is observed as can be seen in all four cases in **Fig.3.8**.Crack width has been observed decreasing when higher strength of concrete grade is used in RC beams.R2 bars corroded upto a level of 30% is observed failing in shear mode (can be seen in **Fig. 3.8b** and **Fig. 3.8d**) even when the concrete strength is increased from M1 to M2. It is observed that increasing yield strength of reinforcement from R1 to R2 for same concrete grade decreases the ductility in RC beam. This type of failure is hazardous for seismic design of structures as deformation capacity in beam will be less with limited energy dissipation capacity.

3.3.1 Effect of 10% Corrosion on R1/R2 RC beam

Load Vs. deflection graph have been plotted in **Figs. 3.9-3.12** of RC beams with no corroded and 10% corroded bars. **Table 3.8** represents maximum moment, length of plastic hinge in mm and in terms of *d* (effective depth of the beam).

Plastic hinge length is the length at which inelasticity occurs or is assumed to occur (Elmenshawi et al. 2011). The values of moment, curvature (*Ø = M/EI*), plastic rotation is calculated from the load-deflection graphs and plastic hinge length is calculated from equation 2 given in next section. It is observed from **Fig. 3.9** that maximum deflection and maximum load (236.28 kN) is occurring in RC beam with no corroded bar used in M2R2 case whereas the highest value of plastic hinge length (shown in **Table 3.9**) is occurring in M2R1 (without corrosion). It is because of the decrease in ductility with increase of yield strength of reinforcement.

TABLE 3.9 Plastic hinge length of RC beams

Beam No.	**RC Beam**	**Maximum Moment (kN-m)**	**Length of Plastic hinge, l_p (mm)**	**l_p (in terms of effective depth of beam)**
A	M1 R1	73.81	117.32	0.43 d
B	M1 R1 C10	72.49	100.72	0.37 d
C	M1 R1 C20	67.61	94.37	0.34 d
D	M1 R1 C30	60.10	83.17	0.30 d
E	M1 R2	70.71	108.84	0.40 d
F	M1 R2 C10	66.04	95.49	0.35 d
G	M1 R2 C20	64.23	87.66	0.32 d
H	M1 R2 C30	60.76	70.44	0.26 d
I	M2 R1	78.41	143.29	0.52 d
J	M2 R1 C10	72.55	126.9	0.46 d
K	M2 R1 C20	68.89	104.45	0.38 d
L	M2 R1 C30	65.57	89.65	0.33 d
M	M2 R2	76.29	129.58	0.47 d
N	M2 R2 C10	71.96	112.84	0.41 d
O	M2 R2 C20	71.86	97.43	0.35 d
P	M2 R2 C30	68.81	78.26	0.28 d

So, all RC beams with no corrosion have ductile failure due to under-reinforced behaviour observed from load-deflection graphs. Beams with a higher concrete grade (M1 to M2) showed around 6-7% increase in load carrying capacity when both R1 and R2 reinforcement bars are used.

When 10% corrosion is imparted in R1C10 and R2C10 bars, maximum load carrying capacity decreased too along with lower displacement capacity, which in turn effects the seismic potential of the beams, where bars get corroded in turn restricting the energy dissipation. Although there is no much difference in the decreasing value of load and deflection in 10% corroded R1 as well as R2 bars used in RC beam when compared to beams with no corroded bars used. Flexure failure is noticed in both 10% corroded RC beam and in no corrosion bar used in RC beam but the crack width is more than 50% as compared to no corroded RC beams in all four cases in 10% corroded RC beam. A 10% decrease in load carrying capacity is observed when 10% corroded RC beam is used due to UTS/YS ratio less than 1.25.

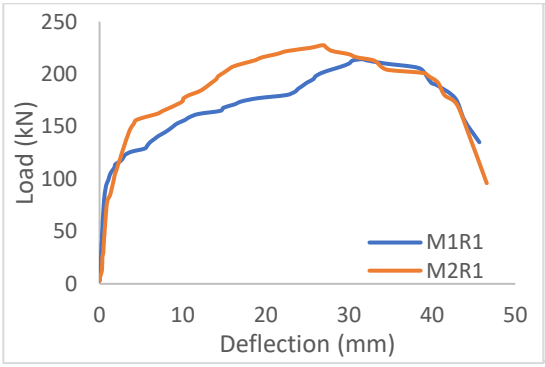

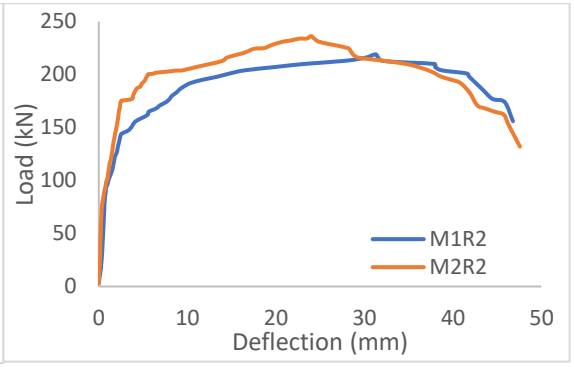

Fig. 3.9 Load-deflection curve of RC beams with R1 bars (Without corrosion) **Fig. 3.10** Load-deflection curve of RC beams with R2 bars (Without corrosion)

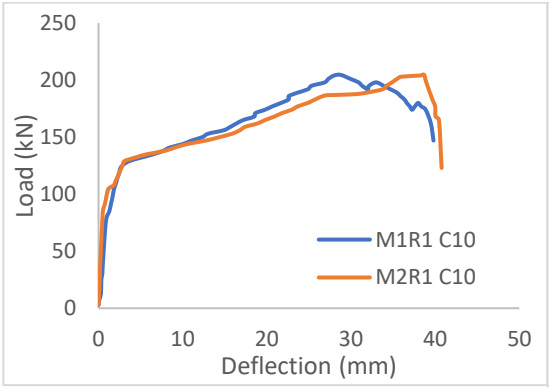

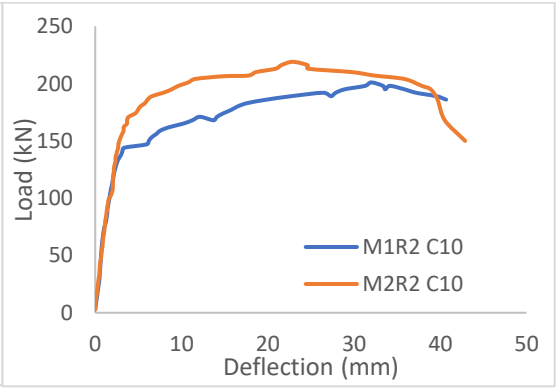

Fig. 3.11 Load-deflection curve of RC beams with R1 bars (10% corroded bars) **Fig. 3.12** Load-deflection curve of RC beams with R2 bars (10% corroded bars)

3.3.2 Effect of 20% Corrosion on R1/R2 RC Beam

The load-deflection curve of RC beams with 20% corroded bars is shown in **Figs. 3.13 and 3.14**. The maximum load carrying capacity decreases upto 17% in RC beams when 20% corroded bars are used

along with much lower displacement capacity making it undesirable to use as seismic efficient structure. With decreasing deflection, the value of plastic hinge length of RC beams with 20% corroded bars also decreases, giving rise to brittle shear failure in high yield strength (R2) bars.

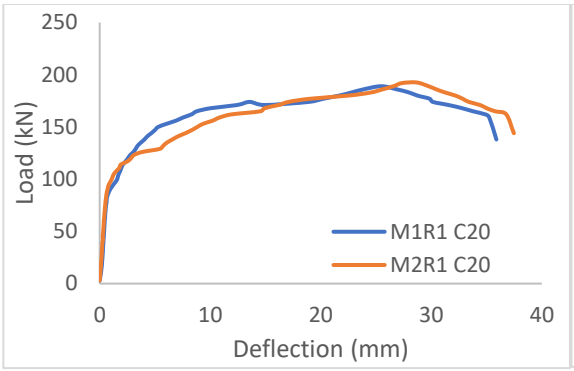

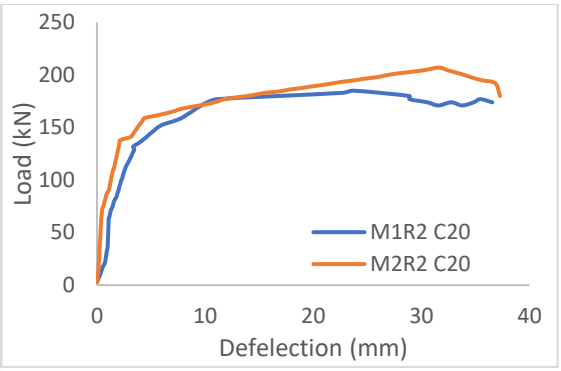

Fig. 3.13 Load-deflection curve of RC beams with R1 bars (20% corroded bars)

Fig. 3.14 Load-deflection curve of RC beams with R2 bars (20% corroded bars)

Crushing of concrete is also observed in both R1 and R2 grade of steel used for the same grade of concrete. It can be seen from **Figs. 3.13 and 3.14** that maximum load carrying capacity is more when high strength of concrete grade is used in 20% corroded bars of both R1 and R2.

3.3.3 Effect of 30% Corrosion on R1/R2 RC Beam

The load-deflection graph of RC beams with 30% corrosion level of reinforcement used is shown in **Figs. 3.15 and 3.16**. It has been observed after performing the tensile test of reinforcing bars that 30% corroded bars have lowest *UTS/YS* ratio which is much lower than 1.25 and therefore the maximum load carrying capacity decreased (as shown in **Figs. 3.15 and 3.16**) upto 25% in RC beams. The plastic hinge length value decreased too and the beams failed in shear (**Figs. 3.8b and 3.8d**) at lowest displacement as compared to less corroded RC beams (10%,20%). This type of behaviour of RC beams with brittle shear failure gives rise to the need of retrofitting old structures where the bars get corroded over a period of time and get damaged by the previous earthquakes so that the energy dissipation capacity of these structures increase during future earthquakes.

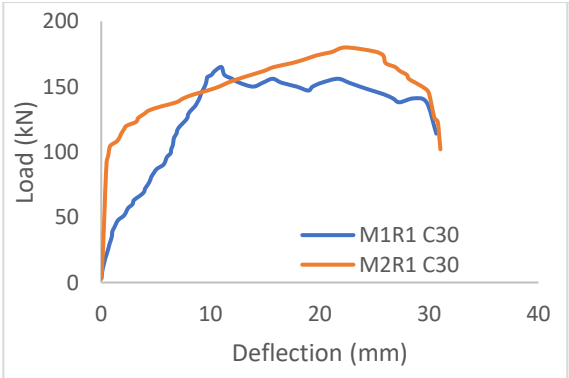

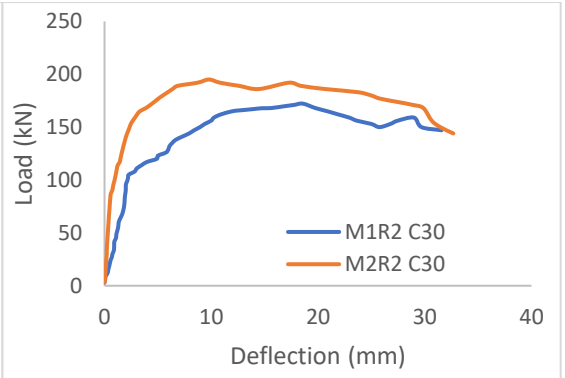

Fig. 3.15 Load-deflection curve of RC beams with R1 bars (30% corroded bars)

Fig. 3.16 Load-deflection curve of RC beams with R2 bars (30% corroded bars)

In all the cases with different percentages of corrosion, the maximum load carrying capacity in both R1 and R2 bars is with the higher strength of concrete grade. The plastic hinge length also increases withincrease in concrete grade as given in **Table 3.9**.

3.4 EXPERIMENTAL MOMENT-CURVATURE BEHAVIOUR

The extent of damage propagated along the shear span depends on the obtained inelastic curvature (Elmenshawi et al. 2011). Distribution of curvature within the plastic hinge region is important especially for deflections beyond the maximum flexural strength of the member under a certain axial load. The moment and curvature values of RC beams at the centre are calculated from the experimental values of load-deflection plot. Curvature is calculated from the deflection obtained at the centre, which is the potential plastic hinge region (Ouaar, A et al. 2007). The influence of concrete strength, yield strength and steel bar quantity on complete moment curvature performance of doubly RC beam sections have been assessed (Lee and Kang. 2000). Moment- curvature curves till the failure of all the beams (each case) is shown in **Figs. 3.17-3.18**.

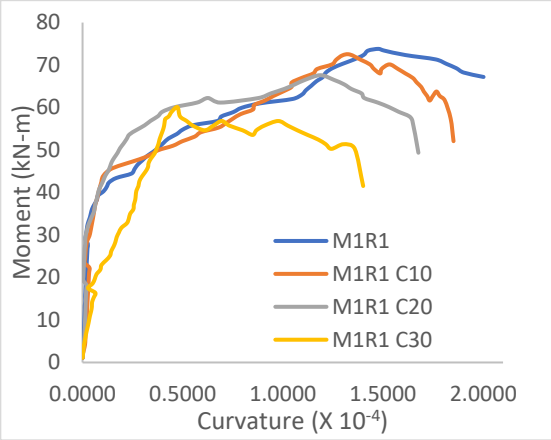

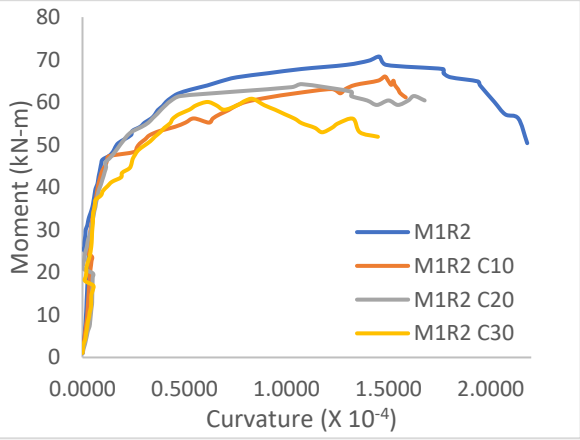

Fig. 3.17 Moment- curvature Curve of M1 R1 (all cases) **Fig. 3.18** Moment- curvature curve of M1 R2 (all cases)

From the above two figures (**Figs. 3.17 and 3.18**) it can be seen that maximum moment values reached 73.81kN-m and 70.71kN-m in M1 R1 and M1 R2 case without any corrosion. The moment value decreased from 10% corroded bar used in RC beam to 30% corroded bar due to low *UTS/YS* ratio of corroded bars. The value of curvature observed is maximum for the RC beam with no corroded bar used which therefore had a capability of producing longer plastic hinge length (**Table 3.9**) thereby making the energy absorption higher in seismic events giving rise to ductile failure of structure.

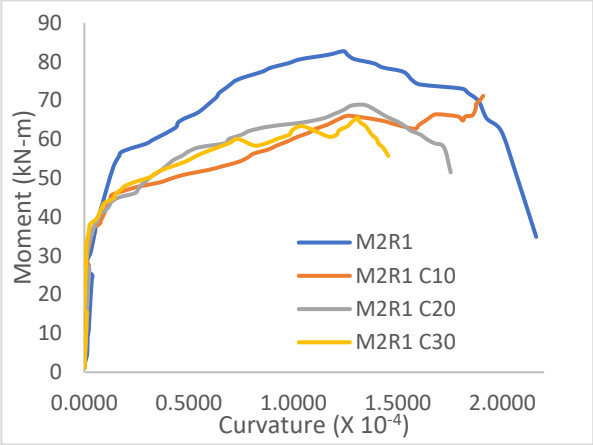

Fig. 3.19 Moment- curvature Curve of M2 R1 (all cases)

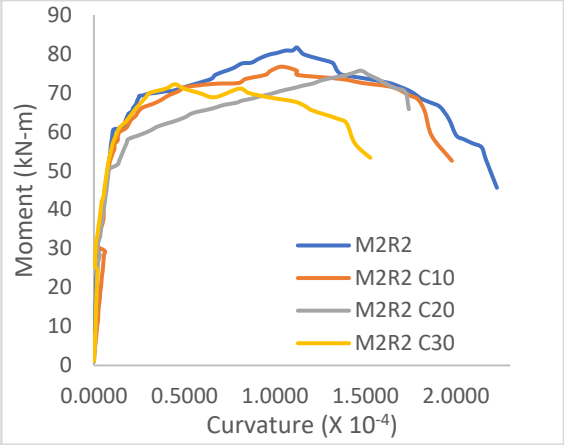

Fig. 3.20 Moment- curvature curve of M2 R2 (all cases)

It can be observed from **Figs. 3.19 and 3.20** that maximum moment values reached 78.41kN-m and 76.29kN-m in M2R1 and M2R2 case without any corrosion and similarly it decreased from 10% corroded bar to 30% corroded bar. It is noticed that moment carrying capacity is increased when concrete grade is increased from M1 to M2. For the same concrete grade when yield strength of the reinforcement is increased from R1 to R2, there is a decrease observed in curvature value. It is because of the ability to deformation without breaking in high yield strength of steel reduces as we go higher in yield strength of reinforcement as observed by Bureau of Indian Standards. Decrease in the value of curvature from 10% corroded bar to 30% corroded bar also affected the failure of RC beams which changed from flexural to shear failure with wide cracks formed in the beams where corroded bars have been used making it unfit as a seismic member.

3.5 ANALYSIS OF PLASTIC HINGE LENGTH

Plastic hinge length, l_p is computed by dividing curvature to plastic hinge rotation as given below in the equation 2. The plastic hinge rotation capacity has also been seen getting influenced by longitudinal reinforcement ratio, concrete strength and also with the loading type (concentrated, two-point etc.) (Lopes and Bernardo. 2003, Douglas et al. 1996).

$$\Theta_p = (\emptyset_u - \emptyset_y)\, l_p = \emptyset_p l_p \qquad (2)$$

Where $\emptyset_u$and $\emptyset_y$are the curvatures calculated from deflection (centre) at ultimate load and yielding, respectively, $l_p$is the plastic hinge length and $\Theta_p$is plastic rotation examined as moment approaches the plastic moment. Yield curvature is calculated at yielding point identified from load-deflection graph of RC beam by considering cracked moment of Inertia for yielding. Ultimate Curvature is calculated after yielding of tension steel, since after yielding, stress remains constant but strain keeps increasing till the point when failure strain of concrete or reinforcement is reached.

The variation of plastic hinge length from no corroded bars to 10%, 20% and 30% corroded bars used in RC beams is shown below from **Figs. 3.21-3.24**.

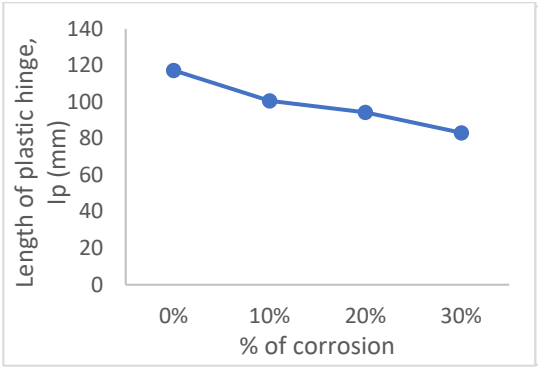

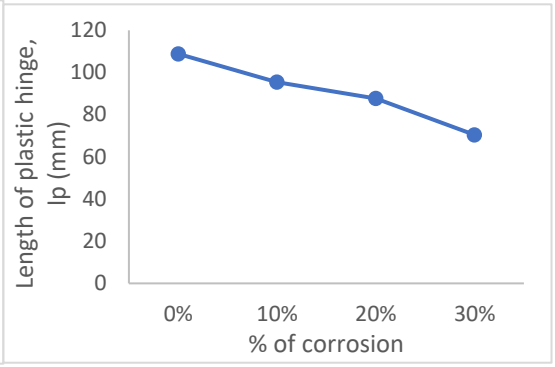

Fig. 3.21 Variation in plastic hinge length for M1R1 (4 cases) **Fig. 3.22** Variation in plastic hinge length for M1R2 (4 cases)

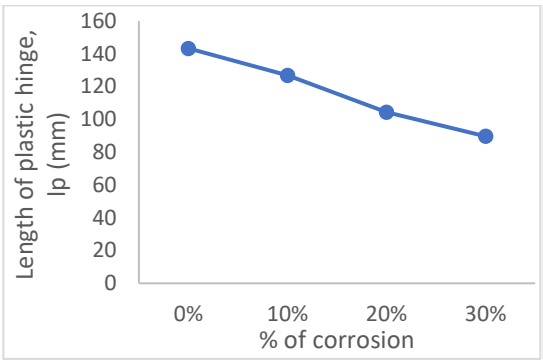

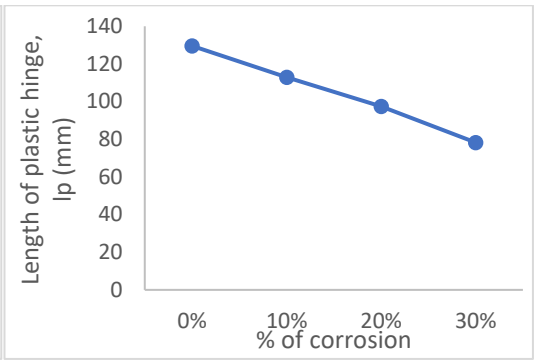

Fig. 3.23 Variation in plastic hinge length for M2R1(4 cases) **Fig. 3.24** Variation in plastic hinge length for M2R2(4 cases)

It has been noticed that plastic hinge length is maximum in RC beams with no corroded bars used and decreases as the corrosion level increases in all four cases. *Lp* has been evaluated and normalised in terms of effective depth of beam, d. From this experimental work, plastic hinge length is observed to be varying from 0.52 *d* to 0.26 *d* when bars are corroded at 10%, 20% and 30% respectively with the variation of concrete grades (M1, M2) and reinforcement bars (R1, R2). The plastic hinge length of beams with no corroded bars used is between 0.4 *d* to 0.52 *d*, which complies with Baker who indicated that for the range of span/d and *z/d* ratios, l_p lies in the range between 0.4*d* and 2.4*d*. Mattock and Corley (1967) and Sawyer et al. (1964) theories give a constant plastic hinge length regardless of reinforcement index, 0.85*d*, 0.78*d* and 0.66*d* respectively. Plastic hinge length increases as grade of concrete is increased and decreases with increase of yield strength of reinforcement bar whereas it is contradictorily indicated by Ou and Nguyen (2014) that *lp* has no strong relationship with the concrete compressive strength or longitudinal tensile steel ratio.

It is also observed that yielding load and ultimate load is increasing with increasing concrete grade and yield strength of reinforcement which is a similar observation to Kheyroddin and Naderpour (2007) who concluded that the yielding load and ultimate load is increasing with tension reinforcement index for two-point loading. The value of maximum load increases with increase in concrete grade for same yield strength of reinforcement bar and therefore it increases the ductility of RC beams thereby increasing the plastic hinge length. Plastic hinge length decreases with increase of steel yield strength as stated by Bureau of Indian standards that the ductility reduces as grade of steel increases, which proves that the

ability of deformation of steel bar without breaking gets weak. So, higher grade of steel should be used only when design usage requires it else, its elongation capacity will be less and it can result in making any component of structure over-reinforced resulting in brittle shear failure, which is ineffective to be called as seismically efficient structure.

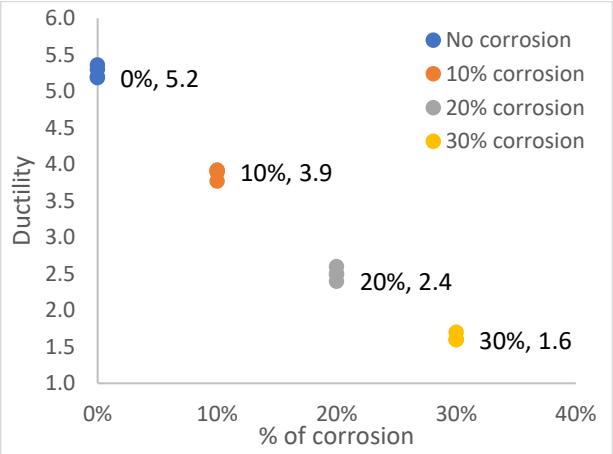

Fig. 3.25 Effect of Ductility on RC beams (all cases)

In seismic design, the ratio of ultimate deformation and deformation at first yield is defined as ductility. Ductility can be demonstrated with regard to many response parameters connected to deformations, namely rotations, curvatures and displacements. Curvature ductility is ratio of curvature at the end of post elastic range *Øu* and at the first yield point of tension steel *Øy*, as stipulated in cl. 3.3 of IS13920:1993. **Fig. 3.25** shows the effect of ductility on RC beams as per different corrosion levels. The values of displacement ductility factor should range from 3 to 5 whereas curvature ductility ratio may be greater than displacement ductility considering post-elastic range when frame is deflected laterally. Ho and Kwan (2008) pointed out the study conducted by various authors (Ho et al. 2004, Kwan et al. 2006), that the minimum ductility should be 3.32 for the design of beams in non-earthquake resistant structures and for beams in earthquake resistant structures, a larger value of minimum ductility could be assigned depending on the actual demand. It can be easily noticed from **Fig. 3.25** that bars corroded from 10% to 30% level used in RC beams had ductility value decreasing from 3.9 to 1.5. RC beams with no corroded bars used had ductility value between more than 5, therefore capability of deforming when subjected to lateral loads under any earthquake will be affected in RC beams with corroded bars. Plastic hinge length is also seen decreasing from 10% to 30% corroded bars used, so it can be stated that structures having corroded bars like an old reinforced building structures designed as per earlier codes should be assessed and retrofitted accordingly based on knowing the percentage of corrosion in RC beams. Therefore, there is a decrease observed in ductility of RC beams with increase in percentage of corrosion of reinforcement. However, ductile behaviour has been observed in 10% corroded bars of RC beams with

ductility value of 3.9 and low ductility of 1.5 has been observed in 30% corroded bars used in RC beam which is unacceptable for RC beams in earthquake resistant structure.

3.6 CLOSING REMARKS

The chapter reports the post yield performance of RC beams with corroded reinforcement. Reinforced concrete beam specimens were designed and reinforcements were subjected to anodic corrosion at a constant voltage. The specimens were tested with varying grade of concrete and type of reinforcement along with the condition of reinforcement (10%, 20% and 30% corroded reinforcement) by applying two-point loading (approximately $1/3^{rd}$ and $2/3^{rd}$ of span). Behaviour of RC beam under flexure loading is monitored and moment-curvature relationships are reported. The results are correlated with analysis of plastic hinge length. From simultaneous monitoring of different corrosion percentages on the flexure behavior of RC beam, effect of different concrete grade and different yield strength of reinforcement on RC beam for plastic hinge analysis have been reported. It can be concluded that rational integration of plastic hinge analysis and ductility of corroded RC beams can reveal the seismic qualification of existing structures.

CHAPTER 4
DEVELOPMENT OF PLASTIC HINGE MODEL WITH CORRODED REINFORCEMENT

4.1 GENERAL

Seismic qualification of existing structures with the help of evaluation of plastic hinge parameters was studied in the preceding chapter, using "moment-curvature" relationship and analysis of "plastic hinge length" of RC beam with corroded reinforcement. The vis-à-vis effect of ductility on RC beams with respect to percentage of corrosion was established. Corrosion was induced in reinforcement bars when inside the RC beam after casting it. Corrosion of longitudinal/transverse reinforcement also decreases bond between concrete and steel. This chapter reports development of plastic hinge model with corrosion induced in reinforcement individually before casting RC beam analytically. The focus is to investigate plastic hinge model of corroded Reinforced Concrete (RC) beams tested experimentally as well as analytically through nonlinear finite element modeling considering the effect of reinforcement corrosion. A simple empirical equation is reported for maximum moment including the percentage of corrosion, using soft computing technique of Genetic Programming (GP). The equation obtained as an output of GP models is investigated to consider the effect of yield strength of reinforcement, concrete grade and percentage of corrosion of RC beam over maximum moment carrying capacity.

4.2 FINITE ELEMENT MODELING

Finite element method of analysis permits complex analyses of nonlinear response of RC buildings to execute in efficient manner (Kumari and Kwatra. 2013). The nonlinear response of the RC components of a structure is predicted fairly well with finite element method.

The details of RC beams used in FE modelling are given in **Table 4.1** where beams have been analysed after taking into account corrosion level at 10%, 20%, 30% and compared with the experimental data from load-deflection graph comparison which is observed to be in close agreement with each other (**Fig. 4.9 to 4.12**). Corroded bars (bottom, top and stirrups) are modelled by taking the stress-strain plots at different levels which are tested for determining residual tensile strength in Universal Testing Machine. Therefore, RC beams with corrosion level at 5%, 15%, 25% and 35% are also analysed by taking the data from tensile tests of extracted reinforcement bars after corrosion through linear interpolation.

Table 4.1 Details of beams used in FEM study

Beam No.	RC beam	Concrete Grade	Reinforcement Bar
A1 (Exp, Anal)	M1 R1	M1	R1
A2 (Anal)	M1 R1 C05	M1	R1C10 (Corroded at 5%)
A3 (Exp, Anal)	M1 R1 C10	M1	R1C10 (Corroded at 10%)
A4 (Anal)	M1 R1 C15	M1	R1C10 (Corroded at 15%)
A5 (Exp, Anal)	M1 R1 C20	M1	R1C20 (Corroded at 20%)
A6 (Anal)	M1 R1 C25	M1	R1C10 (Corroded at 25%)
A7 (Exp, Anal)	M1 R1 C30	M1	R1C30 (Corroded at 30%)
A8 (Anal)	M1 R1 C35	M1	R1C10 (Corroded at 35%)
B1 (Exp, Anal)	M1 R2	M1	R2
B2 (Anal)	M1 R2 C05	M1	R2C10 (Corroded at 5%)
B3 (Exp, Anal)	M1 R2 C10	M1	R2C10 (Corroded at 10%)
B4 (Anal)	M1 R2 C15	M1	R2C10 (Corroded at 15%)
B5 (Exp, Anal)	M1 R2 C20	M1	R2C20 (Corroded at 20%)
B6 (Anal)	M1 R2 C25	M1	R2C10 (Corroded at 25%)
B7 (Exp, Anal)	M1 R2 C30	M1	R2C30 (Corroded at 30%)
B8 (Anal)	M1 R2 C35	M1	R2C10 (Corroded at 35%)
C1 (Exp, Anal)	M2 R1	M2	R1
C2 (Anal)	M2 R1 C05	M2	R1C10 (Corroded at 5%)
C3 (Exp, Anal)	M2 R1 C10	M2	R1C10 (Corroded at 10%)
C4 (Anal)	M2 R1 C15	M2	R1C10 (Corroded at 15%)
C5 (Exp, Anal)	M2 R1 C20	M2	R1C20 (Corroded at 20%)
C6 (Anal)	M2 R1 C25	M2	R1C10 (Corroded at 25%)
C7 (Exp, Anal)	M2 R1 C30	M2	R1C30 (Corroded at 30%)
C8 (Anal)	M2 R1 C35	M2	R1C10 (Corroded at 35%)
D1 (Exp, Anal)	M2 R2	M2	R2
D2 (Anal)	M2 R2 C05	M2	R2C10 (Corroded at 5%)
D3 (Exp, Anal)	M2 R2 C10	M2	R2C10 (Corroded at 10%)
D4 (Anal)	M2 R2 C15	M2	R2C10 (Corroded at 15%)
D5 (Exp, Anal)	M2 R2 C20	M2	R2C20 (Corroded at 20%)
D6 (Anal)	M2 R2 C25	M2	R2C10 (Corroded at 25%)
D7 (Exp, Anal)	M2 R2 C30	M2	R2C30 (Corroded at 30%)
D8 (Anal)	M2 R2 C35	M2	R2C30 (Corroded at 35%)

A three-dimensional FE model with mesh size 50 mm is developed by using software ATENA to produce load-deflection response and failure crack patterns of RC beams (**Fig. 4.1**). The program system provides various material models for different materials and purposes. The most important material models for reinforced concrete building software are concrete and steel. These advanced models consider all important aspects of real material behavior during tension and compression.

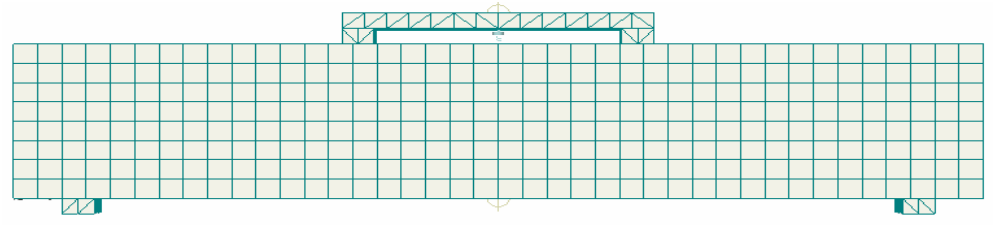

Fig. 4.1. FEM model along with mesh generation

4.2.1 Modeling of Concrete

Element geometric modeling of concrete using 3D solid brick elements with 20 nodes has been executed. A 3D solid brick element with three degrees of freedom at each node: translation in the x, y and z directions of the node. The element can be plastically deformed, cracked and crushed in three orthogonal directions. The main aspect of this element is the analysis of non-linear material properties. Crack formation procedure can be divided into 3 stages, **Fig. 4.2 (a)**. The uncracked stage occurs before reaching tensile strength. Cracks are formed in the processing area of potential cracks. Due to the bridging effect, the tensile stress on the crack surface is reduced. Finally, after the stress is completely released, the crack continues to open without stress. The tensile failure of concrete is characterized by the gradual growth of cracks, which connect together and eventually break larger parts of the building. It is generally considered that crack formation is a brittle process, and after crack formation, the strength in the tensile load direction suddenly becomes zero. Therefore, crack formation is undoubtedly one of the most important nonlinear phenomena, which controls the behavior of concrete buildings (Vladimir, Libor &Jan, 2018).

Smeared crack modelling approach have been employed for crack modelling. Within the smeared concept, fixed crack model is applied. In this study, the fixed crack model (Darwin and Pecknold 1974, Cervenka 1985) has been used, when the principal stress exceeds the tensile strength, the crack direction and the material axis are defined by the principal stress direction at the time of cracking. Darwin and Pecknold (1974) and Cervenka (1985) have developed an inelastic material model to be used in conjunction with the finite element technique to simulate the behaviour of reinforced concrete structures under cyclic, biaxial loading. The model is based on a smeared representation of cracking and reinforcement in plane stress state.

Viktor, Vladimir and Gintaris (2013) investigated accuracy of predictions of short-term deflections of RC beams by computer simulation (finite element software ATENA).

4.2.1.1 Fixed Crack Model

In the fixed crack model, the crack direction is given by the principal stress direction at the time of crack initiation. During further loading, the direction is fixed, representing the orthotropic material axis.

Since the concrete members are assumed to be isotropic, the principal stress and strain directions are the same in uncracked concrete. After the crack, orthotropyis introduced. The weak axis m_1 of the material is perpendicular to the crack direction, and the strong axis m_2 is parallel to the crack. Normally, the principal strain axes $\varepsilon 1$ and $\varepsilon 2$ rotate and do not have to coincide with the axes of orthotropy$m1$ and $m2$. This creates shear stress on the cracked surface as shown in **Fig. 4.2 (d)**. The stress components $\sigma c1$ and $\sigma c2$ represent the stresses in the normal direction and parallel to the crack plane, respectively. They are not principal stresses due to the shear stress. (Vladimir, Libor &Jan, 2018).

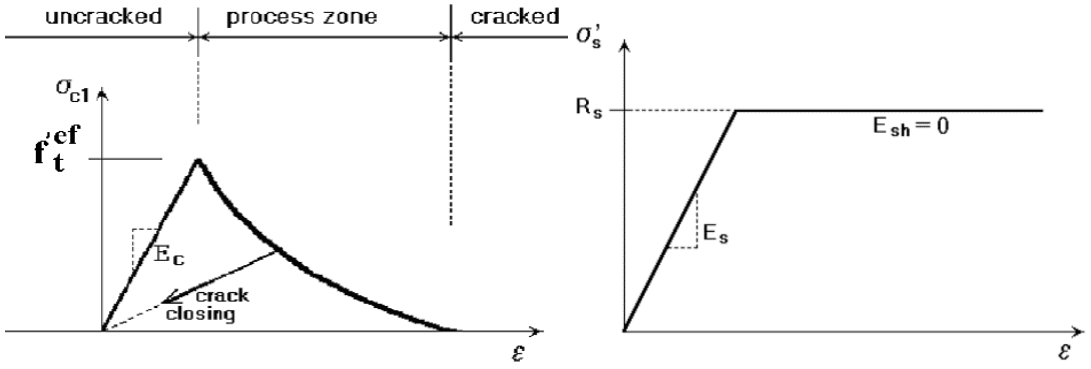

Fig. 4.2(a). Geometry of brick elements and stages of crack openings, **Fig. 4.2(b)**. Bilinear stress-strain law for reinforcement

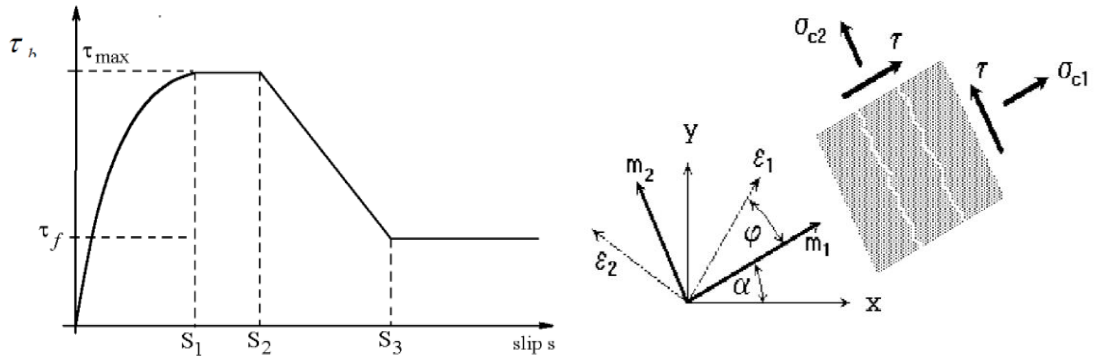

Fig. 4.2 (c). Bond- slip relationship, **Fig. 4.2 (d)**. Fixed crack model. Stress and strain state [Vladimir,Libor& Jan,2018]

4.2.2 Modeling of Reinforcement

Modeling of reinforcement in finite element is much simpler than the modelling of concrete. The reinforcement model can be discrete or smeared. In the current work, the discrete modeling of steel bars has been completed. In the current work, the reinforcement elements have been used to model the reinforcement. It is a 3D bar element, each node has three degrees of freedom, which are translations in node x, y and z directions. Bar elements are uniaxial tension and compression elements. The stress is assumed to be uniform throughout the element. The element has plastic deformation ability, and also has creep, swelling and large deformation ability. Rebar can be modeled in two different forms: discrete and smeared. Discrete steel bars are in the form of steel bars. In this study, the discrete method was used. Assumed to be the law of bilinear, that is, completely elastic plastic as shown in **Fig. 4.2(b)**. The initial

elastic part has the elastic modulus of steel *Es*. The second row represents the plasticity of the hardened steel, and its slope is the hardening modulus *Esh*. In the case of complete plasticity, *Esh* = 0. Limit strain εL means steel has limited ductility.

4.2.3 Modeling of Bond-Slip Relationship

The bond strength of corroded steel reinforcement consists of contributions from concrete τ_{con} and stirrup τ_{st} is defined according to Maaddawy, Soudki & Topper (2005) which is determined as

$$\tau_{max,c} = R\left\{0.55 + 0.24\frac{c_c}{d_b}\right\}\sqrt{f_c'} + 0.191\frac{A_t f_{yt}}{s_s d_b} (f_c' \text{ and } f_{yt} \text{ in MPa}) \quad (3)$$

$$R = (A_1 + A_2 X) \quad (4)$$

Where *R* is calculated by using variables *A1* and *A2*, which depends on corrosion current density level used to accelerate the corrosion procedure (where, *R*=1 for uncorroded condition) (Maaddawy et al., 2005). The reduction of bond strength contribution from stirrup (in Equation (3)) due to corrosion is considered by decreasing the stirrup area and yield strength.

A perfect connection is acquired for modelling interface between concrete and reinforcement. Typical 4-segment envelope conforming to CEB-FIP model code 1990, as defined below (Equation (5)), is adopted and modified using Equation (3) to incorporate corrosion effect and in this study, the bond stress-slip relationship between concrete and steel bars is simulated (Zhao et al. 2011).

$$\begin{aligned} \tau &= \tau_{max}\,(s/s_1)^{\alpha} && \text{for } 0 \le s \le s_1 \\ \tau &= \tau_{max} && \text{for } s_1 \le s \le s_2 \\ \tau &= \tau_{max} - (\tau_{max} - \tau_f)\,[(s - s_2)/(s_3 - s_2)] && \text{for } s_2 < s \le s_3 \\ \tau &= \tau_f && \text{for } s_3 < s \end{aligned} \quad (5)$$

Where α = 0.4, *s1* = *s2* = 0.6 mm, *s3* = 2.5 mm, and τ_f= 0.15 τ_{max}. **Fig. 4.2(c)** shows steel bond stress-slip relationship according to CEB-FIP model code 1990.

Table 4.2 represents all the material properties used in Finite element analysis.

Table 4.2 Material properties used

Material	Material model	Important properties
Concrete	Non Linear Cementitious 2	f_{ck}= M1, M2 (Refer **Table 3.2**)
Reinforcement Bar	Reinforcement (bi-linear stress-strain relationship)	E = 200 GPa f_y = Different for all 16 cases (Refer **Table 3.6**)
Steel Plate	3D elastic isotropic	E = 200 GPa
Bond treated steel-concrete interface		Perfect connection

4.3 RESULTS AND DISCUSSIONS

4.3.1 Load-Displacement Behaviour

The load deflection graph obtained from experimental and FEM simulations is shown in **Fig. 4.3 to 4.6.**

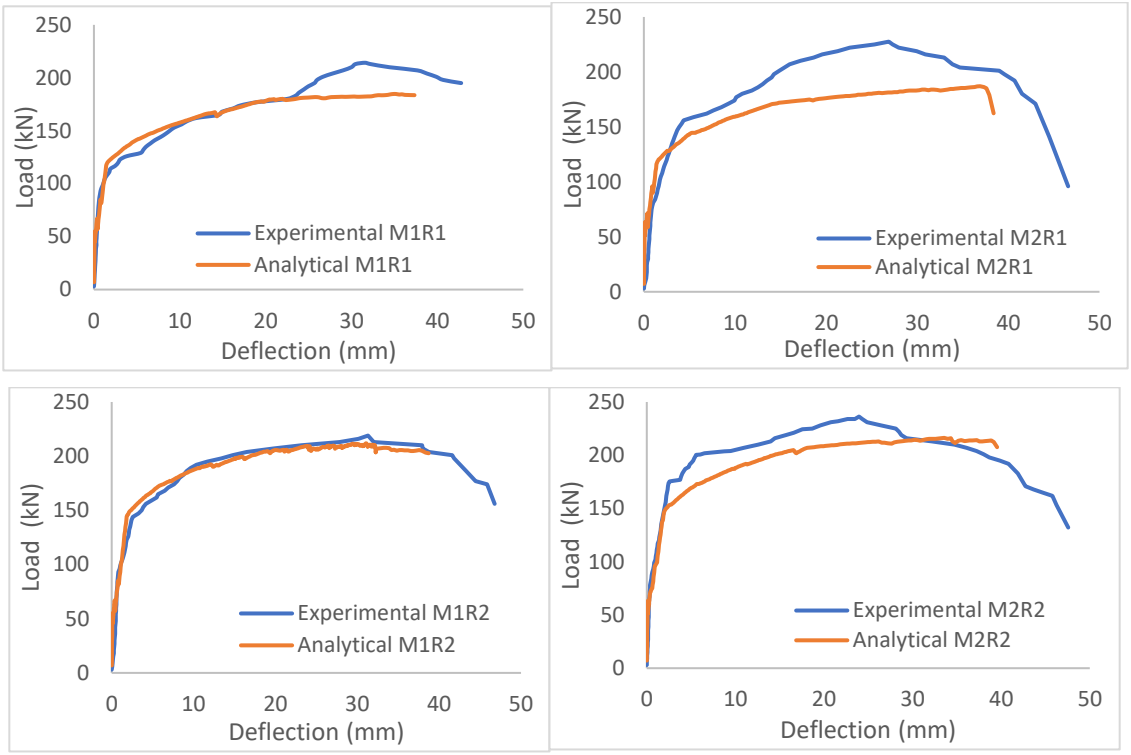

Fig. 4.3. Comparison of Experimental and FEM results (No corrosion)

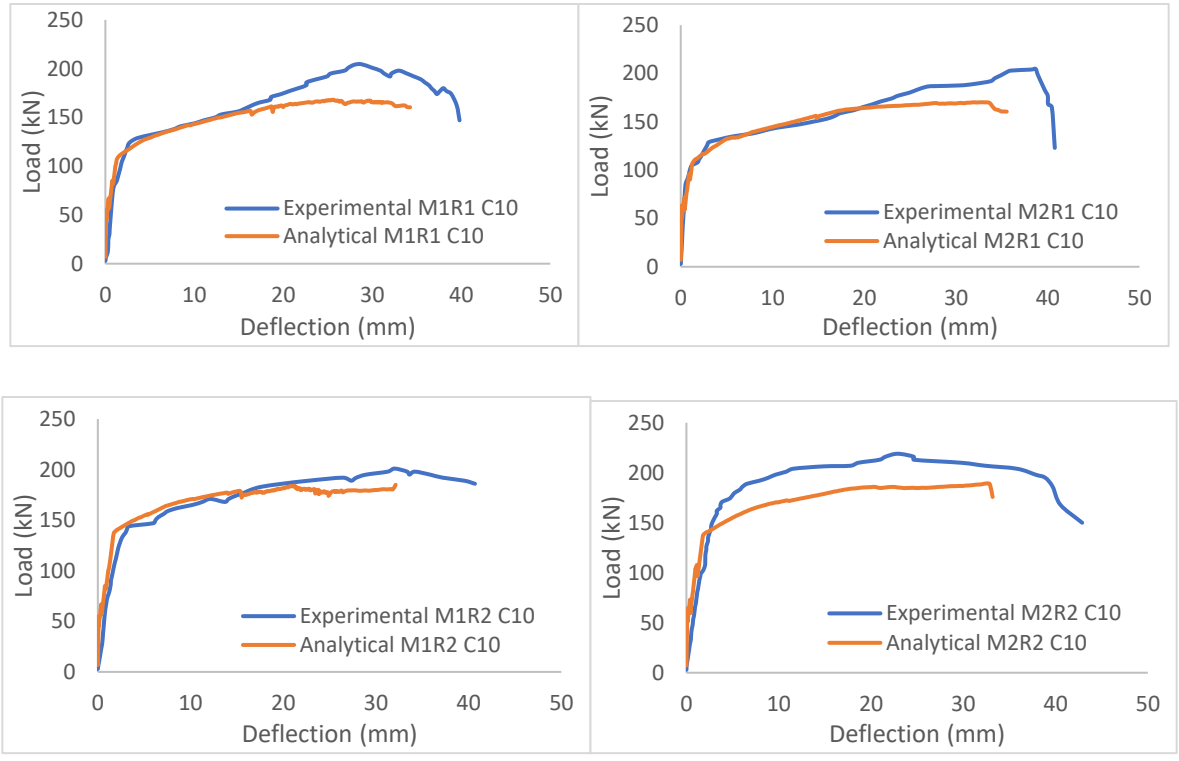

Fig. 4.4. Comparison of Experimental and FEM results (10% corroded)

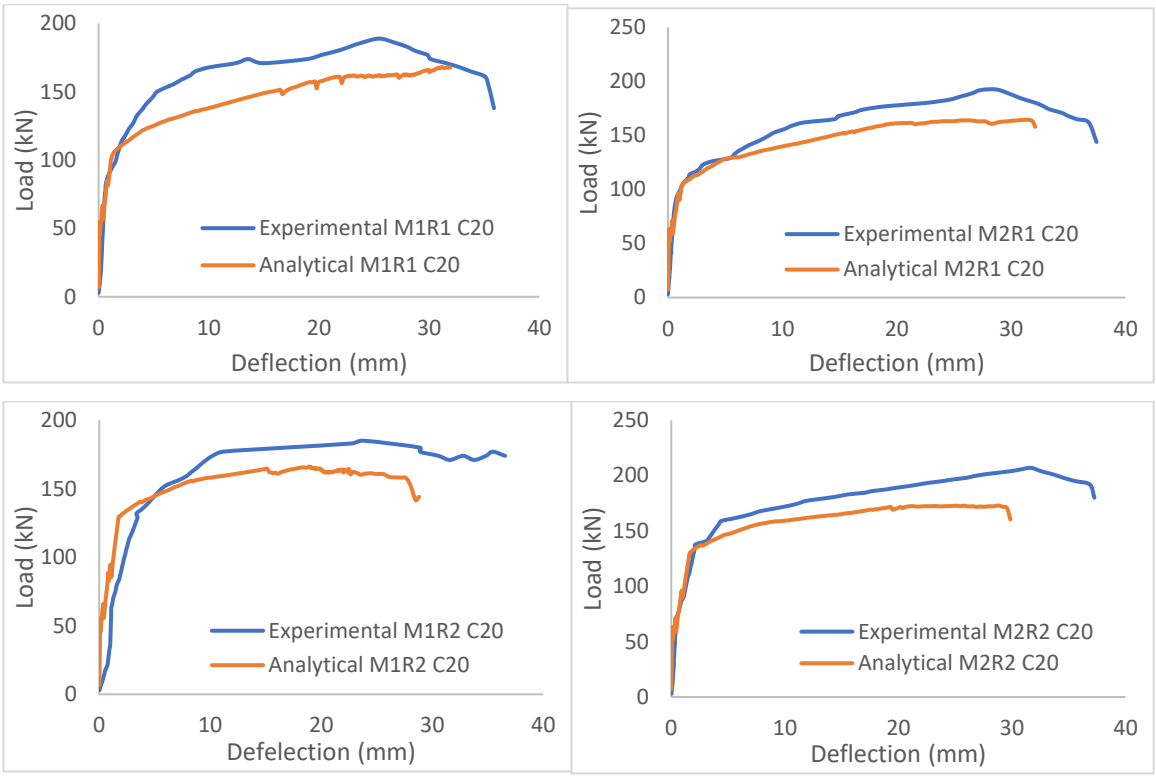

Fig. 4.5. Comparison of Experimental and FEM results (20% corroded)

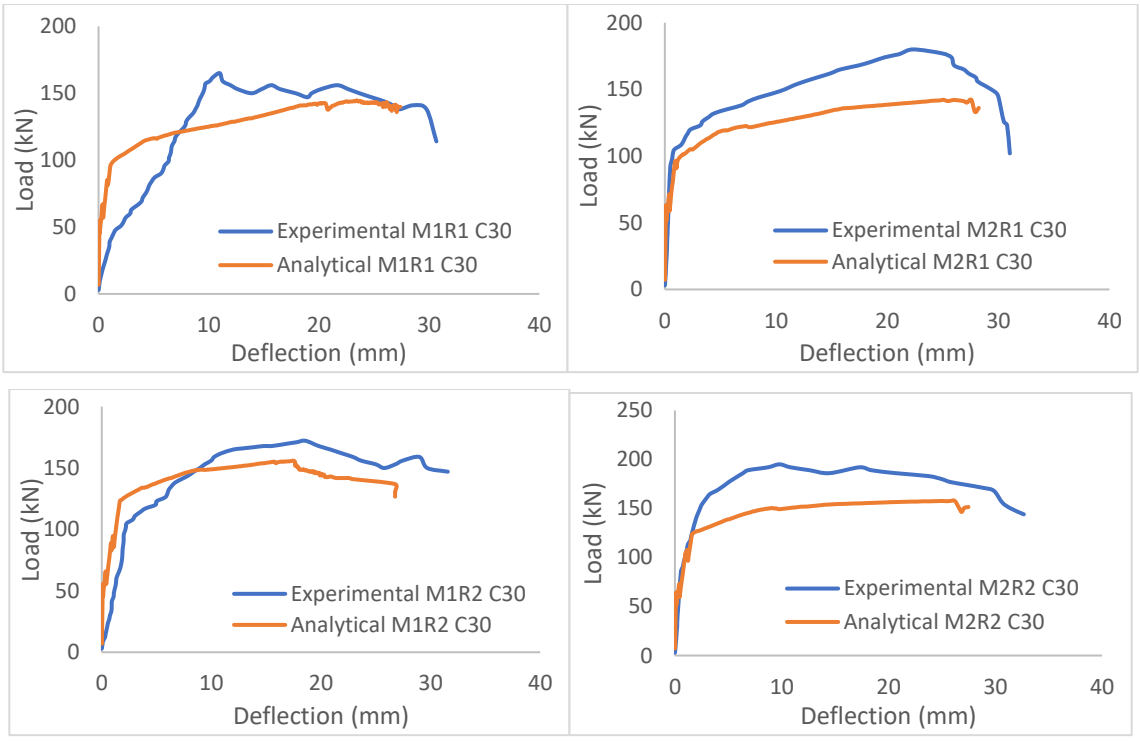

Fig. 4.6. Comparison of Experimental and FEM results (30% corroded)

It can be observed that FEM simulation is close to the experimental curve of RC beams with corrosion level 0%, 10%, 20%, 30% in bottom bars. It is observed from **Fig. 4.3** that deflection and load is observed maximum in RC beam without corrosion in M2R1 as well as M2R2 case. Increase in

compressive strength of concrete, increases load carrying capacity and deflection thereby making it a potential seismic member.

As the level of corrosion in reinforcement bar is increased from 10% to 30%, load and deflection are decreased. Experimental and analytical load-deflection curves of no corroded and 10% corroded bars embedded in RC beams are observed to be in close agreement with each other, whereas 20% and 30% corrosion induced in bars of RC beams show discrepancies in some cases due to high level of corrosion percentages involved. Force and deflection carrying capacity continues to increase with increase of compressive strength of concrete in all cases of RC beams as can be seen in **Fig. 4.3 to 4.6**.

The failure pattern of the RC beam is obtained from FEM analysis. **Fig. 4.7(a),(b)** show the 3d view of cracks formed at ultimate load in RC beam at 0%, 10%,20% and 30% corrosion induced in reinforcement. It can be seen that the maximum cracks are seen at the bottom portion of the RC beam due to tension developed at the bottom. Crack patterns obtained through FEM analysis matches well with the experimental cracks. There is a shear failure observed in 30% corroded reinforcement bars in RC beam of type R2 which is found in close agreement with experimental failure pattern (**Fig. 4.7 (b)**).

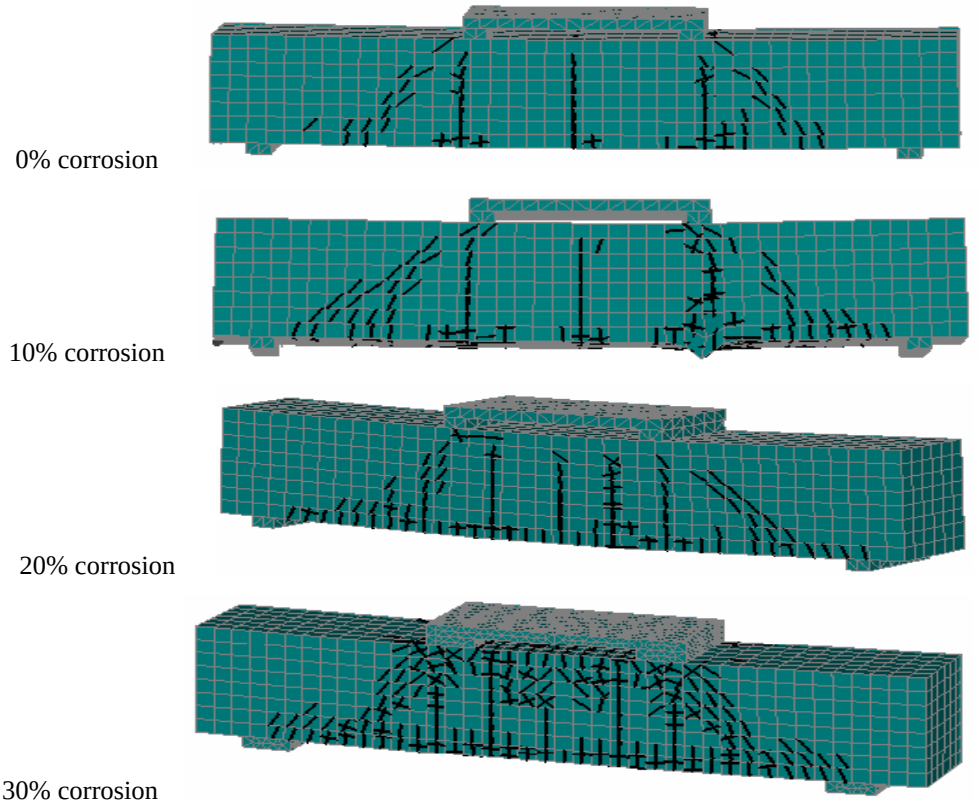

Fig. 4.7(a). Failure patterns of RC beams after FE analysis (flexure in all cases)

M1R2C30/M2R2C30 (30%corroded)

Fig. 4.7(b). Failure patterns of RC beams after FE analysis (shear failure observed)

4.3.2 Moment-Rotation Relationship

A reinforced concrete beam subjected to seismic loading consists of two regions, a small hinge region where flexural cracks occur along with concrete crushing with most of the permanent rotation concentrated around the wide flexural cracks, and the non-hinge region where there are much narrower cracks with no concrete crushing. Once a crack forms, the crack can only widen in a flexure designed beam and the opening of the crack concentrates rotation around the flexural crack. Therefore, moment-rotation relationship can predict the behaviour of RC beams specifically at the hinge region. Moment-rotation relationships are calculated from moment-curvature relationship where curvature is calculated from deformation calculated from experiments. Numerical validation of experiment is done using non-linear FE method as explained in the preceding section above. The analytical moment- rotation curves of all the four cases (M1R1, M1R2, M2R1, M2R2) at different corrosion levels (0%,5%,10%,15%,20%,25%,30%,35%) is shown below in **Fig. 4.8 to 4.11**. The moment-rotation curves obtained after performing finite element analysis with different corrosion percentages of reinforcement bar of RC beams in all the four cases is showing decrease in the moment carrying capacity and rotation capacity with the increase in corrosion percentages of reinforcement bar from 5% to 35% used in RC beams as can be seen in **Fig. 4.8 to 4.11**. Most of the curves are not smooth in RC beam at 35% corrosion level because shear cracks are observed in RC beams at 30% corrosion level and more, thus ultimately reducing the rotation capacity of the member. Furthermore, moment and rotation capacity decreases at more than 25% corrosion level of RC beams due to decrease in confinement capacity of corroded hoops.

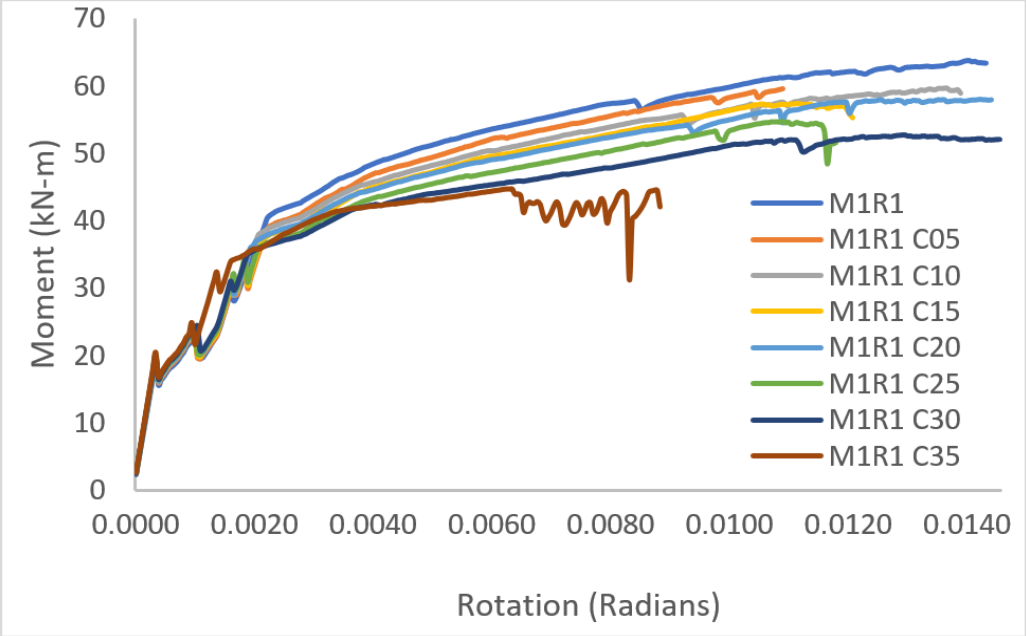

Fig. 4.8. Analytical moment- rotation curve of M1R1

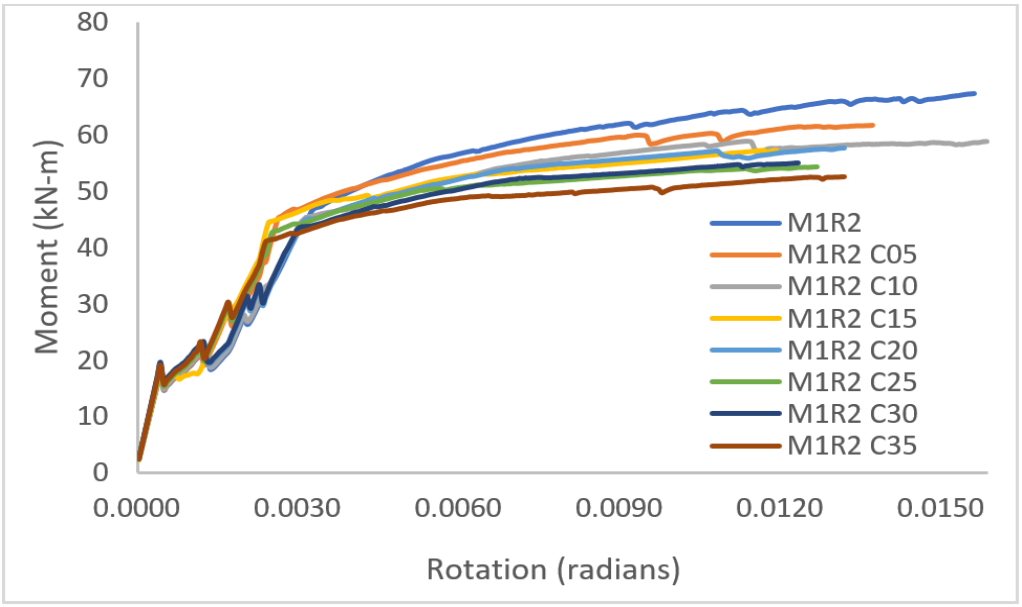

Fig. 4.9. Analytical moment- rotation curve of M1R2

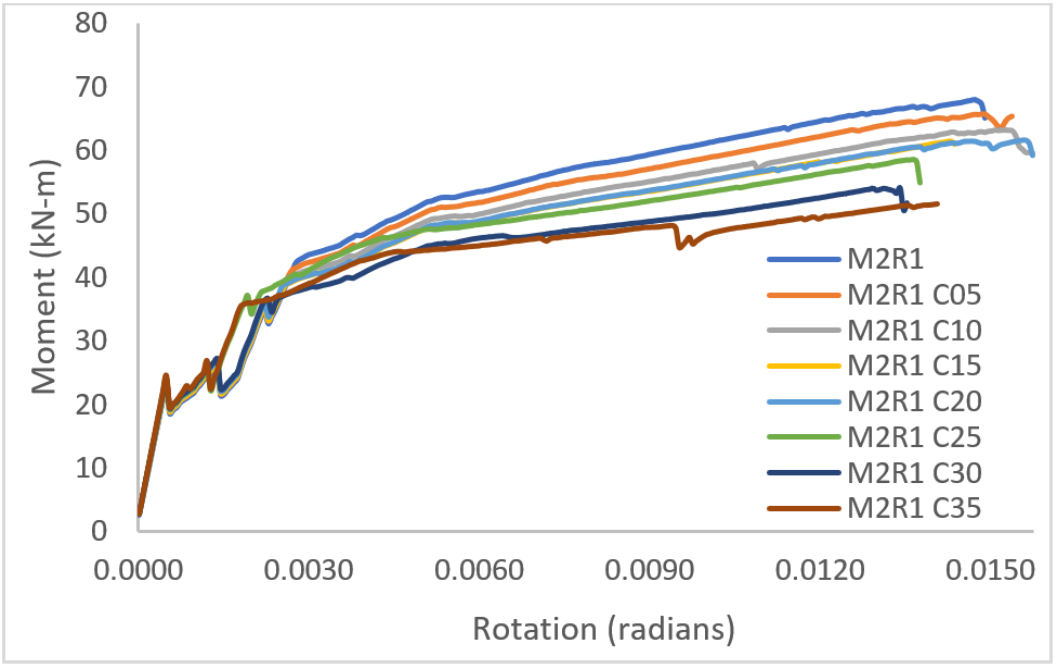

Fig. 4.10. Analytical moment- rotation curve of M2R1

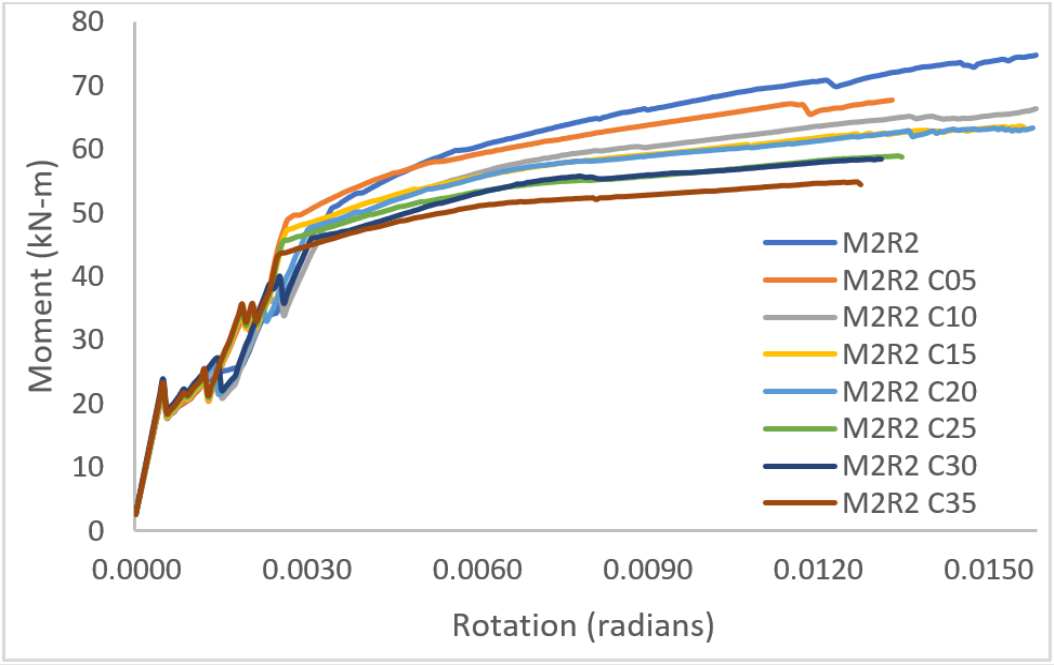

Fig. 4.11. Analytical moment- rotation curve of M2R2

The moment-rotation graphs obtained from experimental and FEM simulations are presented in **Fig. 4.12 to 4.15**. The moment-rotation behaviour obtained from finite element analysis is in close agreement with experimental behaviour of RC beams as can be seen in **Fig. 4.12**. The moment-rotation graphs in **Fig. 4.13 to 4.15**are similarly correlated. The decrease of moment and rotation capacity effects the seismic potential of the RC beams with increase in corrosion percentage from 5% to 35% because of reduced load carrying capacity of reinforcement and inability of hoops to confine core concrete. The moment carrying capacity is observed to be more for higher grade of concrete in every case making it better as seismic member.

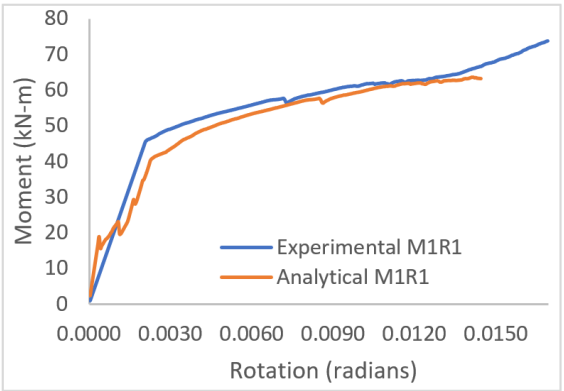

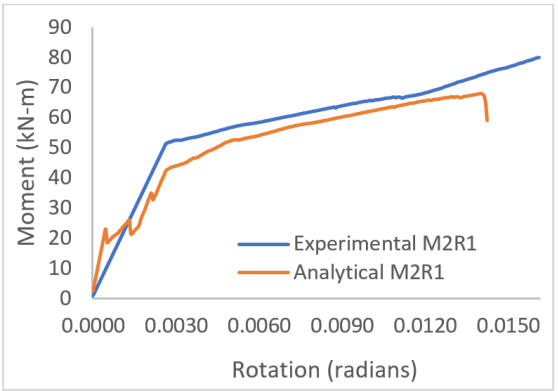

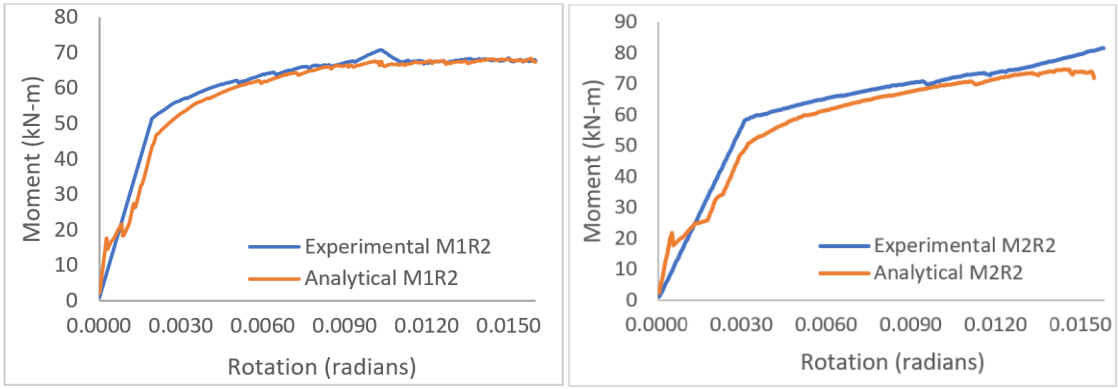

Fig. 4.12. Moment-rotation curve of Experimental and FEM results (No corrosion)

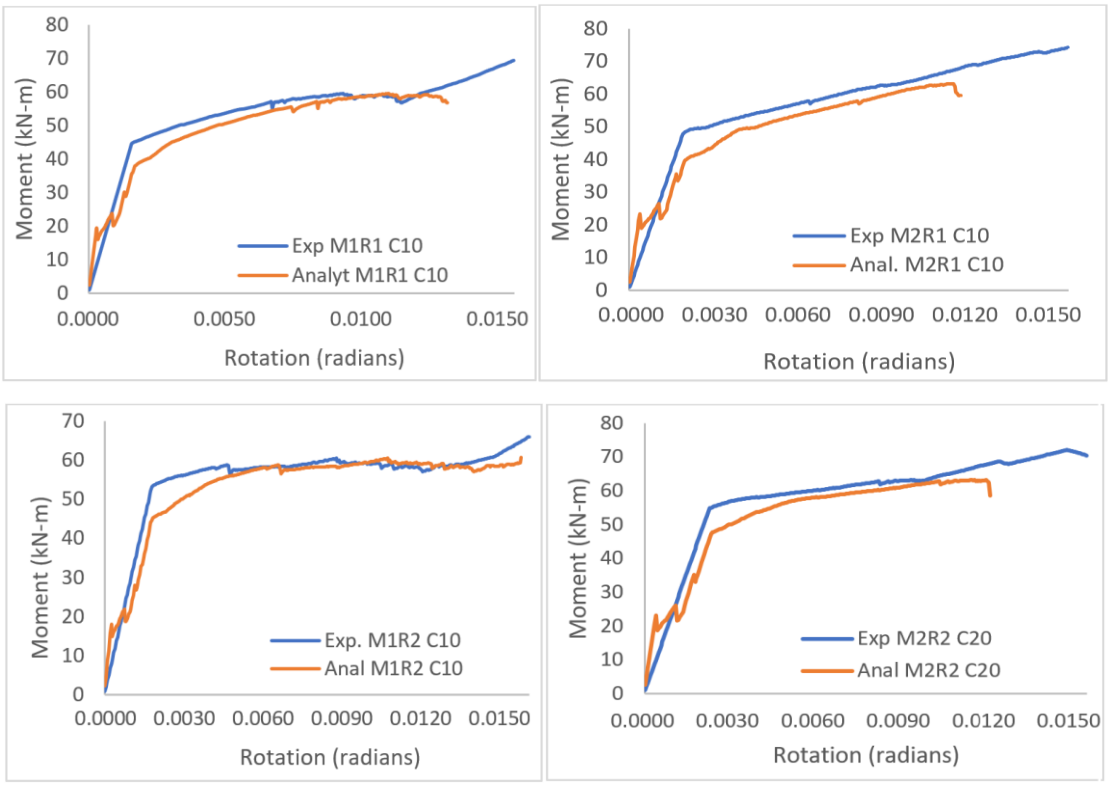

Fig. 4.13. Moment-rotation curve of Experimental and FEM results (10% corrosion)

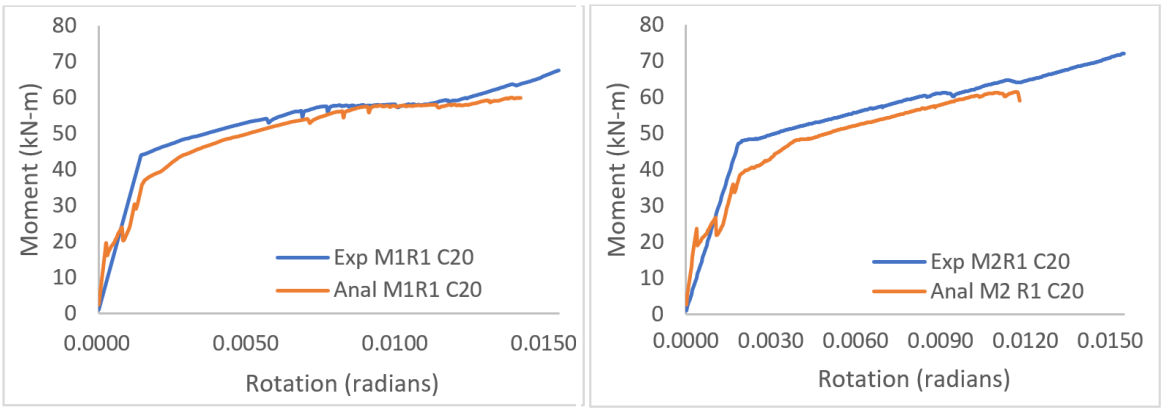

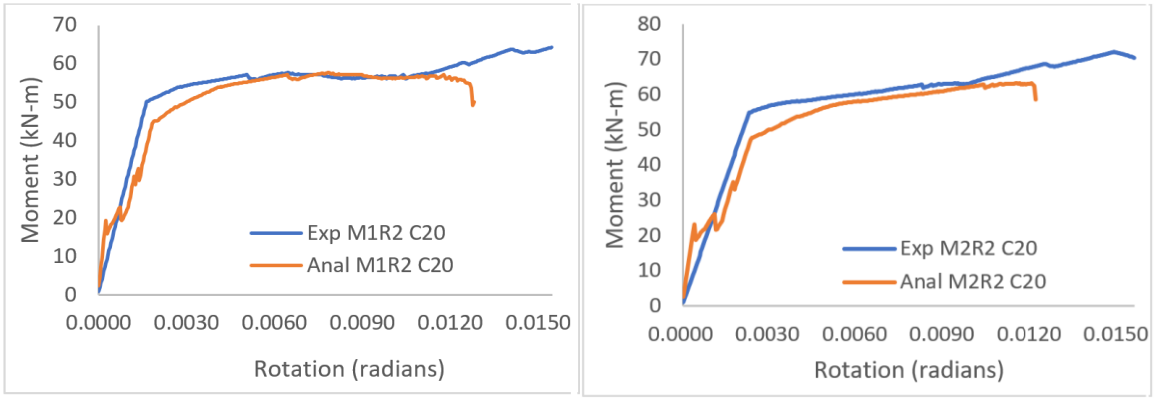

Fig. 4.14. Moment-rotation curve of Experimental and FEM results (20% corrosion)

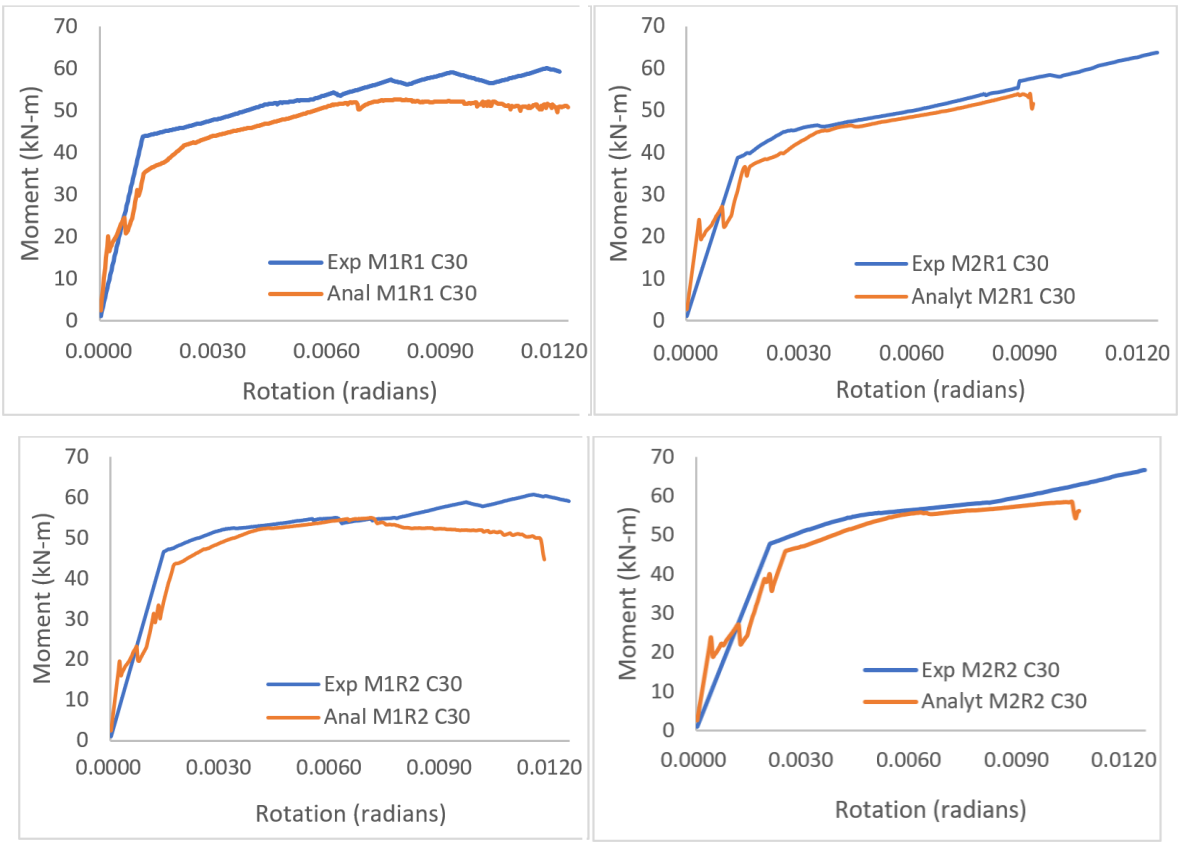

Fig. 4.15. Moment-rotation curve of Experimental and FEM results (30% corrosion)

All the conditions of the RC beam are very consistent, especially after the high rotational yield, the difference in yield at the beginning is partly because finite element model uses stress-strain relationship of bilinear steel as given in **Table 4.2** which tends to over-estimate the initial stiffness but has little effect at high rotations. The Moment and rotation capacity are observed more in experimental testing of RC beams representing its actual behaviour.

It can be seen from **Fig. 4.12 to Fig. 4.15** that rotation decreases with the increase in yield strength of reinforcement due to decrease in ductility of RC beam. It is observed that smaller rotations are associated with increasing corrosion percentage in reinforcement. FEMA-356 defined rotation as modelling parameters and acceptance criteria for nonlinear procedures (Table 6-7 in FEMA-356). The

generalised deformation is taken as rotation in the flexural plastic hinge zone of RC beams in this study and rotation capacities are defined in **Table 4.3**.

As per the Table 6-7 of FEMA-356, the rotation parameters defined in category NC of transverse reinforcement can be compared with rotation parameters of no corrosion case since hoops are spaced at *>d/3* in this study in the flexural plastic hinge region. Rotation at yielding and ultimate stage of FEMA-356 as shown in **Fig. 4.16** is almost similar to rotation capacity observed in no corrosion case (**Fig. 4.17**).

Table 4.3 Modeling parameters and acceptance criteria of RC beams for nonlinear analysis

S.No.	Case	Corrosion level	Modeling parameters			Acceptance criteria		
			Rotation (radians)			Rotation(radians)		
			B	C	D	IO	LS	CP
1	M1R1	No corrosion	0.0094	0.0145	0.2	0.0106	0.012	0.0125
2	M1R2		0.01	0.0136	0.2	0.0126	0.0131	0.0135
3	M2R1		0.0098	0.0161	0.2	0.0105	0.012	0.0132
4	M2R2		0.0111	0.0158	0.2	0.0122	0.0138	0.0145
5	M1R1 C05	5%	0.009	0.0143	0.2	0.0095	0.011	0.0117
6	M1R2 C05		0.0099	0.0133	0.2	0.0111	0.0119	0.0121
7	M2R1 C05		0.0095	0.0154	0.2	0.0115	0.0122	0.0129
8	M2R2 C05		0.0103	0.0153	0.2	0.0114	0.0126	0.0131
9	M1R1 C10	10%	0.0088	0.0141	0.2	0.0092	0.0109	0.0117
10	M1R2 C10		0.0096	0.0130	0.2	0.011	0.0114	0.012
11	M2R1 C10		0.0091	0.0148	0.2	0.0107	0.0115	0.0123
12	M2R2 C10		0.0096	0.0146	0.2	0.0113	0.0124	0.0129
13	M1R1 C15	15%	0.0077	0.0137	0.2	0.0077	0.0107	0.0113
14	M1R2 C15		0.0065	0.0128	0.2	0.0065	0.0108	0.0113
15	M2R1 C15		0.0071	0.0144	0.2	0.0071	0.0111	0.0119
16	M2R2 C15		0.0062	0.0142	0.2	0.0062	0.0122	0.0123
17	M1R1 C20	20%	0.0054	0.0133	0.2	0.0054	0.0106	0.0118
18	M1R2 C20		0.0048	0.0126	0.2	0.0048	0.0107	0.0113
19	M2R1 C20		0.0057	0.0140	0.2	0.0057	0.0111	0.0119
20	M2R2 C20		0.0045	0.0139	0.2	0.0045	0.0119	0.0123
21	M1R1 C25	25%	0.0046	0.0125	0.2	0.0046	0.0104	0.0107
22	M1R2 C25		0.004	0.0121	0.2	0.004	0.0106	0.0107
23	M2R1 C25		0.0048	0.0136	0.2	0.0048	0.0107	0.0114
24	M2R2 C25		0.0044	0.0135	0.2	0.0044	0.0114	0.0114
25	M1R1 C30	30%	0.0040	0.0117	0.2	0.0040	0.0102	0.0084
26	M1R2 C30		0.0025	0.0116	0.2	0.0025	0.0103	0.0108
27	M2R1 C30		0.0029	0.0133	0.2	0.0029	0.0098	0.0105
28	M2R2 C30		0.0024	0.0131	0.2	0.0024	0.0111	0.0109
29	M1R1 C35	35%	0.0038	0.0111	0.2	0.0038	0.0086	0.0067
30	M1R2 C35		0.0022	0.0100	0.2	0.0022	0.009	0.0092
31	M2R1 C35		0.0028	0.0117	0.2	0.0028	0.01	0.0101
32	M2R2 C35		0.0020	0.0105	0.2	0.0020	0.0095	0.0099

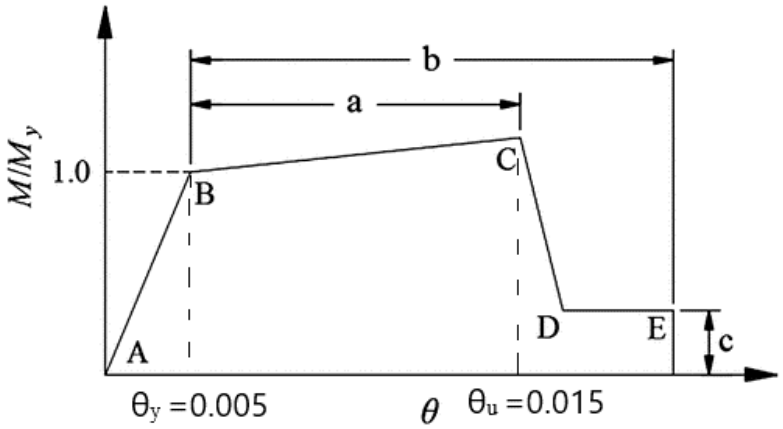

Fig. 4.16. Moment- chord rotation relation of RC plastic hinges in category NC of transverse reinforcement

On the same guidelines of FEMA-356, **Fig. 4.17** below shows the plastic hinges modeled with the moment-rotation relationships calibrated with the experimental and analytical data presented in this study at 0%, 20% and 35% corroded bars used in RC beams. Since shear failure is observed in RC beams with corrosion percentages 30% and above, rotation capacity at IO, CP level can be compared with rotations of beams controlled by shear in FEMA-356 (Table 6-7) which is quite similar. Also, yield rotation decreased from 20% to 35% corrosion level due to shear failure observed in RC beam with corrosion percentages 30% and above. The moment-rotation relation of RC beams with different corrosion percentages of bars taken in this study cannot be further compared with properties of plastic hinges considering moment-chord rotations with no-corroded bars of RC beams in FEMA-356.

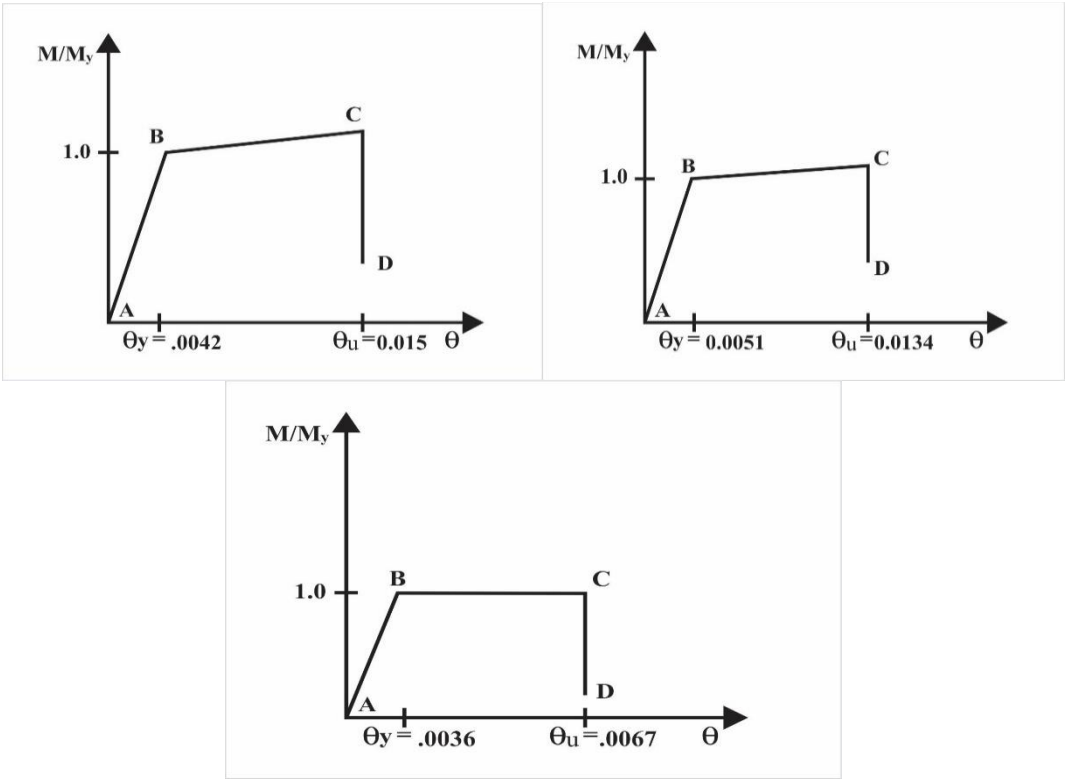

Fig. 4.17. Moment-chord rotation relation for RC beam plastic hinges using 0%, 20%, 35% corroded bar

Development of moment-chord rotation for RC plastic hinges at 0%, 20%, 35% corroded bar in RC beam has shown that ductility is decreasing with the increase in corrosion level of bars making it seismically vulnerable. **Fig. 4.17** shows that the bars corroded at 20% and 35% level used in RC beams had ductility value decreasing from 2.62 to 1.86 respectively. RC beams with no corroded bars used had ductility value more than 3. The moment-rotation behaviour of RC beam with no-corrosion case is observed to be in good agreement with rotation capacity as specified by FEMA-356 and so, it can be used to predict nonlinear behaviour of existing structures by performing pushover analysis. The structural behaviour of existing structures after performing pushover analysis can be well predicted according to the maximum moment capacity equation developed in this study including different corrosion levels in RC beams using genetic programming which is presented in the section below.

4.4 DEVELOPMENT OF MATHEMATICAL RELATION USING GENETIC PROGRAMMING

The concept of genetic programming (GP) is borrowed from the evolutionary process that occurs in nature. Species survive according to the principle of "survival of the fittest" (Joshi et al., 2014). GP is similar to genetic algorithm (GA). Unlike the latter, its solution is a computer program or equation for a set of numbers in GA (Gaur and Deo. 2008). In the search phase of the genetic programming algorithm, the program (for example, the unknown mathematical function that must be approximated by the appropriate sin, cos, polynomial, exp function and x +-* operator) undergoes multiple transformations to make it approximate as much as possible for the input to the desired output. GP equation is created by taking only x + - * operators. Genetic Programming was needed because they can dynamically build very complex programs (functions) to maximize certain utility functions (i.e. min {fitting error}).Pandey et al., developed generalised scour depth equation using multi linear regression (MLR) and Genetic algorithm (GA), where the scour depth predicted by GA is found to be more accurate than MLR. Although the research on GP technology can be traced back to the 1960s and 1970s, GP is a unique subject proposed by Koza (Johari, Habibagahi&Ghahramani, 2006).

4.4.1 Advantages of genetic programming

Compared with traditional modeling methods, the main advantage of GP is that it does not assume any previous functional form of the solution. In GP, the building blocks (input variables and target variables and function sets) are defined first, and then the learning method is followed to find the best structure of the model and its coefficients (Joshi et al., 2014). Use of GP in Civil engineering field is a very recent development and no references are noticed by the author in the field of application of Genetic Programming for plastic hinge models of RC beams although some applications are found in

geotechnical engineering (Johari et al. 2006). Therefore, an attempt is made to derive a simple empirical equation for maximum moment capacity including the yield strength of steel, compressive strength of concrete, geometry of beam, rotation capacity and percentage of corrosion with no corrosion as well using Genetic Programming with GPKERNEL (Babovic and Keijzer. 2000).

4.4.2 Methodology

To achieve best calibration of data with experimental tests and analytically using nonlinear Finite element modelling (FEM), Genetic programming models are developed under 8 different percentages of corrosion (0%,5%,10%,15%,20%,25%,30%,35%) to predict the flexural response of RC beam in terms of maximum moment carrying capacity. The division of the data is arrived at after several trials. So, the division of the data is approximately 70% for training and remaining 30% for testing the model (Joshi et al., 2014). GP model is developed with an attempt to arrive at the minimum possible input parameters. The statistical measures used to evaluate the accuracy of the developed model are Root Mean Square Error (RMSE) and Coefficient of Efficiency (CE). The coefficient of efficiency, E, measures the differences between the observations and predictions relative to the variability in the observed data itself (Guven and Aytek, 2010). These models have been developed using tree-based GP using the GPKernel software developed by Babovic and Keijzer (2000).

4.4.3 Model formulation and Results

In the present study, GP model is developed with 6 input parameters. These input parameters are chosen considering the effect of cross-section, material properties and percentage of corrosion in reinforcement of reinforced concrete beam. Effect of cross-section is incorporated in terms of *D* (depth of beam, mm), whereas material properties are incorporated in terms of *fck* (compressive strength of concrete, N/mm^2), *fy* (yield strength of reinforcement, N/mm^2), *Ast* (area of steel, mm^2), Θ (rotation, radians). The corrosion of reinforcement is defined as *C* (%). Output parameter of the GP model is maximum moment carrying capacity (M_{max}) of the beam.

The results of GP model are presented in **Table 4.4** below.

Table 4.4 Results of GP model

Performance parameters	M_{max}	Lp
RMSE	0.079	0.073
CE	0.92	0.94

The maximum moment capacity expression obtained after running the GP program is presented in Equation 6 below:

$$M_{max} = \left(\frac{fck * A_{st}}{fy}\right) + \left(\frac{D*\Theta*100}{C}\right) + 22.37 \qquad (6)$$

Similarly, length of plastic hinge expression obtained after running the GP program is presented in Equation 7 below:

$$Lp = 3.084\left(\frac{fck*Ast}{fy}\right) - 0.55\left(\frac{D*\Theta*100}{C}\right) \qquad (7)$$

The GP equation of maximum moment capacity and plastic hinge length obtained above is simple, short and meaningful. Since, it is clearly visible from the equation (Equation (6) and (7)) that strength increases with amount of reinforcement and decreases with increase of corrosion level. **Fig. 4.18** shows the relationship between moment carrying capacity and percentage of steel weight loss using Experimental, Analytical & GP based relationships. The resulting values of GP based relationships gives far better agreements with experimental moment carrying capacity as compared to analytical relationships. GP based relationship gives the moment capacity within 11% average error line (range of error line is between minimum 6% and maximum 18%). The performance parameters, RMSE and CE for maximum moment capacity are 0.079 and 0.92 respectively. The results are obtained with reasonable and acceptable accuracy.

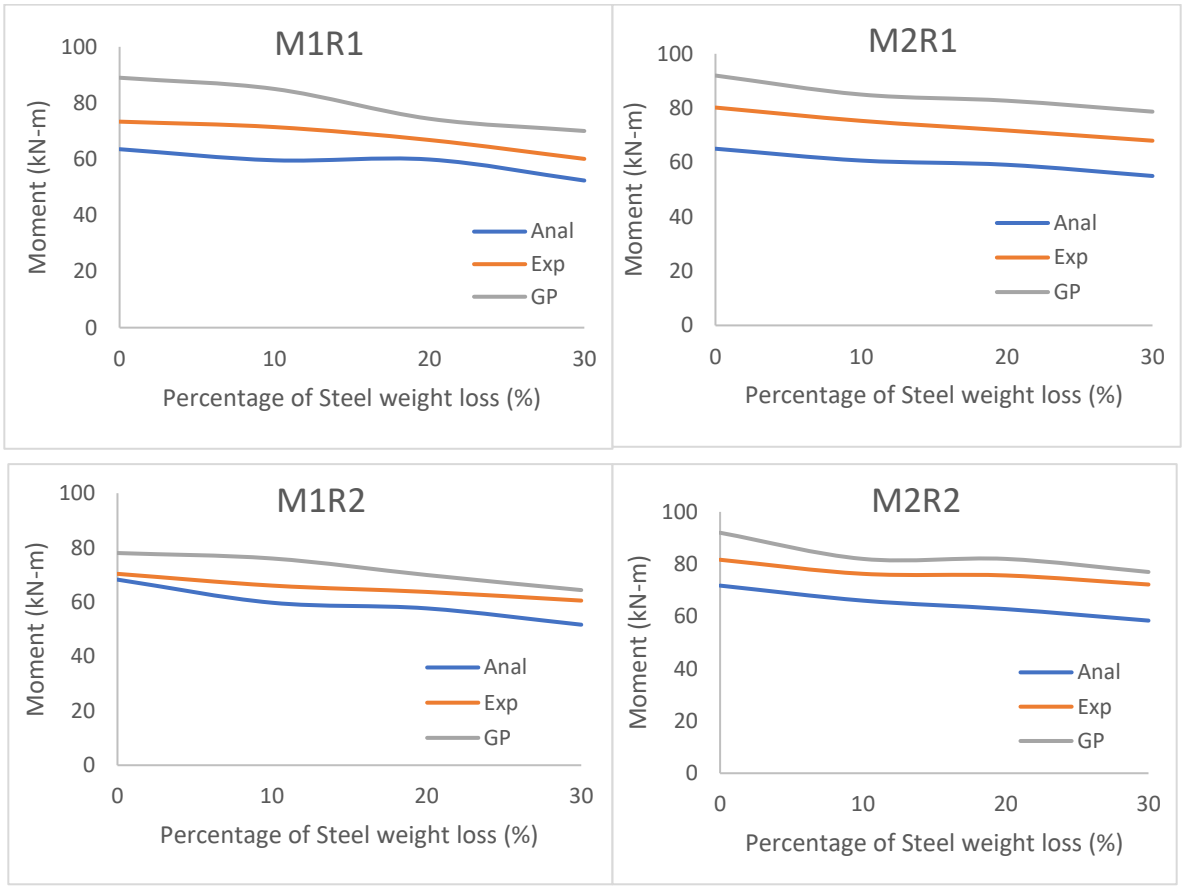

Fig. 4.18. Relationship between moment carrying capacity and percentage of steel weight loss using Experimental, Analytical & GP based relationships

4.5 CLOSING REMARKS

This chapter explores the development of plastic hinge model of RC beams for damage caused by flexural and flexure-shear cracks in plastic hinges with corroded reinforcement after calibration of experimental and analytical data. This parametric study incorporating the experimental results has been compared with finite element method to investigate effect of reinforcement corrosion embedded in RC beams. The moment-rotation relation and failure modes of corroded RC beams were also reported. Moment-chord rotation for RC plastic hinges at 0%, 20%, 35% corroded bar in RC beam was presented to predict the nonlinear behaviour of existing structures by performing pushover analysis. Genetic programming technique was implemented for estimating maximum moment carrying capacity of RC beams with corroded steel by taking different percentages of corrosion of reinforcement bar including no corrosion case as well, which can predict the seismic behaviour of RC beam of any existing structure too.

CHAPTER 5
EFFICACY OF DEVELOPED PLASTIC HINGE MODEL OF RC BEAM BY PUSHOVER ANALYSIS

5.1 GENERAL

Plastic hinge model for corroded Reinforced Concrete (RC) beams are developed based on load-deformation obtained experimentally, as well as analytically through nonlinear finite element modeling considering the effect of reinforcement corrosion. A simple empirical equation is also obtained for maximum moment including the percentage of corrosion, using soft computing approach of Genetic Programming (GP). In this chapter, the work has been expanded to explore the developed plastic hinge model of RC beam on inelastic behavior of all RC buildings by performing pushover analysis. Also, investigations are done to analyse the effectiveness of the plastic hinge models developed (different % of corrosion levels) for the same. While moment-curvature relationship has the potential to monitor the deterioration of RC beams due to corrosion exposure. Also, nonlinear parameters like plastic hinge length has the potential of relating effect of corrosion to inelastic behavior of components of structure as evaluated in Chapter 3. Therefore, a two-storey frame is analysed by incorporating the developed hinge models of RC beam.

5.2 DESCRIPTION AND MODELING OF RC FRAME STRUCTURE

A single bay two storey frame is considered for the analysis. The building frame has the floor height of 3.0m, span of 5m in X-direction and 6 m in Y-direction. All beams have dimension of 230mmX 350mm and dimension of columns are 350mX 350mm. The joints are fixed and properties of frame components are provided in **Table 5.1**. Material properties have been considered as 25 MPa, 30 MPa for concrete compressive strength and yield strength varied for steel bars with different corrosion levels (0 to 30%) as given in **Table 5.2**.

Table 5.1 Member Section Properties

Member	**Diameter of Bar**	**Longitudinal Reinforcement**	**Stirrups**	**Cross-section**
Column	16mm	8No.s -16mm (Dia)	8mm@150mm c/c	350mmX 350mm
Beam	12mm	4No.s -12mm (Dia)	8mm@200mm c/c	230mmX 350mm

Table 5.2 Yield Strengths of Steel bars

Reinforcement Bar	Yield Strength (MPa)
R1	369
R1C10 (10% corroded)	335
R1C20 (20% corroded)	323
R1C30 (30% corroded)	300
R2	445
R2C10 (10% corroded)	425
R2C20 (20% corroded)	360
R2C30 (30% corroded)	340

The RC frame building with the above materials and dimensions has been modeled using SAP 2000 software (**Fig. 5.1**). The user defined option has been used in the analysis and moment curvature behavior of beam (for different % of corroded bars) has been defined using hinge model developed in the preceding section. A bending moment curvature analysis must be performed considering the section characteristics and constant axial load on component for each column. For user defined hinge properties of column, simplest form of length of plastic hinge as 0.5*H* (*H* as column depth) is used.

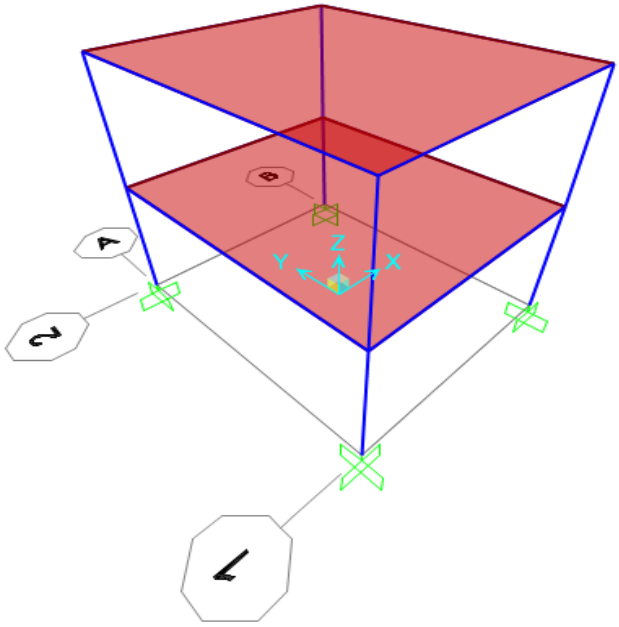

Fig. 5.1 RC frame Model (SAP 2000)

Plastic hinge length is obtained from moment-curvature analysis of RC beams from preceding chapters and has been defined for all the cases.

5.3 PUSHOVER METHODOLOGY

Push-over analysis is performed by subjecting the structure to a monotonically increasing mode of lateral load, which represents the inertial force that the structure will endure when subjected to ground shaking [Kadid and Boumrkik, 2008]. Various structural components may yield sequentially under gradually increasing loads. Therefore, the structure suffers a loss of stiffness in each case. Using pushover analysis, the characteristic nonlinear force-displacement relationship can be resolute.

16 cases are considered in the pushover analysis of each frame, as shown in **Table 5.3**, including variation of concrete strength, yield strength of reinforcement along with corrosion percentages of bars as explained in preceding chapters.

Table 5.3 Pushover Analysis cases

RC Frame No.	Concrete Grade	Yield Strength of Reinforcement	Corrosion % of Reinforcement Bar
A	M1	R1	0%
B	M1	R1	10%
C	M1	R1	20%
D	M1	R1	30%
E	M2	R1	0%
F	M2	R1	10%
G	M2	R1	20%
H	M2	R1	30%
I	M1	R2	0%
J	M1	R2	10%
K	M1	R2	20%
L	M1	R2	30%
M	M2	R2	0%
N	M2	R2	10%
O	M2	R2	20%
P	M2	R2	30%

Pushover analysis includes the application of gravity loads and representative lateral load patterns. The frame shall be subjected to gravity analysis and at the same time lateral loads have also been applied. The pushover analysis is load controlled, where the structure is loaded to full collapse (unstable condition).

In all cases, monotonous stepwise application of lateral force to perform nonlinear static analysis. The applied side load has an acceleration in the X direction, which represents the force that the various components of the RC building bear when subjected to ground vibration. Some elements may yield sequentially, under incrementally increasing loads. Consequently, at each event, the structures experience a stiffness change as shown in Figure 5.2, where IO is immediate occupancy, LS is life safety and CP stand for collapse prevention respectively [Kadid and Boumrkik, 2008].

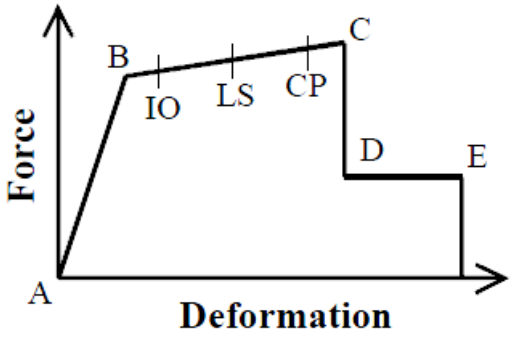

Fig. 5.2 Force-Deformation for pushover hinge

In the pushover analysis, the behavior of building is distinguished by the capacity curve after defining hinge property, which represents relationship between base shear and displacement. The next section discusses moment-curvature and results of pushover analysis (pushover curve, plastic hinge mechanism) of default and developed hinge model.

5.3.2Moment-Curvature and Pushover Curve

The moment curvature curve of default hinge property and developed hinge model (Case M1R1) is shown in **Figure 5.3**.

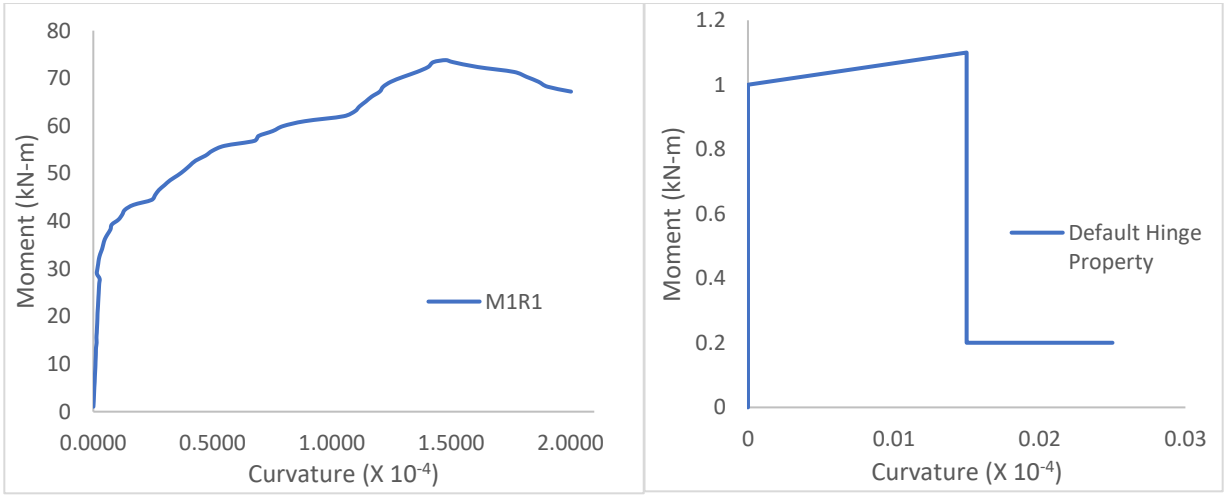

Fig. 5.3 Moment-Curvature of Developed hinge model (Case M1R1) and Default-hinge model

The comparison depicts that moment-curvature relationship of RC beam depicts the actual behaviour based on extreme compression fiber reaching the ultimate concrete compressive strain, as determined by Priestley et al., or the longitudinal steel reaching a tensile strain of 50% of the ultimate strain capacity. However, default-hinge properties are based on FEMA-356. The developed model is better than Default-hinge as it reflects nonlinear behaviour compatible with element properties

The pushover curves for all the sixteen cases of RC frame using developed hinge models are shown in **Figure 5.4**. These curves represent the overall behavior of the frame with ductility and stiffness. The trend in the pushover curves of all four RC frame cases with corroded bars are similar. They are linear at first, but begin to deviate from linearity as beams and columns are subjected to inelastic action. When the building is pushed well into the inelastic range, the curve becomes nonlinear.

It can be observed from Fig. 5.3, that both base shear force and displacement of RC frame is decreasing with the increase in corrosion of reinforcement bars for all the four cases. The base shear of 276.67 kN is observed to be maximum for M2R2 case without corrosion at the maximum displacement of 36.30 mm. This means that RC frame of M2R2 case (no corrosion) has a greater capability to resist lateral load (seismic load) than other three non-corroded cases. The four curves without corrosion case showed no decrease in the load carrying capacity of the buildings suggesting good structural behavior. However, structure with corroded bars experience loss in stiffness, therefore, the slope of the pushover curve is nonlinear and decreasing. The curve is decreasing due to the reduction of steel cross-section because of pitting corrosion. In the frame with both R1 and R2 bars, there is an increase in pushover curve after the decrease due to tensile stresses induced in concrete surrounding rebars through internal pressure generated by increasing volume of corrosion product. The variation in base shear capacity of 10% corroded case is less than 6% in all the cases as compared to no corrosion case. But base shear capacity has been observed to be decreasing with a variation of 8% to 15% in 20% and 30% corroded cases as compared to no corrosion case. It has been observed that 4% to 7% increase occurred in base shear capacity with increase in grade of concrete (M1 to M2). An increase in variation of base shear has been observed between 12% to 17% with the increase in yield strength of steel. In higher steel grade, tension force was higher at ultimate strain and more concrete was active in resisting moment. Therefore, the base shear increases with increase of grade of steel.

To study possible differences in outcome of nonlinear static analysis, frames are modelled with default hinge properties as well to compare with the developed hinge properties. Not more than 5% variation in base shear capacity is observed when compared with default hinge properties. However, default hinge properties have considerable effect in displacement capacity of RC frame. It is due to the fact that, same deformation capacity is assumed by default hinge model for all columns, without considering axial load level and orientation of columns properly (Inel and Ozmen, 2006).

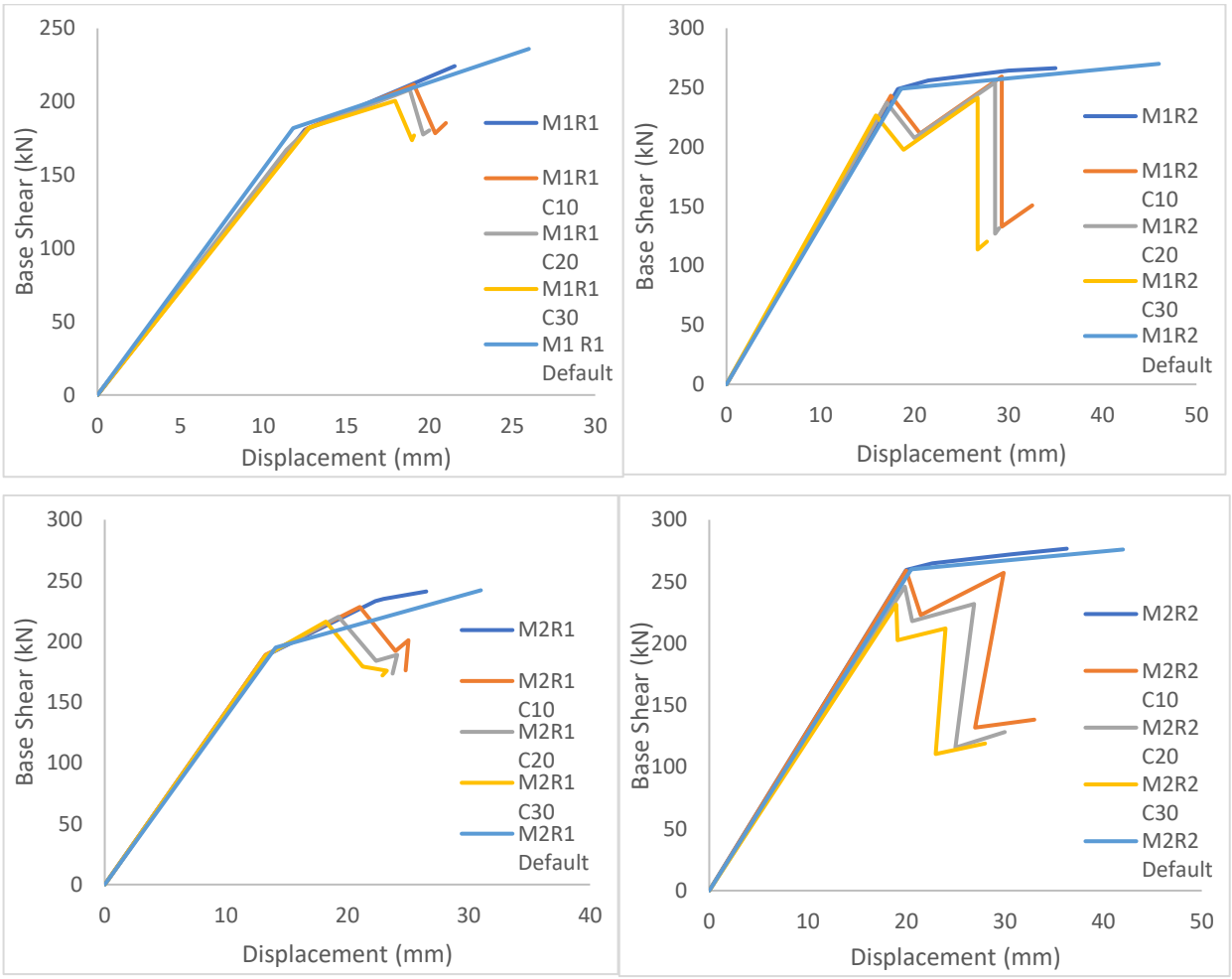

Fig. 5.4 Pushover curves of RC frame for all four cases a)M1R1 b) M1R2 c)M2R1 d) M2R2

The base shear capacities for cases M1R1and M2R1 are quite similar. The comparison of the pushover curve shows that stiffness of frame is almost similar in the initial phase until yielding occurs sequentially due to incrementally increasing lateral loads.

5.3.2 Plastic hinge mechanism

Proposed plastic hinge formation for reinforced concrete frames to provide information about the local and overall failure mechanisms in the building (i.e. soft stories and strong beam- weak column response etc.). The plastic hinge formation mechanism is obtained at the displacement point corresponding to the ultimate displacement as shown in **Figure 5.5 to Figure 5.8**. The ulimate point is considered as the displacement at 20% of the lateral load capacity.

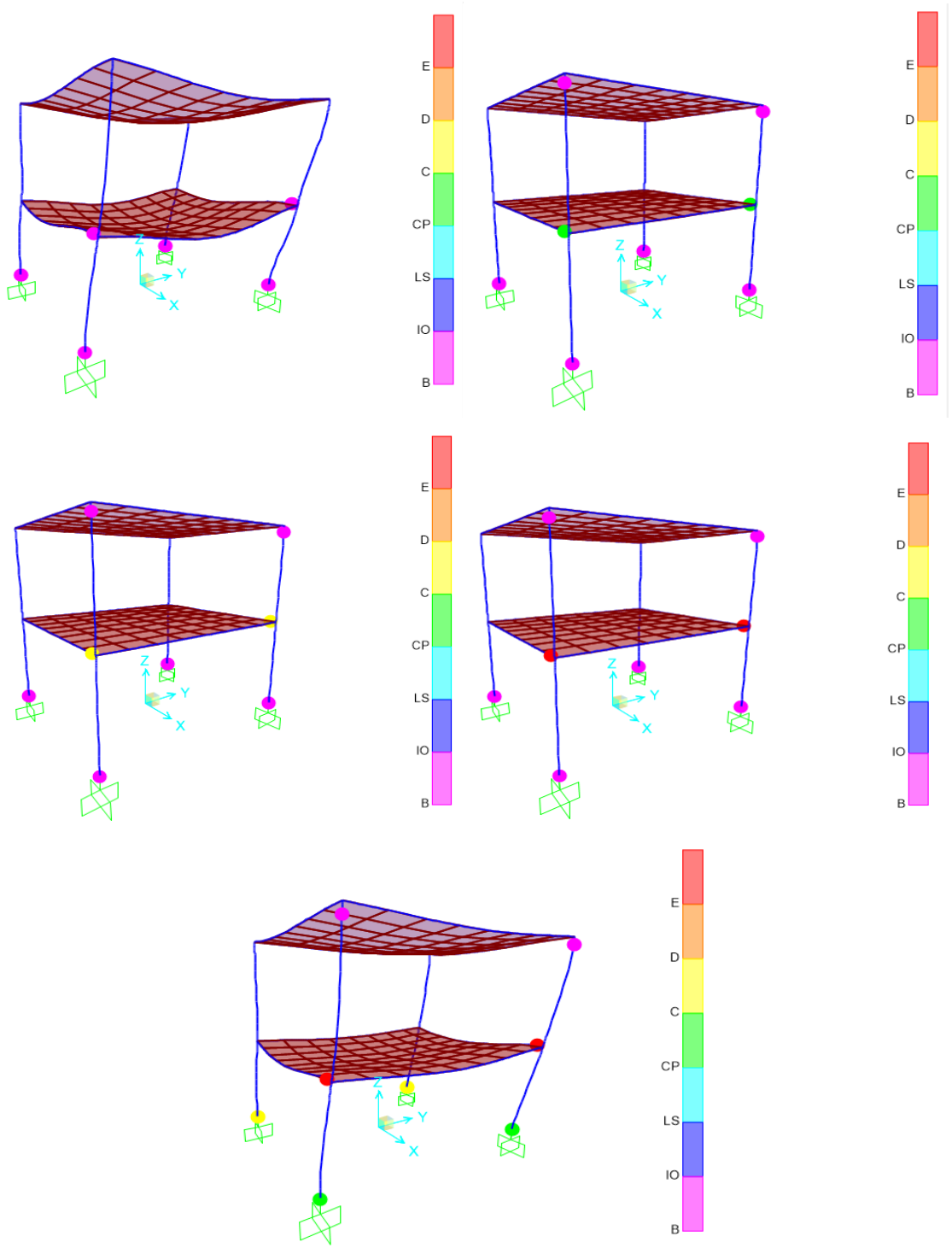

Figure 5.5 Plastic hinge patterns of M1R1 RC frame a) No corrosion b) 10% corrosion c) 20% corrosion d) 30% corrosion (e) Default-hinge model

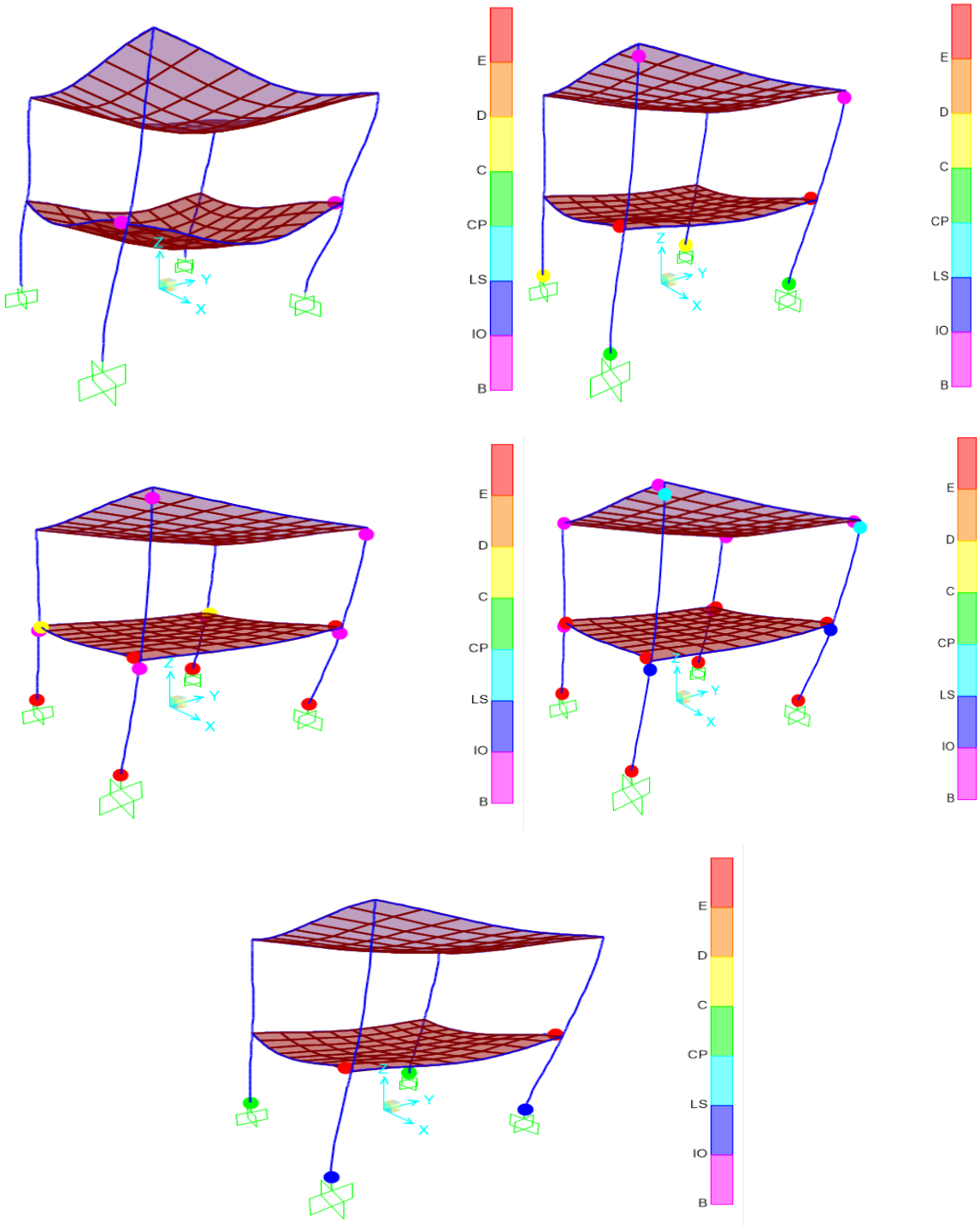

Figure 5.6 Plastic hinge patterns of M1R2 RC frame a) No corrosion b) 10% corrosion c) 20% corrosion d) 30% corrosion (e) Default-hinge model

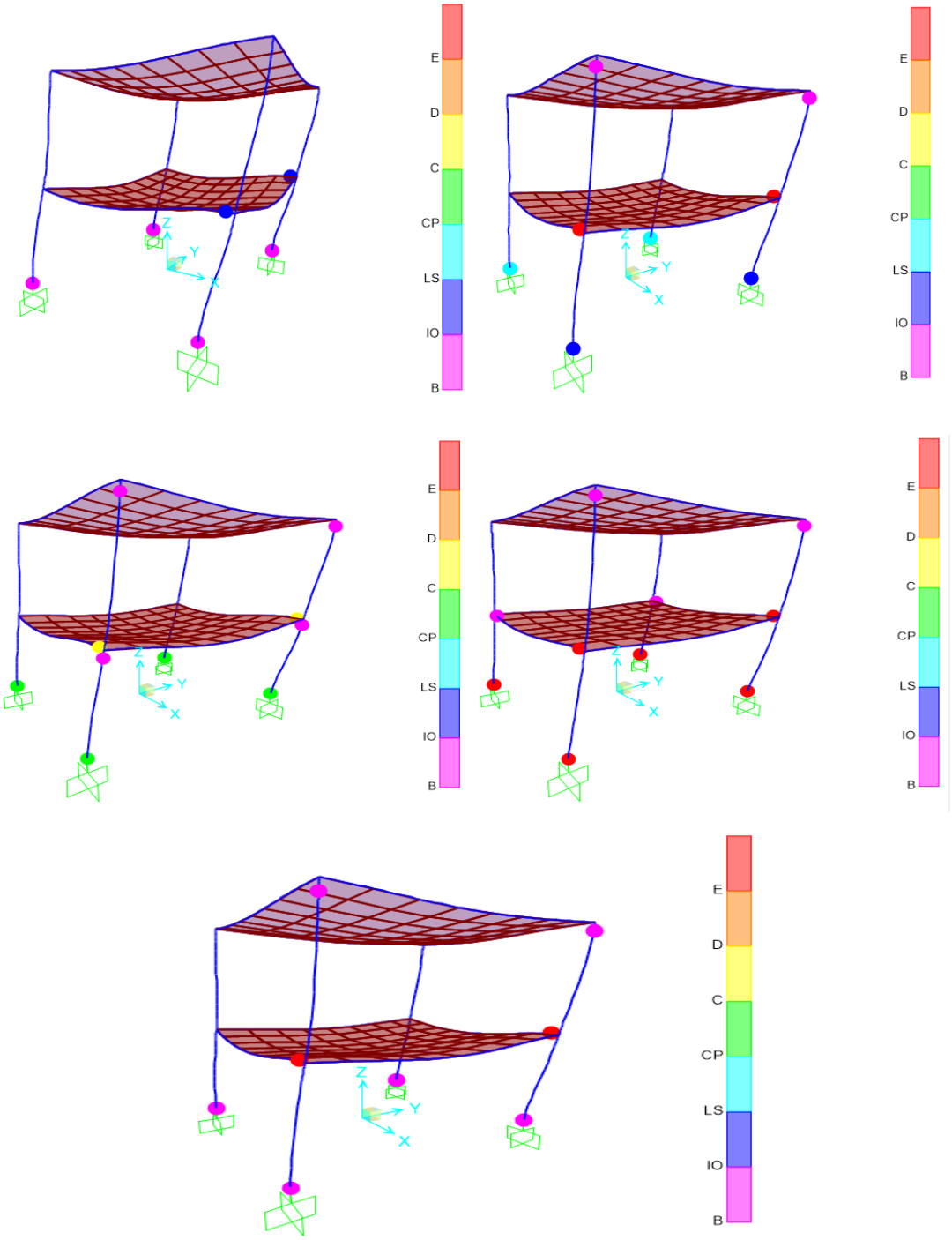

Figure 5.7 Plastic hinge patterns of M2R1 RC frame a) No corrosion b) 10% corrosion c) 20% corrosion d) 30% corrosion (e) Default-hinge model

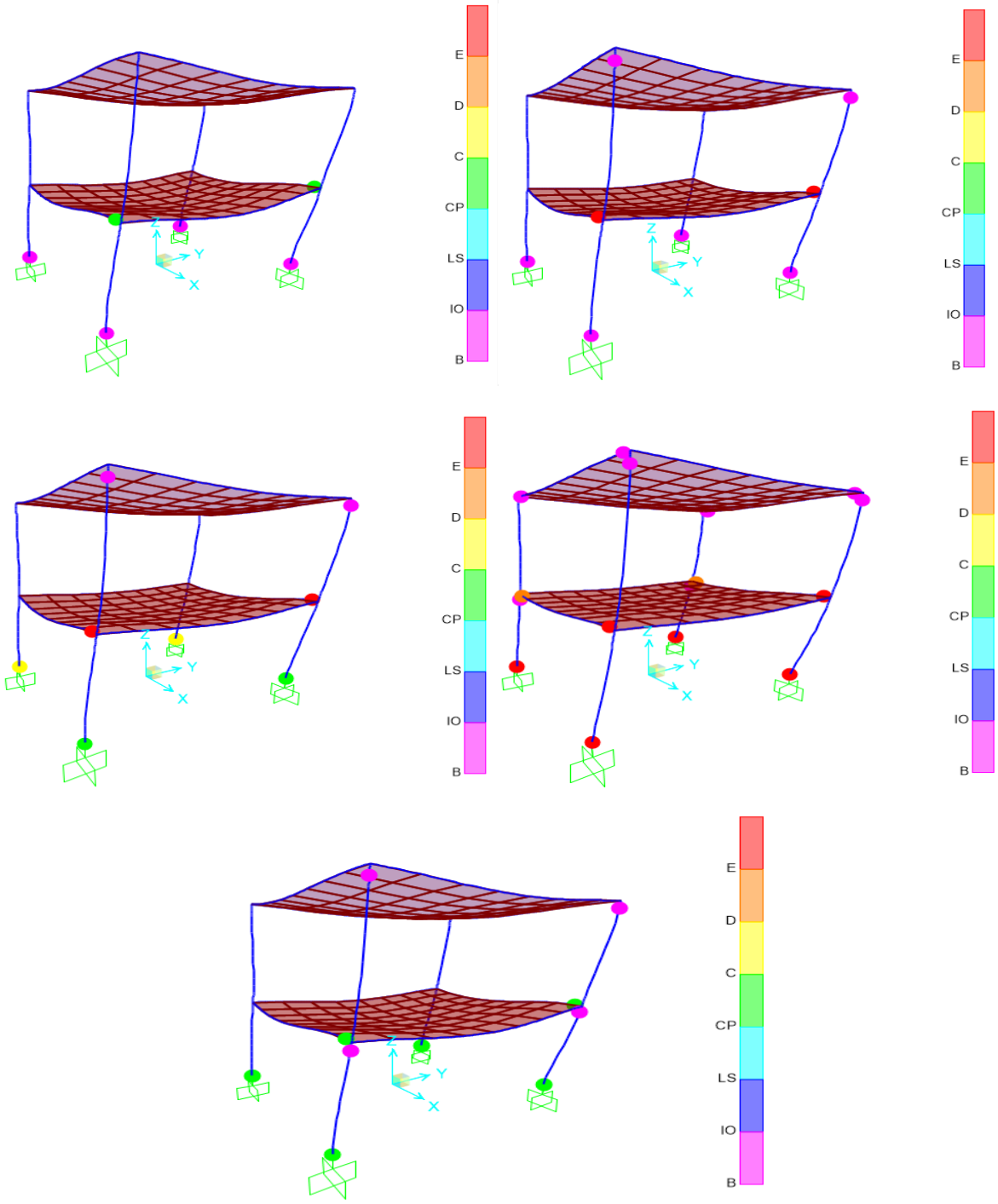

Figure 5.8 Plastic hinge patterns of M2R2 RC frame a) No corrosion b) 10% corrosion c) 20% corrosion d) 30% corrosion (e) Default-hinge model

Comparison of the figures of all cases reveal that the hinge patterns for all cases are similar. Plastic hinges are formed beyond CP point at corrosion level of 20% and 30% in RC frame. Also, plastic hinge formation starts with beam ends and base columns of lower story, then propagates to upper story. Since yielding occurs before ultimate displacement points at yielding, IO (Immediate Occupancy) and LS (Life Safety) respectively, the amount of damage in the frame structure will be limited. Although the hinge positions seem to be the same, in all cases, major damage or failure occurs at beam of the frame. The

hinging pattern of the two-storey frame by incorporating plastic hinge model of RC beams in RC frames is suitable for a ductile beam mechanism in which columns are stronger than beams in no corrosion and 10% corrosion cases (**Fig. 5.5 to 5.8**). Comparison of hinging patterns of default and developed hinge model estimate plastic hinge formation at ultimate state very well. However, significant differences have been observed at the ultimate state in default hinge model. It can be seen from **Fig. 5.5 to 5.8** that ductile beam mechanism has been emphasized through hinge patterns with default hinge model in which columns are stronger than beams. But this mechanism is not guaranteed for the buildings designed according to previous codes in other countries (Inel and Ozmen, 2006).

After carefully checking the observation results, it is visible that column yield occurs at the ground base position where point of CP (Collapse Prevention) in plastic hinge formation is crossed only in RC frames with corrosion cases (20% and 30% corrosion levels).

5.4 CLOSING REMARKS

This chapter explores the efficacy of plastic hinge model of RC beams after calibration of experimental and analytical data on RC frames with different percentages of corrosion. This parametric study incorporating the analytical results by performing pushover analysis has been presented to investigate the displacement capacity and base shear. The pushover curves and the plastic hinge mechanisms of RC frames are also reported. Pushover curve and plastic hinge mechanism has been presented by incorporating different percentage level of corrosion to predict the nonlinear behavior of existing structures by performing pushover analysis.

CHAPTER 6
CONCLUSIONS

6.1 GENERAL

In the present study plastic hinge models of corroded RC beams have been developed. These models can be effectively used to monitor seismic evaluation of old buildings by using pushover analysis. These plastic hinge models of RC beams are better when considering corrosion than the information currently available through FEMA documents. On the basis of present study, following conclusions can be made.

6.2 CONCLUDING REMARKS

6.2.1 Evaluation of plastic hinge parameters with corroded reinforcement

1. Bars corroded to 10% still have ductility as the *UTS/YS* ratio is close to 1.25 with high value of plastic hinge length. Whereas bars corroded to 20% and 30% have undesirable shear failure as *UTS/YS* ratio is much less than 1.25 resulting in low value of plastic hinge length.
2. Deflection carrying capacity of RC beams is decreasing from 10% to 30% corroded bars. Shear failure has also occurred in some of the R2 corroded bars in RC beams since the shear capacity reached earlier than flexure capacity of corroded beam.
3. Moment-curvature values of corroded RC beams decreases from 10% corroded bar to 30% corroded bar changing the failure from flexure to shear with wide cracks formed and making it unfit as a seismic member.
4. RC beams with no corroded bars have curvature ductility value more than 5. The curvature ductility for RC beams with corroded reinforcement reduced from 3.9 to 1.6 for corrosion level changing from 10% to 30%.
5. The plastic hinge length decreases from 0.52 *d* to 0.26 *d* as the corrosion of reinforcement bar is increased.
6. Length of plastic hinge increases as the grade of concrete is increased and decreases with the increase of yield strength of reinforcement bar from R1 (369 MPa) to R2 (445 MPa) as the ductility gets reduced when grade of steel increases.

6.2.2 Development of plastic hinge model with corroded reinforcement

1. The moment-rotation relation and the failure modes of corroded RC beams from experiments are well matching with the finite element model including load-displacement relation.

2. The moment carrying capacity and rotation capacity decreases with the increase in corrosion percentages of reinforcement bar from 5% to 35% used in RC beams. The moment carrying capacity is more for higher grade of concrete.
3. RC beams are able to sustain flexure failure approximately till 25% of corrosion loss. A further increase of corrosion level in reinforcement bars at 30% and above in RC beams change the failure mode of the beam from flexure to shear failure.
4. RC beams with corrosion percentages 30% and above are failing in shear, which is showing rotations at CP (Collapse Prevention) level almost similar to the rotations of beams controlled by shear as given in FEMA-356.
5. Moment-chord rotation for RC plastic hinges at 0%, 20%, 35% corroded bar in RC beam is reveal that ductility decreases with the increase in corrosion level of bars making it seismically vulnerable and it can be used to predict the nonlinear behaviour of existing structures by performing pushover analysis.
6. The analytical model developed using Genetic Programming equation depicts that the maximum moment carrying capacity of beam depends on size of member, material properties and percentage of corrosion of reinforcement bar.

6.2.3Efficacy of developed plastic hinge model of RC beam by pushover analysis

1. Base shear force and roof displacement of RC frame is decreasing with the increase in corrosion of reinforcement bars.
2. The base shear of 276.67 kN is observed to be maximum for M2R2 case without corrosion at the maximum displacement of 36.30 mm.
3. Base shear is increasing with an increase in both concrete and steel grade. But significant increase in base shear of about 13% to 17% is noticed with increase in grade of steel.
4. Plastic hinges are formed beyond CP point at corrosion level of 20% and 30% in RC frame. Also, plastic hinge formation starts with beam ends and base columns of lower story, then propagates to upper story.
5. The hinging pattern of the developed model with defining moment-curvature of beams in RC frames is suitable for a ductile beam mechanism in which columns are stronger than beams as observed after performing pushover analysis.

6.3 RECOMMENDATIONS FOR FUTURE RESEARCH

The proposed research work developing plastic hinge models of RC beams for seismic evaluation of RC structures can be further extended as:

1) Development of plastic hinge model of RC beams, columns and RC beam-column joints for pushover analysis of RC structures considering variation in section properties of member, type of loading, modes of failure (by considering shear stirrups & without shear stirrups) and end support conditions (moment rotation relationships-confined or unconfined concrete) with corrosion.

2) Investigation of the efficacy of plastic hinge models developed for damage monitoring in other civil engineering structures of bigger and complex dimensions and sizes.

3) Study on plastic hinge behaviour and its development can be extended to stainless steel and other materials with corrosion.

LIST OF PUBLICATIONS

[1] Yadav, D., Kwatra, N. and Agarwal, P., 2019. Post-yield deformation parameters of reinforced concrete beam with corroded reinforcement. *Structural Concrete, 20*(1), pp.318-329.

[2] Yadav, D., Kwatra, N. and Agarwal, P., 2020. Comparative post-yield performance evaluation of flexure member with corroded reinforcement. *Structure and Infrastructure Engineering*, pp.1-21.

REFERENCES

ASCE/SEI 41-06. (2007). Seismic Rehabilitation of Existing Buildings.

ATC. Seismic evaluation and retrofit of concrete buildings—volume 1 (ATC-40). Report No. SSC 96-01. Redwood City (CA): Applied Technology Council; 1996.

ATC 55. Evaluation and improvement of inelastic seismic analysis procedures. (2001).

ATC, NEHRP Guidelines for the Seismic Rehabilitation of Buildings, FEMA 273 Report, prepared by the Applied Technology Council for the Building Seismic Safety Council, published by the Federal Emergency Management Agency, Washington, D.C. 1997a.

ATC, Next-Generation Performance-Based Seismic Design Guidelines: Program Plan for New and Existing Buildings, FEMA 445, Federal Emergency Management Agency, Washington, D.C. 2006.

Baker, ALL. (1956), "Ultimate load theory applied to the design of reinforced and prestressed concrete frames", *London: Concrete publications Ltd*

Babovic, V. and Keijzer, M. (2000). *Genetic programming with GPKERNEL*. Documentation by David Rodriguez Aguilera, University of Cordoba, Spain.

Biskinis, D. and Fardis, M.N. (2010). Deformations at flexural yielding of members with continuous or lap-spliced bars. *Structural Concrete, 11 (3)*, 127-38.

Biskinis, D. and Fardis, M.N. (2010). Flexure-controlled ultimate deformations of members with continuous or lap spliced bars. *Stuctural Concrete, 11(2)*, 93-108. http://dx.doi.org/10.1680/stco.2010.11.2.93.

Carpinteri, A., Corrado, M., Mancini, G. and Paggi, M., 2009. Size-Scale Effects on Plastic Rotational Capacity of Reinforced Concrete Beams. *ACI Structural Journal*, *106*(6).

Cervenka, V. (1985). Constitutive Model for Cracked Reinforced Concrete. *Journal ACI*, *82*, No.6 pp.877-882.

Colajanni, P., Recupero, A. and Spinella, N., 2019, October. Push-Over Analysis of RC Frame with Corroded Rebar. In *IOP Conference Series: Materials Science and Engineering* (Vol. 627, No. 1, p. 012020). IOP Publishing.

Corley, G.W. (1966), “Rotation capacity of reinforced concrete beams”, *J. Struct. Div.,***92**:121-46.

Dadi, V.S.K. and Agarwal, P., 2015, June. Comparative post-yield performance evaluation of flexural members under monotonic and cyclic loadings based on experimental tests. In *Structures* (Vol. 2, pp. 72-80). Elsevier.

Darwin, D., Pecknold, D.A.W. (1974). Inelastic Model for Cyclic Biaxial Loading of Reinforced Concrete. Civil Engineering Studies, University of Illinois, July.

Douglas, K.T., Davidson, B.J. and Fenwick, R.C. (1996), “Modelling of reinforced concrete plastic hinges”, *Proceedings of Eleventh World Conference on Earthquake Engineering,*ISBN: 0 08 042822 3.

Erdem, I., Akyuz, U., Ersoy, U. and Ozcebe, G., 2004, August. Experimental and analytical studies on the strengthening of RC frames. In *13th World Conference on Earthquake Engineering*.

Eligehausen, R. and Langer, P. (1986), “The rotation capacity of plastic hinges in reinforced concrete beams and slabs”, *Proceedings of International symposium on Fundamental Theory of Reinforced and Prestressed Concrete,* Nanjing, China.

Elmenshawi, A., Brown, T. and Metwally, S. (2011), “Plastic hinge length considering shear reversal in reinforced concrete elements”, *J. Earthq. Eng.*, **16**: 188-210, 2012, doi: 10.1080/13632469.2011.597485.

FEMA. NEHRP guidelines for the Seismic rehabilitation of buildings (FEMA 273). Washington (DC): Building Seismic Safety Council; 1997.

Federal Emergency Management Agency (2000). *Prestandard and commentary for the seismic rehabilitation of buildings*, FEMA-356. Washington, D. C., U.S.

FEMA-440. (2005). Improvement of Nonlinear Static Seismic Analysis Procedures.

Gaur, S. and Deo, M.C. (2008). Real time wave forecasting using genetic programming. *Ocean Engineering, 35 (11-12),* 1166-1172.

Goel, R.K. and Chopra, A.K., 2001. Improved direct displacement-based design procedure for performance-based seismic design of structures. In *Structures 2001: A Structural Engineering Odyssey* (pp. 1-10).

Habibullah, A. S.E. and Stephen Pyle, S.E., 1998. Practical three-dimensional nonlinear static pushover analysis. *Structure magazine, winter*.

Ho, J.C.M., Kwan, A.K.H. and Pam, H.J. (2004), *"Minimum flexural ductility design of high-strength concrete beams",* Magazine of concrete research, 56:1, 13-22.

Ho, J.C.M. and Kwan, A.K.H. (2008), "Flexural ductility assessment and concurrent flexural strength and ductility design of reinforced concrete beams", *Proceedings of 14th World Conference on Earthquake Engineering*, Beijing, China.

Hou, L., Liu, H., Xu, S., Zhuang, N. and Da Chen. (2017) "Effect of corrosion on bond behaviours of rebar embedded in ultra-high toughness cementitious composite", *Constr. Build. Mater.*,**138**, 141-150. http://dx.doi.org/10.1016/j.conbuildmat.2017.02.008.

Hsiao, F.P., Yeh, Y.K. and Hwang, S.J., SEISMIC EVALUATION OF RC SCHOOL BUILDINGS WITH PUSHOVER ANALYSIS.

Inel, M. and Ozmen, H.B., 2006. Effects of plastic hinge properties in nonlinear analysis of reinforced concrete buildings. *Engineering structures*, *28*(11), pp.1494-1502.

IS 13920 (1993), "*Ductile detailing of reinforced concrete structures subjected to seismic forces- code of practice*", Bureau of Indian standards, India.

Johari, A., Habibagahi, G., and Ghahramani, A. (2006). Prediction of soil-water characterstic curve using genetic programming. *Journal of Geotechnical and Geoenvironmental Engineering, 132(5)*, 661-665.

Joshi, S.G., Londhe, S.N., and Kwatra, N (2014). Determination of natural periods of vibration using genetic programming. *Earthquakes and structures, 6,* No.2. doi: http://dx.doi.org/10.12989/eas.2014.6.2.000

Juarez, C.A., Guevara, B., Fajardo, G. and Castro-Borges, P. (2011). "Ultimate and nominal shear strength in reinforced concrete beams deteriorated by corrosion." Engineering Structures, **33**.

Kadid, A. and Boumrkik, A., 2008. Pushover analysis of reinforced concrete frame structures.

Kheyroddin, A. and Naderpour, H. (2007). Plastic hinge rotation capacity of reinforced concrete beams. *International Journal of Civil Engineering, 5(1)*, 30-47.

Krawinkler, H. and Seneviratna, G.D.P.K., 1998. Pros and cons of a pushover analysis of seismic performance evaluation. *Engineering structures*, *20*(4-6), pp.452-464.

Krishna, A. and Sengupta, P., (2017). Effect of reinforcement corrosion on seismic performance of reinforced concrete structures. International Journal of Advances in Mechanical and Civil Engineering, ISSN: 2394-2827 Volume-4, Issue-6.

Kumari, B. and Kwatra, N. (2013). Finite element modelling of a multi-storeyed retrofitted reinforced concrete frame. *IOSR Journal of mechanical and civil engineering (IOSR-JMCE), 8, Issue 3,* 08-22. e-ISSN:2278-1684.

Kwan, A.K.H, Chau S.L. and Au F.T.K. (2006), "Improving flexural ductility of high-strength concrete beams", *Proceedings, Institution of civil engineers,* Structures and buildings **159**, 339-347.

Lopes, S.M.R. and Bernardo, L.F.A. (2003). Plastic rotation capacity of high strength concrete beams. *Materials and Structures, 36,* 22-31.

Lopes, S.M. and Carmo, R.N.F. (2006). Deformable strut and tie model for the calculation of the plastic rotation capacity. *Computers and Structures, 84,* 2174-2183. doi: 10.1016/j.compstruct2006.08.028.

Lee, H.S. and Kang, K.Y., 2000. Correlation of Experimental and Analytical Responses of a 1: 12 Scale 10-Story Reinforced Concrete Frame Having Nonseismic Details.

Lopez-Lopez, A., Tomas, A., and Sanchez-Olivares, G. (2016). Behaviour of reinforced concrete rectangular sections based on tests complying with seismic construction requirements. *Structural Concrete*. http;//dx.doi.org/10.1002/suco.201500107.

Lopez-Lopez, A., Tomas, A., and Sanchez-Olivares, G. (2016). Influence of adjusted models of plastic hinges in nonlinear behaviour of reinforced concrete buildings. *Engineering Structures, 124,* 245-257.

Marques, M. and Delgado, R. (2010). Pushover Analysis of R/C Buildings Using a Plastic-Hinge Nonlinear Approach – Modelling Issues. Proceedings of the 14th European Conference of Earthquake Engineering, Ohrid, Macedonia.

Mattock, A.H. and Corley, W.D.G. (1967), "Discussion of rotational capacity of reinforced concrete beams", *J StructDiv,* 93:519-22.

Maddawy, T.E., Soudki, K. and Topper, T. (2005), "Long term performance of corrosion-damaged reinforced concrete beams", *ACI Struct J,* **105**(5); 649-56.

Olteanu, I., Alistar, A. and Budescu, M., 2011. Non-linear Analysis of Reinforced Concrete Frames with ATENA 3-D Program. *BuletinulInstitutuluiPolitehnic din lasi. SectiaConstructii, Arhitectura*, *57*(2), p.93.

Ouaar, A., Doghri, I., Delannay, L. and Thimus, J.F., 2007. Micromechanics of the deformation and damage of steel fiber-reinforced concrete. *International Journal of Damage Mechanics*, *16*(2), pp.227-260.

Ou, Y.C. and Chen, H.H. (2014). Cyclic behaviour of reinforced concrete beams with corroded transverse steel reinforcement. *Journal of structural engineering, 140(9)*, -1—1. doi: 10.1061/(ASCE)ST.1943-541X.0000932.

Ou, Y.C. and Nguyen, N.D. (2014), "Plastic hinge length of corroded reinforced concrete beams" *ACI Structural Journal*,**111**(5), doi: 10.14359/51686872.

Ou, Y.C. and Nguyen, N.D. (2016), "Influences of location of reinforcement corrosion on seismic performance of corroded reinforced concrete beams", Eng. Struct., **126**, 210-223, http://dx.doi.org/10.1016/j.engstruct.2016.07.048.

Ou, Y.C. and Nguyen, N.D. (2016), "Modified axial-shear-flexure interaction approaches for uncorroded and corroded reinforced concrete beams", Eng. Struct., **128**, 44-54, http://dx.doi.org/10.1016/j.engstruct.2016.09.031.

Ouglova, A., Berthaud, Y., Hild, F., Bompard, P., Foct, F. and Lazar, I. P. (2004), "Influence of corrosion on the mechanical behaviour of rebars in reinforced concrete structures", EUROCORR 2004

Pandey, M., Zakwan, M., Sharma, P.K. and Ahmad, Z. (2018). Multiple linear regression and genetic algorithm approaches to predict temporal scour depth near circular pier in non-cohesive sediment. *ISH Journal of Hydraulic Engineering*. DOI: 10.1080/09715010.2018.1457455.

Panagiotakos, T.B. and Fardis, M.N., 2001. Deformations of reinforced concrete members at yielding and ultimate. *Structural Journal*, *98*(2), pp.135-148.

Pandit, P., Gogoi, I. and Babunarayan, K.S., 2011. Effect of Corrosion on Performance of Reinforced Concrete structure using Pushover analysis. *International Journal of Earth Sciences and Engineering*, *4*(6), pp.885-888.

Paul, G. and Agarwal, P., 2012. Experimental verification of seismic evaluation of RC frame building designed as per previous IS codes before and after retrofitting by using steel bracing.

Paulay, T. and Priestley, M. N. J. (1992), "Seismic design of reinforced concrete and masonry buildings", John Wiley & sons, Inc., New York.

Poluraju, P. and Rao, N., 2011. Pushover analysis of reinforced concrete frame structure using SAP 2000. *International Journal of Earth Sciences and Engineering*, *4*(6), pp.684-690.

Presti, A.L., Recupero, A. and Spinella, N., 2018. Influence of rebar corrosion on RC frame push-over response. In *High Tech Concrete: Where Technology and Engineering Meet* (pp. 2118-2126). Springer, Cham.

Priestley, M.J.N, Seible, F. and Calvi, G.M., 1996. *Seismic Design and Retrofit of Bridges*, John Wiley Sons, New York, NY, USA.

Rai, D. C., Jain, S. K. and Chakrabarti, I. (2012), "Evaluation of properties of steel reinforcing bars for seismic design", *Proceedings of 15WCEE LISBOA.*

Saetta, A., Simioni, P., Berto, L. and Vitaliani, R., 2008. Seismic response of corroded rc structures. In *International fib symposium, Amsterdam, the Netherlands*.

Sawyer, H.A. (1964), "Design of concrete frames of two failure states", *Proceedings of the International Symposium on the Flexural Mechanics of Reinforced Concrete,* ASCE-ACI, 405-31

Seifi, M., Noorzaei, J., Jaafar, M.S. and Panah, E.Y., 2008. Nonlinear static pushover analysis in earthquake engineering: State of development. In *Proceeding of International Conference on Construction Building Technology, Kuala Lumpur*.

Sharma, A., Sharma, S., Sharma, S., and Mukherjee, A. (2017). Investigation of deterioration in corroding reinforced concrete beams using active and passive techniques. *Construction and Building Materials, 161,* 555-569. https://doi.org/10.1016/j.conbuildmat.2017.11.165.

Shuraim, A. and Charif, A., 2007. Performance of pushover procedure in evaluating the seismic adequacy of reinforced concrete frames. *King Saud University ashuraim@ gmail. com.*

Tu, Y.H., Hwang, S.J. and Chiou, T.C., 2006, October. In-Site Pushover Tests and Seismic Assessment on School Buildings in Taiwan. In *Proceeding of 4th International Conference on Earthquake Engineering* (No. 147).

Valente, M. (2012), "Bond strength between corroded steel rebar and concrete", *International Journal of Engineering and Technology,* **4**(5).

Viktor, G., Vladimir, C., and Gintaris, K. (2013). Deflection prediction of reinforced concrete beams by design codes and computer simulation. *Engineering Structures, 56,* 2175-2186. http://dx.doi.org/10.1016/j.engstruct2013.08.045.

Vladimir, C., Libor, J., and Jan, C (January 26, 2018). *ATENA theory manual*, part 1, Prague, Czech Republic.

Wang, X.H., Liu, X.L. (2010), "Simplified methodology for the evaluation of the residual strength of corroded reinforced concrete beams", *J Perform ConstrFacil,***24**(2); 108-19.

Yadav, D., Kwatra, N., and Agarwal P. (2018). Post Yield deformation parameters of reinforced concrete beam with corroded reinforcement. *Structural Concrete, 20,* 318-329. https://doi.org/10.1002/suco.201800037.

Yalçiner, H. and Marar, K., 2012. Seismic Performance Evaluation of Corroded Reinforced Concrete Structures by Using Default and User Defined Plastic Hinge Properties. *Earthquake Engineering*, pp.281-302.

Yu, L., François, R., Dang, V.H., L'Hostis, V. and Gagné, R., 2015. Structural performance of RC beams damaged by natural corrosion under sustained loading in a chloride environment. *Engineering Structures*, *96*, pp.30-40.

Yuksel, I. and Coskan, S., 2013. Earthquake behaviour of reinforced concrete frames subjected to rebar corrosion. In *Proceedings of Third International Conference on Sustainable Construction Materials and Technologies*.

Zhao, X., Wu, Y.F., Leung, A.Y. and Lam. H.F. (2011), "Plastic hinge length in reinforced concrete flexural members", *Procedia Eng*, **14**, 1266-1274, doi: 10.1016/j.proeng.2011.07.159.

Zhao, X.M., Wu, Y.F. and Leung, A.Y.T. (2012), "Analyses of plastic hinge regions in reinforced concrete beams under monotonic loading", *Eng. Struct.,***34**, 466-482, doi: 10.1016/j.engstruct.2011.10.1016.

Zhou, H., Zhao, C., Zhang, Y. and Yang, C. (2015), “RC beam pure bending plastic hinge parameter calculation considering size effect and experimental research”, *Proceedings of International Conference on Architectural, Civil and Hydraulics Engineering (ICACHE 2015).*